Analysis and Optimization of the Graz Cycle: A Coal Fired Power Generation Scheme with Near-Zero Carbon Dioxide Emissions

by

Brentan R. Alexander

SUBMITTED TO THE DEPARTMENT OF MECHANICAL ENGINEERING IN PARTIAL FULFILLMENT OF THE REQUIREMENTS FOR THE DEGREE OF

BACHELOR OF SCIENCE
AT THE
MASSACHUSETTS INSTITUTE OF TECHNOLOGY

JUNE 2007

Signature of Author:_____
Department of Mechanical Engineering
May 11, 2007

Certified by:_____
Ahmed F. Ghoniem
Professor of Mechanical Engineering
Thesis Supervisor

Accepted by:_____
John H. Lienhard V
Professor of Mechanical Engineering
Chairman, Undergraduate Thesis Committee

Analysis and Optimization of the Graz Cycle: A Coal Fired Power Generation Scheme with Near-Zero Carbon Dioxide Emissions

By

Brentan R. Alexander

Submitted to the Department of Mechanical Engineering
On May 11, 2007 in partial fulfillment of the
Requirements for the Degree of Bachelor of Science in
Mechanical Engineering

Abstract

Humans are releasing record amounts of carbon dioxide into the atmosphere through the combustion of fossil fuels in power generation plants. With mounting evidence that this carbon dioxide is a leading cause of global warming and with energy demand exploding, it is time to seek out realistic power production methods that do not pollute the environment with CO_2 waste. The relative abundance and low cost of fossil fuels remains attractive and clean coal technologies are examined as a viable solution.

This paper helps identify the many options currently available, including post-combustion capture, pre-combustion capture, and a number of oxy-fuel combustion schemes. One cycle design in particular, the Graz cycle, holds some promise as a future power generation cycle.

A model of the Graz cycle developed in this paper predicts a cycle efficiency value of 56.72%, a value that does not account for efficiency losses in the liquefaction and sequestration of carbon dioxide, or the efficiency penalty associated with the gasification of coal. This high efficiency number, coupled with the low technological barriers of this cycle compared to similar schemes, is used as a justification for investigating this cycle further.

A sensitivity analysis is performed in order to identify key system parameters. Using this information, a computational optimization algorithm based on a simulated annealing scheme is devised and used to alter the parameters until an overall efficiency of 60.11% is achieved. Another optimization scheme which accounts for hardware limitations and plant capital costs is also discussed. This optimization yields a total efficiency of 58.76% while limiting the system high pressure to 110 bar.

With such high efficiency values for this cycle, it is suggested that further study with more advanced models be conducted to better assess the viability of the Graz cycle as a clean technology.

Thesis Supervisor: Ahmed F. Ghoniem
Title: Professor of Mechanical Engineering

Contents

Global Warming: The Carbon Dioxide Problem

The Industrial Age ushered mankind into a new and exciting world of mechanical automation and assistance that brought about manufacturing efficiency never before seen. Society, long accustomed to nominal energy consumption through wood stoves, sought to find new sources of energy to power these new machines that promised wealth and comforts for more people. Fossil fuels began to be consumed in large quantities to satiate the exploding demands for energy across the globe.

Over a century and a half later, the ramifications of this widespread and ever growing use of fossil fuels is beginning to be understood. The by-products of the combustion processes used to extract energy from fuels such as coal, oil, and natural gas, are substances that can be dangerous and have unintended effects when released en masse into the earth's atmosphere. Besides NO_x and SO_x, which are potent poisons that can cause serious health issues in short periods of time to those exposed, carbon dioxide is increasingly becoming a danger to the earth and those that inhabit it.

The earth's atmosphere is a complex and delicate blanket necessary for life. Without this layer, the earth would lose a majority of the energy that impacts it, leaving the average surface temperature at -19°C, a far cry from the comfortable average of 15°C the earth feels now. [(1)] The atmosphere keeps the earth warm, and this phenomenon, known as the greenhouse effect, is one of the most important functions of the atmosphere, which despite consisting mostly of nitrogen and oxygen, has the carbon dioxide in its upper reaches to thank for this effect. Radiation from the sun hitting the earth has a wavelength of between 0.4 and 0.7 µm. [(1)] When reflected back from the earth's surface, the emanating radiation wavelength is larger, at 4-100 µm. [(1)] Carbon dioxide, which absorbs energy in the 13-19 µm range, traps some of this reflected energy in the atmosphere and as a result the surface temperature rises. [(1)]

Carbon dioxide is dangerous as a pollutant because its increased concentration in the atmosphere will trap more energy in the earth's atmosphere, leading to a rise in the global mean temperature. Figure 1 shows data revealing the steady increase in

global atmospheric CO_2 concentrations as measured in Hawaii and the overall rise in the global mean temperature during the same timeframe: [2]

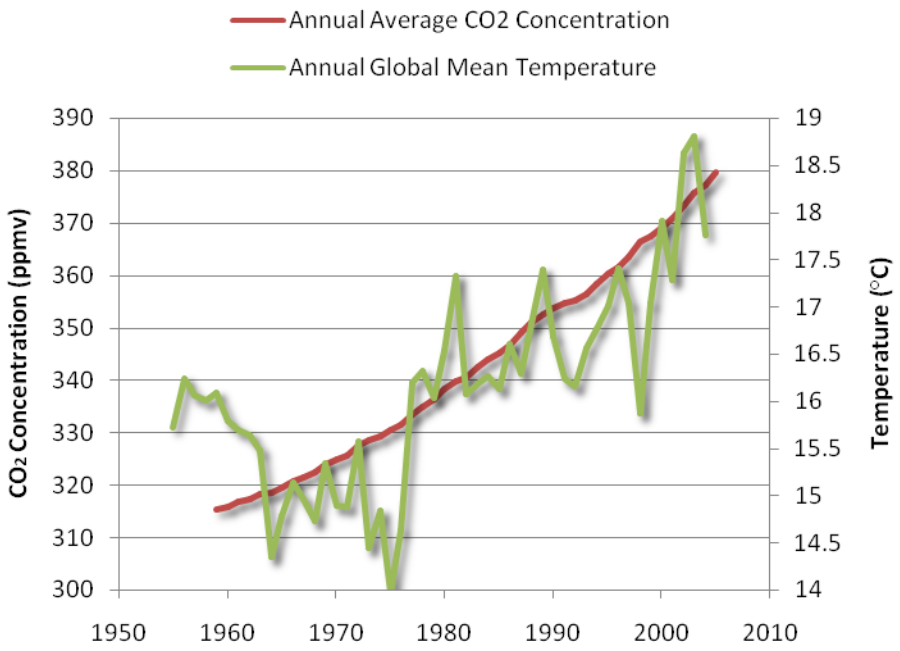

Figure 1: The correlation between the yearly atmospheric CO_2 concentration at Mauna Lao, Hawaii, and the annual global mean temperature is shown [2]

It has been argued by some that the increase in mean temperature over this time could have been caused by natural variations in the earth's climate that have occurred periodically over the millennia, however the change in temperature has been so fast and drastic that it can only fully be explained by the rapid increase in carbon dioxide concentration in the atmosphere, which had remained relatively constant at 280 ppmv until the early 1800s and the dawn of the Industrial Revolution. [1] When a larger time-scale is observed, going back hundreds of thousands of years, it becomes evident that atmospheric carbon dioxide concentrations do naturally fluctuate over time. Comparison to modern concentration levels, however, show that the current levels of CO_2 in the atmosphere are higher than at any point in history. Even if a portion of the increase in carbon dioxide concentrations is natural, human interaction is only speeding the process, and the ramifications of the extra CO_2 may prove disastrous.

A rise, even very slight, in the earth's mean temperature would have far reaching effects on the planet and its ecosystems. If energy usage and CO_2 concentrations continue to grow at the current rates shown in Figure 2, the average terrestrial temperature will increase 0.3°C every decade. [4]

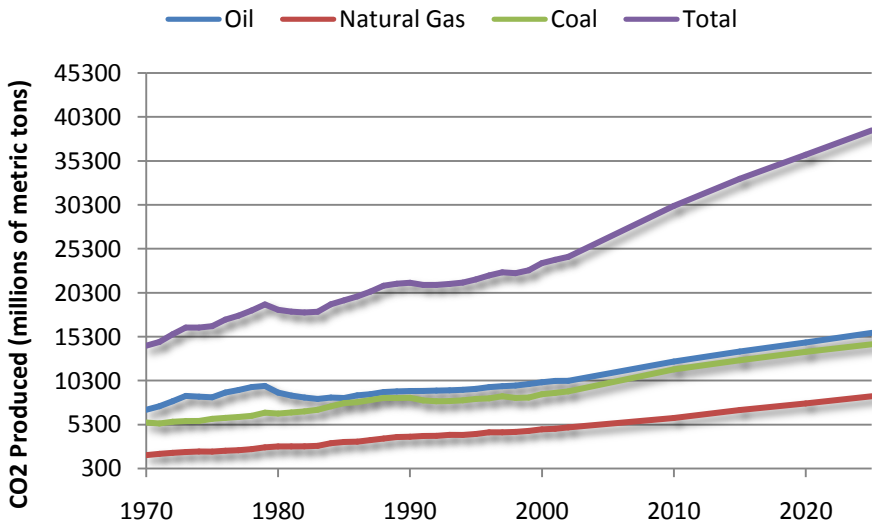

Figure 2: CO_2 emissions by fuel source, 1970-2025 (estimated) [3]

One important ramification of this increased mean temperature is a rise in ocean levels. As the temperature rises, polar ice will begin to melt and return to the oceans, resulting in an average six centimeter rise in the ocean levels per decade if energy usage trends continue. [4] Such a rise in ocean levels would be devastating to low-lying coastal communities like those found in Egypt, Southeast Asia, and the Caribbean. This rise in temperature would also trigger droughts leading to food shortages in areas of the globe already vulnerable to famine, like desert regions in North Africa and South America. [4] As vegetation changes in regions due to the climate change, animal populations will also have to move with their food sources. This movement of large plant and animal populations could weaken ecosystems and have particularly damaging effects on systems already facing extinction. [4] Even disease can spread to new populations as the animal species that carry them move to different latitudes in response to climate changes. Some scientists suggest that more severe weather systems will result from warmer oceans caused by the increased greenhouse effect. [4]

No one is certain of the extent to which global warming will cause devastation. What is certain is that an unabated rise in terrestrial carbon dioxide concentration will lead to an unwanted outcome, which even in the best-case scenario is far too destructive to ignore.

Coal as a Fuel Source

Fossil Fuels: A Necessary Evil

With global warming causing increased concern and leading to possible taxes on what power plants and chemical plants spew into the atmosphere, it seems counterproductive and misguided to place resources into fossil fuels, let alone coal, as the fuel of choice for the future. Indeed, fossil fuel fired power plants are the chief source of carbon dioxide emissions worldwide, and coal plants around the world are among the worst pollution offenders, often pouring tons of carbon dioxide, sulfur oxides, and other toxic gases into the air.

Fossil fuels, however, are a necessary evil. Figure 3 shows projected energy demand, broken down by economy type:

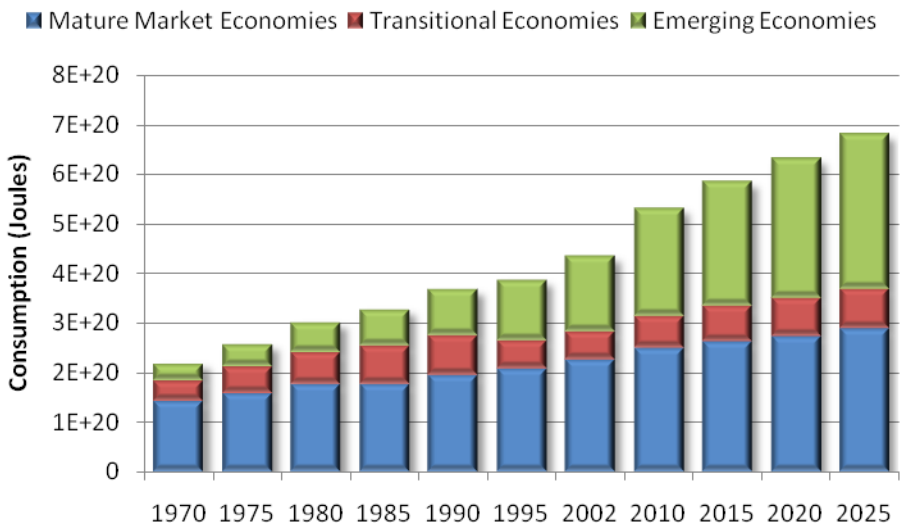

Figure 3: Energy demand by economy type, projected to 2025 [3]

Energy demand is growing steadily worldwide, and as more emerging economies, like China and India, begin and continue to modernize, their energy demands will increase as well. Indeed, in the 20 year period between the year 2000 and 2020, energy demand worldwide is expected to grow by more than 50%.

Where will all this energy come from? Figure 4 shows the breakdown in energy production by type in 2006:

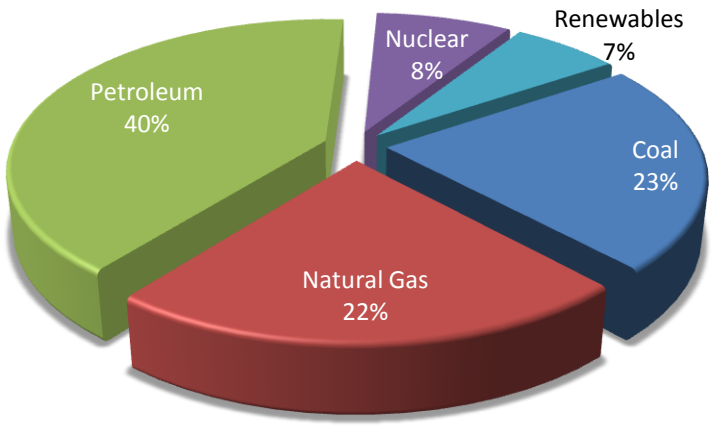

Figure 4: 2006 Energy consumption by fuel type [5]

The fossil fuel family accounted for 85% of all energy produced worldwide. Even with new renewable energy technologies and increasing interest in nuclear energy, the higher costs of renewable energy and nuclear energy make them undesirable economically as a fuel source. [5] As a result, it is clear that fossil fuels will remain the dominant fuel source worldwide for energy production.

Choosing Coal

Despite a continued use of fossil fuels, the choice to use coal as a primary fuel source still seems odd. Coal has been a traditionally dirty technology, often associated with acid rain and other environmental disasters. Natural gas, or methane, on the other hand, burns very cleanly through the following equation:

$$CH_4 + 2O_2 \longrightarrow CO_2 + 2H_2O$$

It seems that natural gas would be the correct choice for the fuel to make carbon dioxide capture and removal as cheap and easy as possible. Even oil, when properly refined and burned, is cleaner than coal and requires less toxin removal to make it a truly clean technology. If it is necessary to pay to remove carbon dioxide from the exhaust of a fossil fuel plant, why would it be desirable to still pay further to remove other pollutants trapped within coal?

The realities of supply limitations and the complexities of the global economy help to explain the attractiveness of coal. Figure 5 shows the prices of both natural gas and oil over the last 35 years:

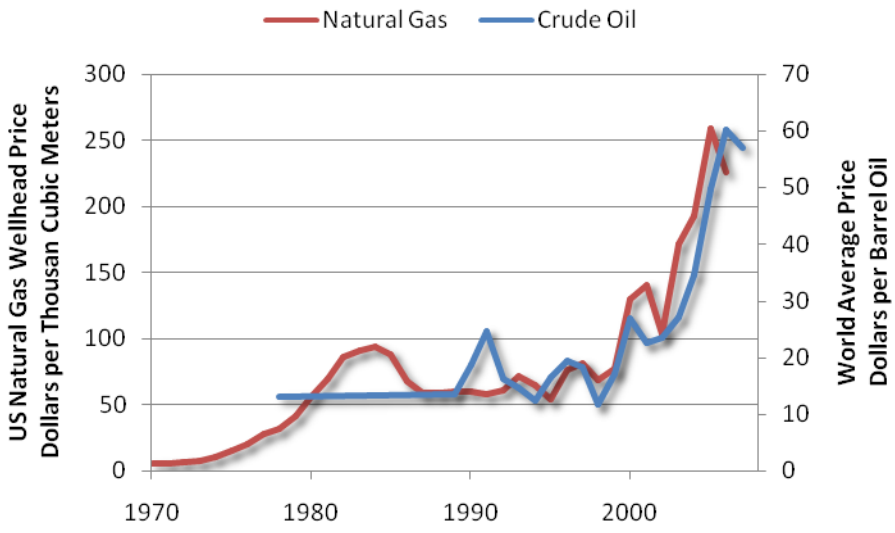

Figure 5: Natural gas and oil prices over time [6] [7]

Since the late 1990s, the prices of both fuels have more than tripled. The reasons behind this spike in prices are complex. One important factor has been the increased demand of both fuel types. For oil, worldwide demand has increased significantly in the last decade and is projected to grow further (see Figure 5). Natural gas suffers a similar demand problem; high efficiency natural gas combined cycle power plants were the choice for new construction in the United States throughout the 1990s, and as more of these plants came online, demand for fuel spiked. [6]

This surge in demand, however, is not the only factor behind the rise in prices. Another equally important factor is the depletion of resources within the United States. Natural gas reserves in the United States in particular have dwindled in the last ten years, and as a result there is an increased dependency on imported gas. [6] Europe has a similar problem, with little reserves of its own. With a volatile political situation in the Middle East, the largest oil producing sector in the world, added to this equation of dwindling domestic supply, the supply of oil and natural gas becomes unstable and unreliable. As a result, prices fluctuate wildly and foreign control artificially raises prices.

The price of coal, however, has remained fairly flat over the last half-century, as exhibited in Figure 6:

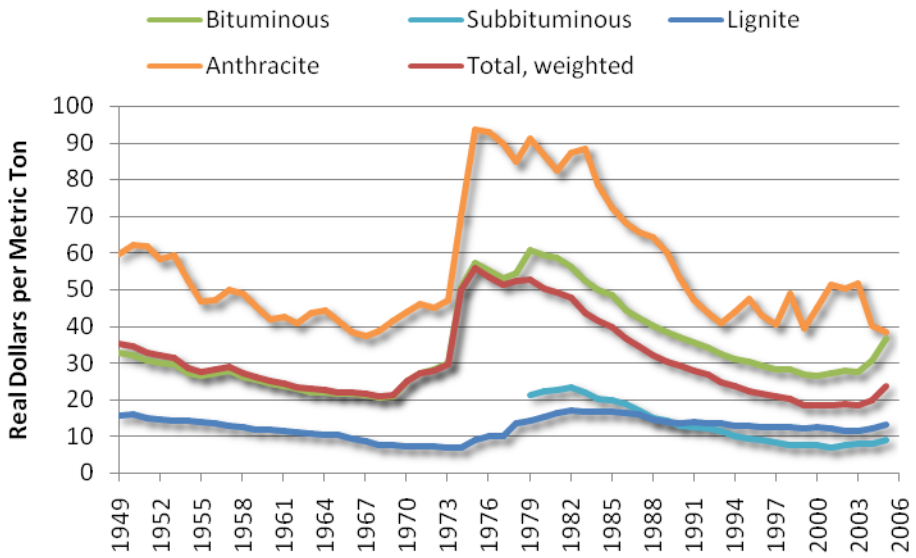

Figure 6: Price of different coal types over time [8]

This shows coal to be a cheap and stable fuel with respect to both oil and natural gas.

The prospects for the growth of coal as a fuel source are encouraging as well. Figure 7 shows a 2006 EIA estimation of remaining coal, oil, and methane reserves both worldwide and in the United States:

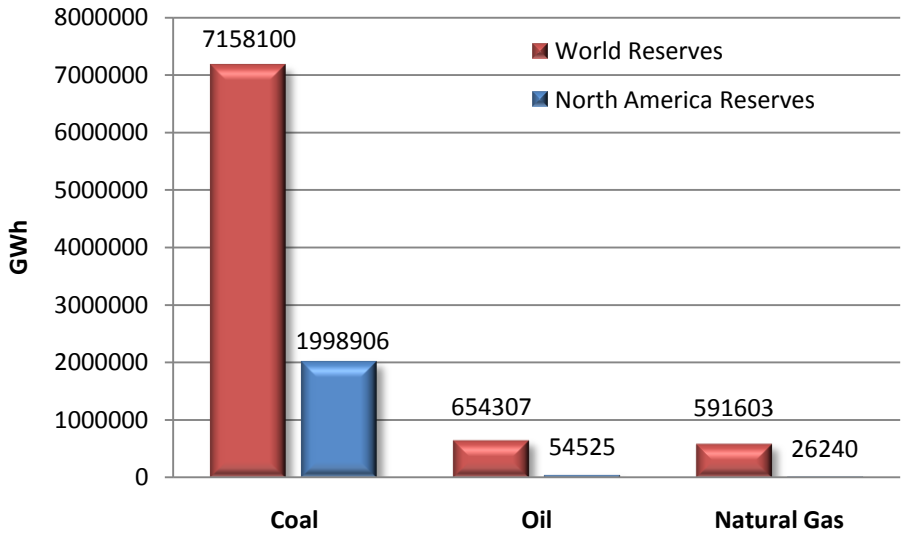

Figure 7: 2006 estimated recoverable resources by fuel type [8]

The study shows coal as a clear winner. Worldwide, there is over ten times the energy available through coal reserves as oil reserves. The types of supply shortages currently seen in the oil industry would not be an issue with coal for hundreds of years. Domestically, coal has an advantage as well. In North America, the estimated coal reserves are larger than the sum of the worldwide estimated oil and natural gas reserves. In addition, the North American coal reserves are estimated to be 36 times larger than the North American oil reserves, and over 76 times larger than the natural gas reserves. [8] This fact means coal can be produced locally near the point of power production, eliminating the supply uncertainties that currently drive the oil market.

All this together means that coal can provide a cheap, stable, domestic fuel supply for centuries, making it an economically clear choice between the fuels. But the problems associated with coal as a dirty fuel source remain, and technologies to address this fact and produce clean burning coal to ease carbon capture are required.

Gasification

The most important component in clean coal technology is the gasifier. Gasification is a relatively old technology that oxidizes a fuel in an oxygen deprived environment. This environment does not allow enough oxygen for full combustion to

occur, and as a result a syngas is produced which can be used as a fuel source later. In general, gasifiers convert fuel using the following reaction:

$$C_nH_m + \frac{n}{2}O_2 \rightarrow nCO + \frac{m}{2}H_2$$

The product synthesis gas, or syngas, that is made up of carbon monoxide and hydrogen, can then be used as a fuel. In practice, the synthesis gas also contains carbon dioxide, sulfur dioxide, methane, and other trace components.

Gasification takes place in three major stages: drying, devolatilization, and gasification. During the drying stage, the input fuel, or feedstock, is heated to over 100°C, at which point the water content in the fuel vaporizes and leaves. During the devolatilization stage, the feedstock is heated to between 500°C and 900°C, where the bonds between volatiles and char structure rupture. The products of this process are tars, hydrocarbon based liquids, hydrocarbon based gases, carbon dioxide, carbon monoxide, hydrogen, and water. These products are then further heated and pressurized. At these high temperatures and pressures, some of the products will fully combust to provide thermal energy for the other stages. The majority of the products will, however, gasify, leaving an output stream of syngas. The unusable remnants of this process, known as slag, are removed as a liquid or a solid from the gasification chamber and disposed.

Gasifiers all fall into one of three categories, depending upon the way in which they perform their gasification: Fixed bed, fluidized bed, and entrained flow gasifiers.

Fixed Bed Gasification

Fixed bed gasifiers make use of a system of grates, spaced throughout the gasifier vessel. As large chunks of feedstock are fed into the top of the unit, they fall upon the grates and begin the gasification process. As the pieces of feedstock lose mass and become smaller, they are able to fall through the grate to the next grate below. As the particle falls, the holes in the grate become smaller and smaller.

In these systems, drying occurs first at the top of the vessel, with devolatlization occurring next as the particle falls. Gasification occurs in the zones at the bottom of the vessel, producing the thermal energy to heat the feedstock in the stages above.

This type of gasifier has been used successfully for many years in South Africa, and is known as the Lurgi fixed bed gasifier. Despite this success, however, interest in fixed bed gasifiers has waned due to their inability to handle caking and low quality coals and their high residence times for particles in the vessel.

Fluidized Bed Gasification

Fluidized bed gasifiers use technology similar to fluidized bed combustors. In these systems, fine coal particles are fed into a highly turbulent environment and mixed with oxygen and water. The coal particles remain suspended within the fluidized bed as slag components fall to the bottom of the vessel and gasification products flow to the top and out.

These systems have the advantage of fast residence times on the order of a few seconds, as well as the ability to accept a wide range of feedstocks, including coals of various quality, wood, and solid waste. Unfortunately, the exhaust stream from the vessel is rich in char, meaning full gasification does not take place within the vessel. As a result, the exhaust gases must be extensively recycled to the gasifier in order to reach a satisfactory conversion efficiency, which increases the energy requirements of the system.

Entrained Flow Gasification

Entrained flow gasifiers represent the current state of the art technology, and it is in these designs that the most interest today is paid. Entrained flow gasifiers, like the other gasifiers, come in many versions and flavors. All these devices work in a similar fashion. One design, produced by Texaco, is shown in Figure 8.

In these gasifiers, a coal slurry or a stream of finely ground coal is passed into the gasification chamber. Drying, devolatilization, and gasification all occur very quickly as the entrained flow moves down the body of the gasifier. The largest portion of the

gasifier body is used for cooling the syngas exiting the gasifier. This cooling raises steam that can be used in a bottoming cycle, while also cooling the syngas to allow slags and other undesirable components to fall out of the flow. Other designs employ a quench cooling scheme, where the syngas is passed through a water bath to cool and remove slags. [9]

These entrained flow gasifiers have the desirable ability to be able to gasify any coal, regardless of its caking characteristics or rank. It also features very short residence times and uniform temperatures. The problems with these gasifiers involve the need to finely grind the feedstock before injection as well as higher oxidant requirements than the other designs.

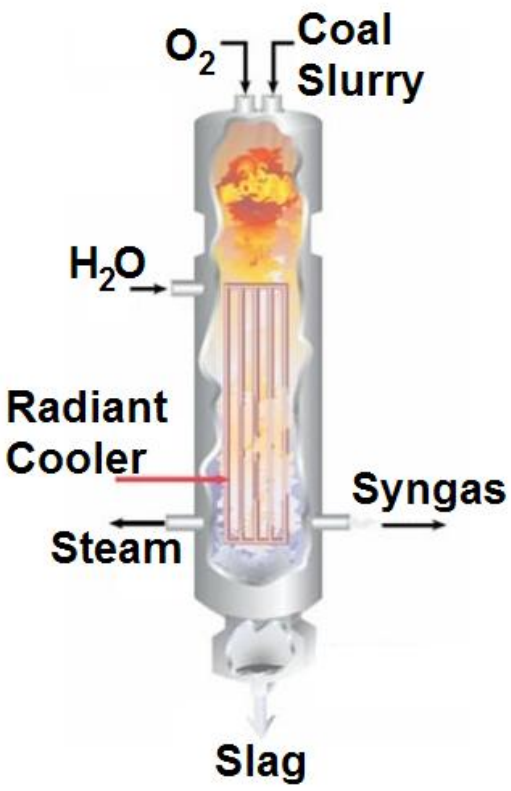

Figure 8: A Texaco entrained flow gasifier [9]

Despite these shortcomings, the entrained flow gasifier is now the gasifier of choice, with most new installations that use gasifiers employing entrained flow designs.

The Advantages of Gasification

There are many barriers to the wide adoption of gasification technology. System cost is a large issue. Gasifiers large enough to serve a few hundred megawatt power plant are massive in scale, often ten or more stories tall. The construction of a vessel able to contain pressures of 40 bar on such a scale are expensive. Few have been built on this large scale and the overall operation of the gasifiers is still not well understood, leaving the door open for possible refinements and improvements to the system.

Reliability is also an issue for these plants, since gasifiers need to be shut down more often than the normal down time for a conventional plant. Most of the proposed designs also employ an air separation unit to provide the oxygen for the gasification process and as a result, significant power must be used from the plant to power the air separation unit. Another pitfall of gasifiers is their poor response times, meaning plants using these units cannot be used for load following.

Despite these issues, gasification provides many distinct advantages over a conventional coal burner. One is the ability to burn virtually any coal, as well as other feedstocks such as solid fuels and wood. This is a significant advantage as current coal power plants are often designed for a specific coal grade. The gasification process also removes corrosive ash elements that are often found in coal, including chloride and potassium compounds, which would normally corrode the insides of components used in a traditional coal plant.

The most obvious advantage of gasification, however, is the high quality syngas that is produced by the process. This syngas can be used in a conventional combined cycle plant, which affords overall plant efficiencies greater than what can be achieved in a traditional coal plant. Gasification is also particularly well suited for carbon capture since the synthesis gas that is produced, once removed of sulfur, is nearly as clean as methane, which means carbon capture can be performed with the smallest penalty possible.

Carbon Capture Technologies

There are many power cycles and plant layouts that have been proposed to capture the carbon dioxide emissions that a normal power plant produces. All of the schemes work independent of fuel source, and many have been developed with natural gas firing in mind. All of these cycles can be used to remove carbon emissions in a clean coal power plant utilizing a gasifier.

These schemes all fall into three general categories defined by the point in the cycle that carbon dioxide is removed, as well as the way in which the fuel is combusted

in the cycle: pre-combustion, post-combustion, and oxy-combustion. Each cycle type has distinct advantages and disadvantages associated with their implementation. A general introduction to the workings of each type of cycle, as well as some proposed designs within each cycle category, is presented here to help determine the power generation designs with the most promise.

Post-Combustion Technology

Post-combustion cycles utilize current power plant designs and proven technologies with an added carbon dioxide stripping plant added to the exhaust stream of the power plant. Figure 9 shows how this technology can simply be added to the exhaust of any power cycle:

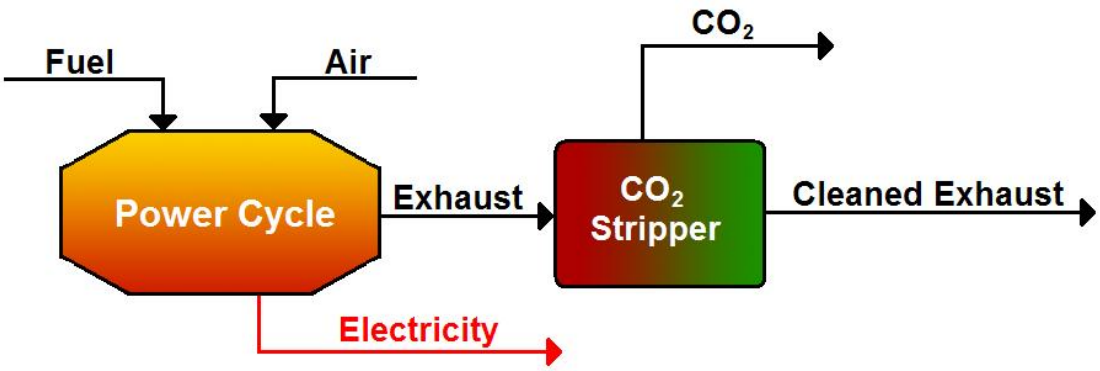

Figure 9: A post-combustion power cycle

There have been many proposals to perform the carbon dioxide stripping. One interesting possible solution involves the use of specialized membranes to separate carbon dioxide from the flue gas. At this time, however, membranes that can perform this task on an economically viable level are not available, and due to the similar size of the atoms in the exhaust gas, the production of a usable membrane that could perform better than currently available systems that employ other methods is unlikely. [10] It has been proposed that a Rectisol cycle, which uses methanol as a solvent to absorb carbon dioxide, be used, as is done for feed gas streams. This process seems ill suited for this application since it is a physical stripping method using a pressure swing. Due to the low concentration of carbon dioxide in the exhaust streams of power plants, physical

stripping means are impractical, which leaves only chemical stripping with temperature swing absorption. These stripper systems use an amine based solution to chemically bond with the carbon dioxide in the flue gas and pull it out of the exhaust stream. Multiple amines and mixtures of amines have been studied to determine the optimum solution mix, although the amine monoethanolamine (MEA) is most often employed. Figure 10 shows a typical amine plant setup, with the flue gas coming from a traditional power cycle:

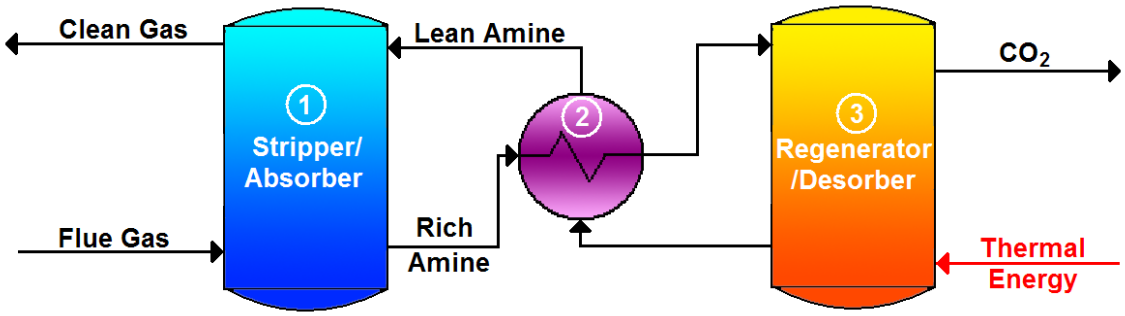

Figure 10: An amine based carbon dioxide stripper

The amine reacts with the carbon dioxide in the exhaust stream within an absorber unit to form a carbonate ion that is dissolved in the water based solution by the following exothermic chemical reaction (1):

$$2MEA + CO_2 \rightleftharpoons MEAH^+ + MEACOO^- \quad (11)$$

The carbon-dioxide-rich amine solution is then heated in a heat exchanger (2) and passed into a regenerator (3) where input heat is used to reverse the above equation and regenerate the amine solution for use once more. This lean amine solution is then passed back trough the heat exchanger (2) and into the absorber.

In a study on the efficiency penalties associated with using amine stripping techniques for post-combustion carbon removal, Desideri and Paolucci note an efficiency penalty of 11.6 percentage points when including carbon dioxide liquefaction on a coal fired plant. [11] Bolland and Undrum, in a similar analysis, find a final plant

efficiency of 49.6%, representing an 8.4 percentage point penalty.[12] It should be noted that the Bolland study assumes a natural gas fired plant, and Desideri and Paolucci note that a methane fired plant would see efficiency pentalties 3-4 percentage points lower than those for coal based plants.[11] This extra efficiency drop is due to gas cleanup which must be performed on coal flue gases to remove sulfur components before carbon dioxide stripping can be performed. This must be included because the amine solutions are very susceptible to poisoning, and sulfur in the exhaust stream will react with the amine and block its regeneration. These studies together place the total efficiency hit for post-combustion plants in the 11 percentage point range for coal.

The single largest advantage of the post-combustion technologies is their current availability as 'off the shelf' components. The power cycles, with only minor modifications, can be used in their current designs. The amine stripping units are also commercially available now for immediate construction,[11] although Bolland et al note that the technology has not been sufficiently proven for large scale applications.[12]

Despite its immediate availability, this technology is in no ways a 'slam dunk' answer to the carbon removal problem. The high heat requirements for the amine regeneration, which are higher still for MEA based amines, represents a large and non-trivial loss to the overall energy output of the plant. Simply adding this unit to all current power cycles would reduce their total energy output by approximately 30%, requiring the construction of more plants and drastically increasing the price of electricity. The amine separation equipment also involves a large capital cost, and estimates place the price of electricity after such an upgrade at more than double its current price.[11] Another problem lies in the efficiency of the separation process itself, as it is only capable of removing at most 90% of the carbon dioxide from the plant exhaust. Extra care must also be taken with respect to the amine solution used, as the amines in the separator are corrosive and reactive, requiring a dilute solution to avoid damage to internal piping. And as noted previously, the amines also require gas cleanup before the stripper to remove SO_x and NO_x emissions (or the more expensive solution of

simple amine solution replacement), as these other pollutants bind with the amine and prevent its regeneration. [11]

Pre-Combustion Technology

Cycles in the pre-combustion category involve designs that remove the carbon atoms from the fuel source as carbon dioxide before the fuel is combusted in the presence of oxygen in a burner. Figure 11 shows the typical layout for a pre-combustion carbon removal power plant:

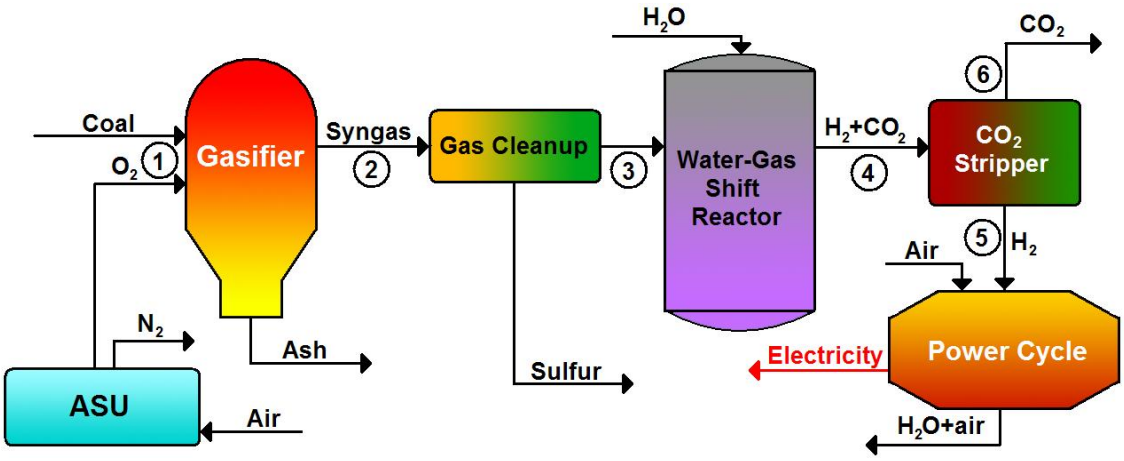

Figure 11: A Coal fired pre-combustion capture power cycle

These plants employ methane reformers or gasifiers (1) to produce a stream of syngas, composed of carbon dioxide, carbon monoxide, and hydrogen (2). This stream is cleaned (3) and mixed with water and passed through a shift reactor which turns the carbon monoxide and water in the stream into carbon dioxide and hydrogen (4). In this way, it operates similarly to current IGCC power cycle designs. Before this final mixture of carbon dioxide and hydrogen is passed into a burner, however, a separator is employed. The nearly pure hydrogen stream is burned in a normal combined cycle plant (5) while the carbon dioxide is passed to a plant for liquefaction and storage (6).

The water-gas shift reactor works via the following chemical equation:

$$CO + H_2O_{(g)} \rightarrow CO_2 + H_2$$

This reaction is exothermic and results in $\Delta_r H$=-41.16 kJ/Mol. This reaction requires temperatures in excess of 900°C in order for the pace of the reaction to be sufficiently fast. [10] They also require excess water to be included in the reactor vessel to ensure full CO conversion. In practice, reactors typically use multiple stages at different temperatures to reduce size and energy utilization while increasing conversion efficiency. These reactors, known as the 'Catalytic clean gas CO shift conversion', can produce over 99% maximum CO conversion in two stages: high temperature conversion and low temperature conversion.

High temperature CO shift conversion works in operating temperatures between 300°C and 530°C. [10] Using Ni/Cr-oxide or Fe/Cr-oxide as the reaction catalyst, these reactors have an advantage of rapid conversion with a minimal size but suffer from incomplete conversion.

Low temperature CO shift conversion operates with temperatures between 180°C to 270°C and employ a Cu/Zn-oxide based catalyst. This reactor operates slower and with a larger volume; its chief purpose is to fully convert the remaining CO which passed through the high temperature stage.

These reactors are a middle-aged technology usually employed to turn methane into hydrogen fuel. They suffer, however, from a sensitivity to impurities, and as a result sulfur cleanup must be employed prior to this stage for plants fired by coal. The gas cleanup employed most often today is known as 'Wet Scrubbing' and is a physical separation scheme using a pressure swing. The process involves mixing the sulfur-rich syngas, known as a 'sour' syngas, with an alkaline based slurry in a turbulent environment. The most common slurry uses limestone ($CaCO_3$). Its interaction with sour gas produces the following reaction:

$$CaCO_{3\,(s)} + SO_{2\,(g)} \rightarrow CaSO_{3\,(s)} + CO_{2\,(g)}$$

In this way, the sulfur is removed from the stream as a solid (calcium sulphite). The sulfur rich slurry is then passed to a regeneration unit where a pressure swing liberates

the sulfur, where it is removed as a solid. The treated syngas, now known as a 'sweet' sygnas, is passed on to the shift reactor. In practice, these systems can reach sulfer removal efficiencies of greater than 90%. [10] These systems are also a middle-aged technology, having been heavily developed in the late 1960s and early 1970s to combat a growing acid rain problem.

This gas cleanup presents a problem, however, because it must be done at low temperatures. As the temperature of the gas inside the scrubber increases, sulfur dioxide oxidizes further to form sulfur trioxide, which cannot be removed by a lime-based slurry. This fact requires the hot sour syngas leaving the gasifier to be cooled substantially before entering the desulfurization unit. The gas must then be reheated after sulfur removal for entry into the high temperature CO shift reactor. [10]

This cool and reheat results in an energy penalty that negatively affects the overall efficiency of the entire plant and is a direct result of two technologies being used for a purpose they were not originally intended for. To combat these losses, two possible solutions have been discussed. The first is known as 'hot gas cleanup' and involves performing the desulfurization at an elevated temperature to reduce or eliminate the cooling and reheating currently required. Although test plants of this type have been constructed and successfully tested, they suffer in the removal efficiencies. In addition, none has been scaled and tested on a large power plant producing in excess of 100MW. Although promising, hot scrubbing technology is not efficient enough to prevent the poisoning of the catalysts in the shift reactor at this point.

Another potential solution would simply swap the places of the desulfurization unit and the shift reactor in the plant layout. Such a swap would allow the gas to be cooled in the shift reactor and again in the sulfur cleanup unit to raise steam for a Rankine bottoming cycle. The cooled sweet syngas could then be directly fed into a combustor in a power cycle. Such a swap would require a shift reactor with catalysts that are immune to sulfur and other impurities. Such systems employ a CoMo/Al-oxide based catalyst and operate between 230°C and 500°C. Shift reactors of this design fail to reach conversion efficiencies greater than 90% [10] and the energy saved by using this

method is more than outweighed by the energy lost in CO that is passed into the rejected CO_2 stream in the CO_2 separator.

The carbon dioxide separation unit is responsible for the remaining efficiency loss. Bolland and Undrum propose in their analysis of a pre-combustion system the inclusion of a carbon dioxide scrubber attached to the exhaust of the shift reactor. [12] Some designs incorporate a scrubber that utilizes stripping chemicals that bind with the carbon dioxide in the gas flow and pull it out of the mixture. This CO_2-rich chemical is then passed to a regeneration unit which, after significant heat input, releases the carbon dioxide into a second stream. Now clean, the chemical can be reused to strip more carbon dioxide from the shift reactor exit flow. These devices work in a near identical fashion to the temperature swing strippers used in post-combustion capture.

Other designs have been proposed which take advantage of the high CO_2 concentrations in the syngas stream by utilizing a pressure swing reactor to remove the carbon dioxide. One popular proposal employs a methanol based solution to physically absorb carbon dioxide, as well as other pollutants like hydrogen sulfide. The rich methanol solution is passed to another reaction vessel at a lower pressure, where the pollutants are released from the methanol. One implementation of this cycle is known as the Rectisol cycle, which operates at -40°C and 40 bar in the absorber vessel. Although used in industrial applications to clean feed gases, the extensive refrigeration required for this design is expensive.

Another proprietary physical stripping method uses the solvent Selexol to strip out the carbon dioxide. This solvent operates in a very similar fashion to Rectisol and has all the same disadvantages, but is also more expensive compared to the Rectisol solution.

Although the technology for these stripping operations exist, their integration into an IGCC flowpath is in no way a mature technology and more research and testing would need to be focused in this area. [12] The power requirements for this unit also present a significant problem, as the function of percentage of carbon dioxide removed versus work required is exponential in nature. As a result, these plants do not

completely capture their carbon emissions, releasing on average 10% of the produced carbon dioxide into the exhaust gases. [12]

An alternative to the chemical or physical stripping techniques proposed involves using membrane technology to separate the large carbon dioxide molecules from the much smaller hydrogen molecules. The work loss in this method comes in the form of a pressure loss across the membrane surface. This method also suffers from an exponential function relating carbon removal percentage to power requirements. This technology is in its infant stage and it is unclear whether membranes will become technologically possible or economically viable as an alternative to chemical stripping methods. [13]

An analysis of a pre-combustion power cycle by Bolland and Undrum produced a final theoretical plant efficiency, including carbon dioxide liquefaction for sequestration, of 45.3% when using methane as the fuel with a reformer. [12] This value compares with a theoretical efficiency of 58% for a combined cycle running on a methane fuel source, representing a 12.7% efficiency point drop. [12] One cause of the efficiency drop for this style plant comes from the air separation unit that is required to produce the pure oxygen stream needed in the methane reformer (or gasifier if the plant was coal fired). It is safe to assume that a coal based plant would run with efficiencies lower than this due to the efficiency losses related to coal cleanup discussed above. [11]

This cycle presents other difficulties outside of the carbon dioxide separator. The burning of the hydrogen based fuel in the combined cycle may require minor alterations to current gas turbine designs. [12] Despite the myriad technical hurdles that need to be overcome, the pre-combustion cycle is heavily discussed and has had significant investment put into its development. Indeed, the DOE FutureGen project is based on a pre-combustion capture design that utilizes a gasifier to allow coal as the primary fuel, and is scheduled to come online in 2012. [14]

Oxy-Fuel Combustion Technology

Oxy-fuel combustors utilize an air separation unit (ASU) to burn a fuel stoichiometrically in pure oxygen, leaving only carbon dioxide and water as the

combustion products, which can be easily separated by condensing out water into its liquid phase. This process results in capture rates of 99%, with the only release being the carbon dioxide that is dissolved in the rejected water. The cycles are all relatively new designs, with their flowpaths being designed from scratch with the demands of the future energy market, including coal firing and carbon capture, in mind. When combined with a power cycle utilizing a gasifier, which also requires an air separation unit for most designs, the added capital costs for the air separation unit can be offset by combining the unit with the one required for the gasifier and integrating the two systems. Within the oxy-combustion world, there have been many proposed plant layouts that must be considered and studied independently.

The Oxy-Fuel Combined Cycle and the CC-Matiant Cycle

The oxy-fuel combined cycle is the simplest of the oxy-fuel cycles. The cycle is similar in layout to a traditional combined cycle plant, with the important difference being that the combustor burns the input fuel (either a syngas or natural gas) in an oxygen rich environment. To control combustion temperatures, a portion of the exhaust stream is recirculated into the combustor. Multiple studies, including one by Bolland and Mathieu, place the efficiency of this cycle in the 43%-47% range with 99% carbon capture. [15] [16] It is important to note that this efficiency is related to the higher heating value (HHV) of syngas fed into the combustor and does not account for efficiency losses originating in the gasifier.

A plant similar to the oxy-fuel combined cycle is known as the CC-Matiant cycle. This cycle is identical to the oxy-fuel combined cycle, except that a recuperator is used on the turbine exhaust before the heat recovery steam generator (HRSG) to warm the gases entering the combustor. [17] Figure 12 presents this cycle layout (note that an oxy-fuel combined cycle has an identical layout if the recuperator step (3) is removed from the flowpath):

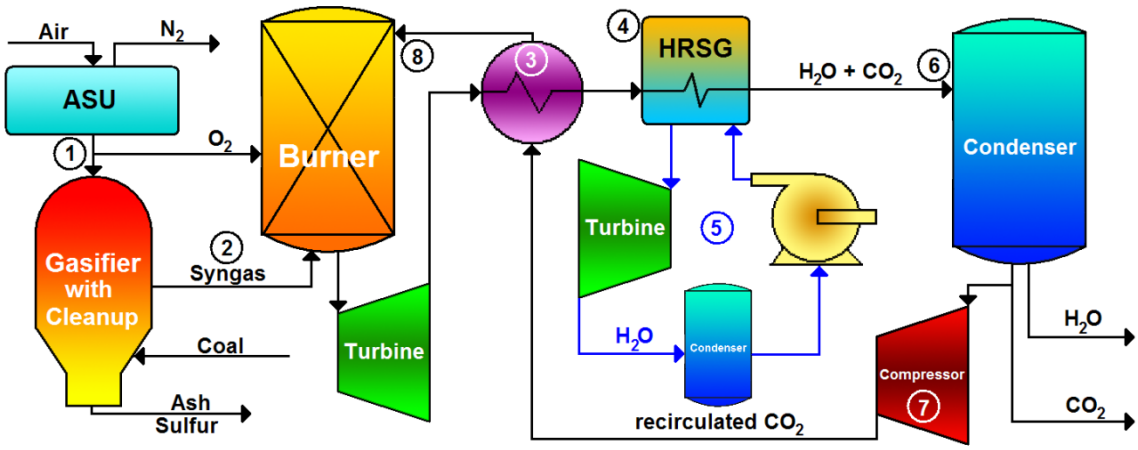

Figure 12: The CC-Matient cycle

An air separation unit is used to inject oxygen into the burner and gasifier (1). The gasifier turns coal into a syngas and the syngas is passed through cleaup before being injected into the burner (2). After combustion, the products pass through a heat exchanger (3) and then a heat recovery steam generator (4). The steam produced from the HRSG is used to run a rankine steam cycle (5). The cooled exhaust from the HRSG, consisting of only water and carbon dioxide, passes into a condenser (6) where the water is condensed and separated. A portion of the carbon dioxide is then compressed (7), fed through the heat exchanger (3) and injected into the burner (8).

The idea behind the addition of a recuperator in the CC-Matiant cycle is to lower the temperature differences in both the steam generator and the combustor to reduce entropy generation in the cycle. In a study of the cycle, Houyou, Mathieu, and Nihart estimate the efficiency of this cycle at 47-49%. [18] Again, this efficiency does not account for losses in the gasification of coal but is based upon the high heating value of the syngas burned. The recuperator that the CC-Matient cycle proposes has been criticized. It has been suggested that when parasitic losses, including pressure losses of ducting and valves, are taken into account, the recuperator contributes little with respect to overall plant efficiency, and the capital expenditure for the recuperator unit is not economically justified. [17]

Both cycles suffer from technological limitations. Because of the air separation unit, the working fluid in the turbines is a mixture of carbon dioxide and water, and no

nitrogen is present. Current gas turbine technology is designed around streams with nitrogen based working fluids. The necessary changes that would need to be made to current turbine technology would not be minor, with changes in the blade shape, flow area, number of stages, and possible alloy changes necessary to produce a working carbon dioxide-based turbine.[10] Indeed, this would not be a modification of current technology, but an entirely fresh design. In a DOE report produced in February 2004, the current status of carbon dioxide turbomachine technology was summed up by a statement claiming that no gas turbines of this type are available or under serious development.[10] Bolland, in his analysis of oxy-fuel combined cycles, agrees, stating that although a large company could possibly create the needed technology in a five to ten year time span, the technology right now does not exist and will not for the foreseeable future.[12]

Possible headway on the issue may be made with the help of the nuclear power industry. Researchers are hoping to start using supercritical carbon dioxide to cool nuclear reactors, as opposed to water, which is the current choice. Supercritical carbon dioxide allows smaller (by orders of magnitude) turbomachinery, leading to a more compact and less complex plant layout. Fourteen British nuclear facilities currently operate with carbon dioxide as the cooling medium, although these plants utilize the gas at moderate (650°C) temperatures.

Despite this help from the nuclear industry, severe problems still remain. One large problem is that supercritical carbon dioxide at high temperatures may react and attack the turbomachinery itself. As a result, special materials may be needed to prevent the deterioration of the turbine blades. The nuclear application is also run as a closed cycle, which means they can guarantee a very pure carbon dioxide stream. Turbines for oxy-fuel use, however, will have a water component in the stream greater than 10% by molar mass flow, and the semi-open nature of the cycles will result in other gases and components, including sulfur dioxide, sulfer hydroxide, and methane, among others, being present in the gas flow. The turbine will have to be able to handle the other constituents and be forgiving to the molar fractions of each. Even with these

problems, designs have been proposed for high temperature carbon dioxide-based gas turbines for use in oxy-fuel cycles, but none have been built or tested. [19]

Another potential problem that has been brought forth in these cycles lies in the condenser, which separates the water from the carbon dioxide in the exhaust stream. As the water liquefies in the condenser, carbon dioxide, which is readily dissolvable in water at high pressures, will dissolve into the water and form carbonic acid under the following reaction:

$$CO_2 + H_2O \rightleftharpoons H_2CO_3$$

This acid could potentially corrode the condenser walls and require expensive replacement. [17] At 1 bar, approximately 1% of the carbon dioxide in the exhaust flow will be dissolved in the water. [17] Of this percentage that is dissolved, only a fraction will turn into carbonic acid and pose any threat. Indeed, the equilibrium constant and rate constant at room temperature are 1.7×10^{-3} and $0.039\ s^{-1}$ respectively, suggesting that roughly 0.2% of the carbon dioxide dissolved in the water will turn into acid, and the water will most likely leave the condenser before the equilibrium is ever reached. [10] As a result, only 2×10^{-5} % of the original carbon dioxide in the exhaust path will turn to carbonic acid in the worst case scenario. Despite this seemingly small number, the pH of such a solution can be calculated to be on the order of 4.5, suggesting a moderately acidic outlet solution. This pH value is out of bounds of specs on most common condenser units, and a condenser for this application would likely need a coating of a special alloy to protect against deterioration.

Once this acidic water solution leaves the plant and encounters open air, where the carbon dioxide partial pressure is much lower than in the condenser unit, most of the carbon dioxide dissolved in solution will leave into the atmosphere, leaving a water solution that is nearly acid free. It is this carbon dioxide escape that accounts for the only carbon dioxide emissions of the entire plant.

The Water Cycle

The water cycle is a more advanced oxy-fuel combustion cycle that utilizes reheat and a recuperator in a Rankine-like power cycle that features water recirculation. Figure 13 shows the cycle layout:

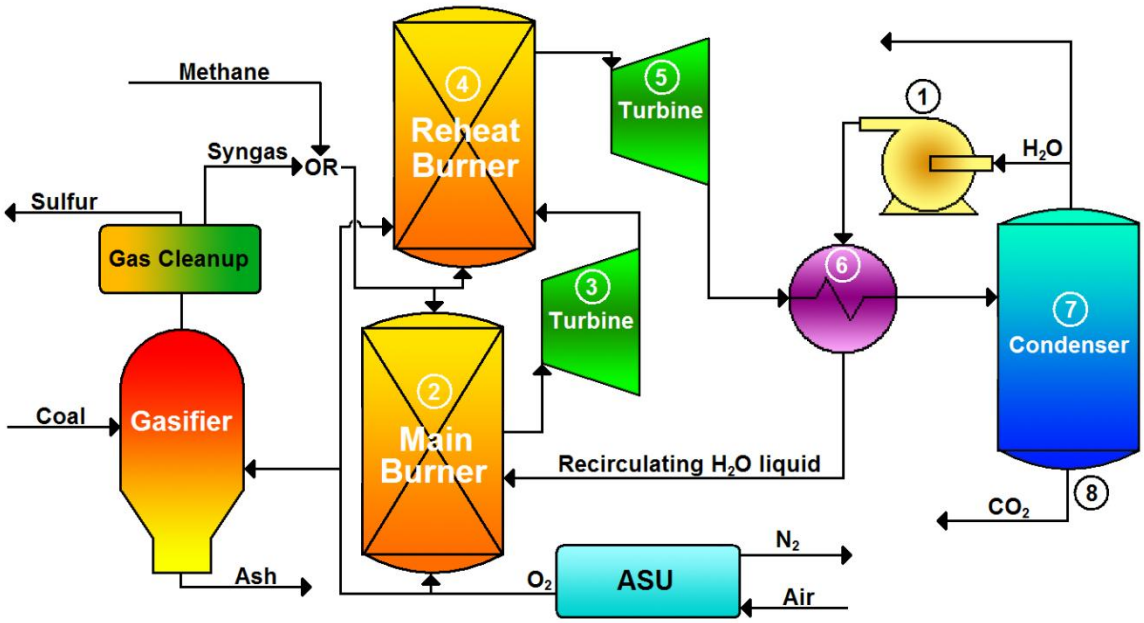

Figure 13: The water cycle

The attractiveness of this design is that the working fluid, which is mostly water, is compressed to its highest pressure of 83 bar in the liquid phase (1), vastly reducing the energy requirements for compression.[16] In the combustor at 83 bar, the liquid water is flashed into steam and heated to 1173 K through the combustion process (2) and expanded to 8.3 bar in a high pressure steam turbine (3). The water is then passed through a reheating combustor where it is heated to an exhaust temperature on the order of 1573 K (4). After expansion to 0.1 bar (5), the stream is passed through a recuperator (6), condensed (7), and carbon dioxide is removed (8). Some of the water is also removed before it is pumped to 83 bar (1), sent through the recuperator (6), and fed into the combustor.[16] The entire cycle is fed with a gasifier running on coal that cleans the syngas of sulfur before injection into the burner. Like all oxy-fuel designs,

combustion is done stoichiometrically with only oxygen, so an air separation unit is required to provide the oxygen to the burners and the gasifier.

Analysis on this type of power cycle has produced estimated efficiencies in the lower 40% range, including carbon dioxide liquefaction. [17] Again, it is important to note that these efficiencies do not account for losses in coal gasification. Bolland, Kvamsdal, and Boden, in their analysis of the water cycle, note that the overall efficiency of the plant is highly sensitive to the outlet pressure of the first combustor, claiming 0.7-1.3 percentage point efficiency gains for each 100 degrees K the temperature is raised. [17] By their calculations, a high pressure of 200 bar with an exit temperature from the combustor of 1673 K would produce a total plant efficiency of 53%. [17]

This leads directly into the largest problem with the water cycle. The cycle is designed to use water as a working fluid in order to take advantage of steam turbines, which are a mature technology. Unfortunately, the best steam turbines cannot handle the high pressures and temperatures needed to push the efficiency values beyond those of simple post-combustion technology. It is suggested that steam turbine technology can perhaps be mixed with high pressure and temperature gas turbine technology to produce a working prototype plant capable of 50% efficiencies, but it is recognized that current technology places the plant at the 40% efficiency level. Much work and research would have to be done to reach a level where the plant can reach higher efficiency. [16] Such technologies would take many years to develop and the investment would most likely not be sound, considering the alternative carbon capture technologies have development times promised to be some years less. [17]

The Matiant Cycle

The matiant cycle makes use of a regenerative Brayton-like cycle with a supercritical CO_2 Rankine-like cycle with carbon dioxide recirculation. Its layout is similar to that of the water cycle, with some exceptions being that carbon dioxide is the working fluid being recirculated, and the pressures and temperatures at each stage are different. Figure 14 shows the cycle layout:

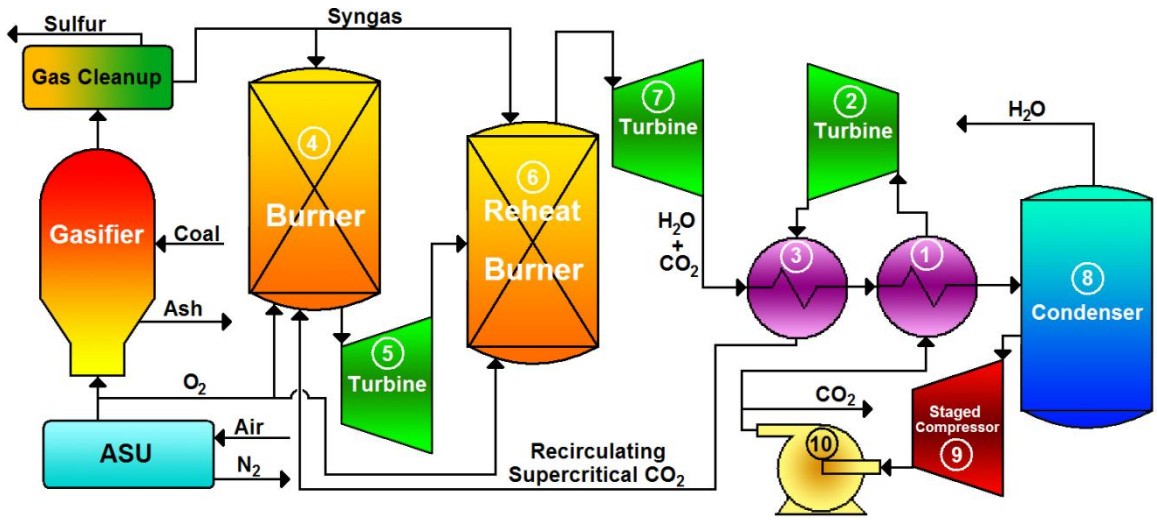

Figure 14: The Matiant cycle

Supercritical CO_2 at 300 bar is heated in a recuperator (1) before being expanded in a gas turbine to 40 bar (2). After this stage, the gas is heated again through a second recuperator (3) before being burned in a high pressure combustor at 40 bar to 1573 K (4). After passing through a gas turbine and being dropped to 9.3 bar (5), the gas is reheated in a reheat combustor to a temperature of 973 K (6). The fluid expands through a second turbine to 1 bar (7) before losing more energy to the recuperator that heats the supercritical CO_2 (1 and 2). After this stage, water is condensed (8) and removed before the carbon dioxide is compressed in an intercooled compressor to 70.5 bar and liquefied at 302 K (9). After excess carbon dioxide is removed, the liquefied CO_2 is then pumped (10) to 300 bar and passed into the recuperator (1).

The attractiveness of this cycle is that the carbon dioxide can be pumped in its liquid phase to 300 bar, saving compression work. Analysis of this cycle by Mathieu and Nihart finds efficiencies between 44-45%. [20] This efficiency figure does not take into account losses associated with the gasification of coal.

The Matiant cycle faces the most daunting technological challenges of all the proposed oxy-fuel cycles. Although it faces the same technological hurdles as the oxy-fuel combined cycle plants with respect to CO_2 based gas turbines, the Matiant cycle has an additional hurdle in the production of a supercritical CO_2 turbine that can expand the fluid from a high pressure of 300 bar and a temperature of 873 K. The cycle architects

suggest that such a turbine could be adapted from current steam based turbines in UltraSuperCritical Rankine type cycles within a 2-3 year timeframe, [20] but it seems that this prediction is overly optimistic. At the very least, this cycle design requires the invention of more new technologies than many other proposed layouts.

Another problem associated with this cycle scheme is the requirement of large amounts of internal heat exchange between hot streams. In particular, the exhaust stream that is cooled enters the heat exchange equipment at 1 bar and 1200 K, which implies problems for the heat exchanger technology. [17] It is highly likely that cooling would be needed to control the temperature of the heat exchange equipment, which would introduce additional efficiency penalties beyond what is currently considered. The size and capital costs of these heat exchangers could also prove problematic. Here again, as with the carbon dioxide based turbines, the nuclear industry is of help. The cycle designs being considered in the nuclear industry include the use of supercritical carbon dioxide heat exchangers of the type necessary for use in these cycles as well. Some proposed designs in the nuclear field include the use of printed circuit heat exchangers instead of shell and tube style heat exchangers. The printed circuit version allows a large reduction in size and capital expenditure for the same heat exchanger effectiveness.

In addition, analysis on this plant design by Bolland et al has shown that it is highly sensitive to parasitic losses and an actual working model of the plant may produce far lower efficiency values than calculated due to unforeseen losses. [17] It is noted that the intercooled compressor is of extreme importance to the cycle, and a drop in isentropic efficiency of 10% for the compressor stack results in a 5% drop in efficiency for the entire plant, and it is openly questioned whether the 90% isentropic efficiency value assumed by the cycle architects is too high. [20]

The E-Matiant Cycle

A cycle based upon the Matiant cycle attempts to address many of the issues with the matiant cycle itself. The E-matiant cycle is a fully Brayton type cycle that removes the high pressure expander and eliminates the reheat combustor. The carbon

dioxide in this cycle stays entirely in the gaseous phase and is totally compressed through an intercooled compressor stack. The maximum pressure in this cycle is reduced to 110 bar. Figure 15 shows the cycle layout:

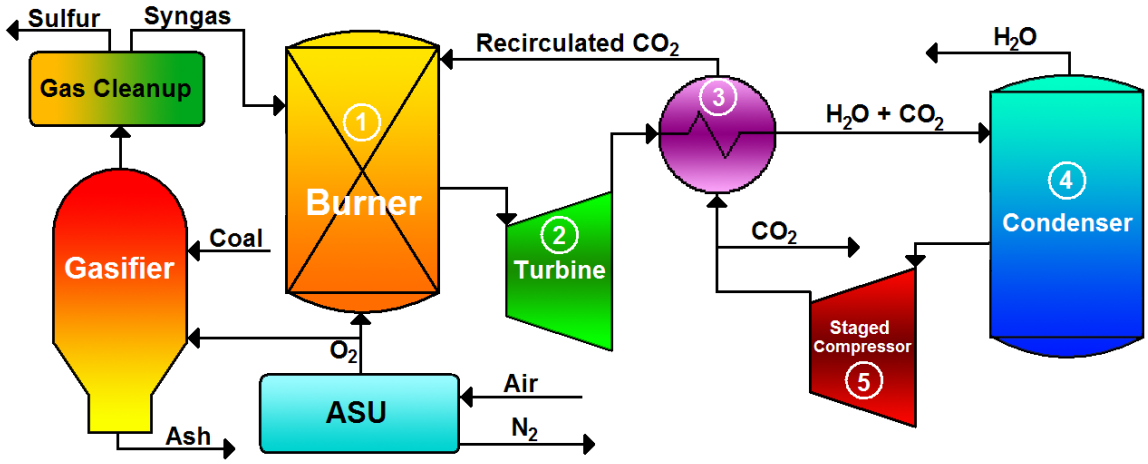

Figure 15: The E-Matiant cycle

A cleaned syngas from a gasifier enters the burner (1) and combusts. The exhaust gas, consisting of only carbon dioxide and water, is passed through a turbine (2) and then a recuperator (3) before passing into a condensor (4). The carbon dioxide is compressed in a staged intercooled compressor (5) before a portion is heated in the recuperator (3). This gas is then fed back into the burner to control combustion temperatures (1).

Cycle analysis by Houyou, Mathieu, and Nihart places the cycle efficiency in the 47% range. [18] This efficiency value does not include losses associated with the coal gasifier. The major draw to this design is that it eliminates the high pressure and temperature supercritical CO_2 turbine that would have had to have been developed for the Matiant cycle. It makes the production of a CO_2 gas turbine more difficult, however, by pushing its high pressure from 40 bar at the combustor outlet to 110 bar. There is also trouble with producing a combustor and associated equipment that can operate at 110 bar. In addition, the cycle still contains large amounts of internal heat exchange equipment and its overall efficiency is still highly dependent upon the isentropic efficiency of the intercooled compressor stack, which was again assumed to be 90%. [18]

Like the traditional Matiant design, it is doubtful that an actual plant utilizing this cycle would come close to the theoretical efficiency values claimed here.

The Graz Cycle

The Graz cycle is another innovative oxy-fuel combustion method that is essentially a high temperature Brayton cycle combined with a low temperature Rankine cycle. [21] Figure 16 shows the plant layout:

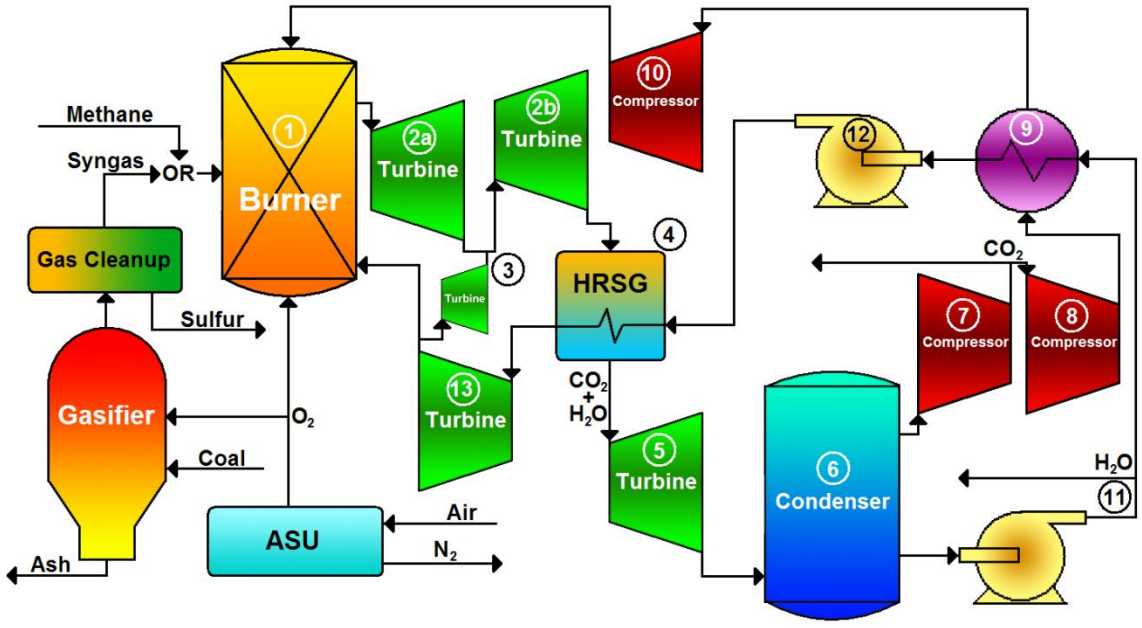

Figure 16: The Graz cycle

The cycle utilizes recirculation of both water and carbon dioxide from the exhaust stream into the combustor to control flame temperatures and produce a humid carbon dioxide working fluid. The combustor operates at 40 bar and increases the exhaust to 1623 K (1). After the burner, the gas is expanded to 10 bar (2a) before more recirculated water is added to the stream (3). The fluid is then expanded to 1 bar (2b) before passing through a boiler where it loses heat to a water stream (4). After this point, the gas is expanded once more to .25 bar (5) where it passes through a condenser to separate the carbon dioxide and water (6). After this separation, the carbon dioxide is compressed to 1 bar and excess CO_2 is removed for later liquefaction and storage (7).

The remaining CO_2 is compressed to 2.7 bar (8) before passing through a heat exchanger where it gives up heat (9). It is then finally compressed to 40 bar and fed back into the burner (10). The water from the condenser is pumped to 5 bar before excess water is removed (11). The remaining water is heated in the heat exchanger (9) before being pumped to a high pressure of 180 bar (12). The water is then sent through the boiler where it is turned to gas and heated to 840 K (4). The stream is passed through a high pressure steam turbine and dropped to a pressure of 40 bar before being inserted into the burner (13).

Analysis of the cycle by Heitmeir, Sanz, Göttlich, and Jericha in one paper and Bolland et al in another places the cycle efficiency, including CO_2 liquefaction, in the 50-52% range. [17] [21] This cycle efficiency does not include the efficiency penalty associated with the gasification of coal.

The use of gas turbines in this cycle based on a CO_2 dominated working fluid presents the same problems that the oxy-fuel combined cycle and Matiant cycle face with respect to CO_2 gas turbine production. The cycle is also rather complex, and it is unclear whether the capital costs for a plant of this complexity would make it economically viable. In addition, this plant fails to incorporate a liquefaction plant for the CO_2, something the Matiant cycle does, and also fails to integrate with the gasifier used to produce syngas from a coal, a problem that all these cycles face.

The high pressure steam turbine, asked to bring steam from 180 bar and 560°C to 40 bar, is also of concern. These entry requirements are higher than what off-the-shelf steam turbine technology is able to offer.

A Comprehensive Study of the Graz Cycle

The choice of the Graz cycle

Despite its problems, the Graz cycle represents the most promising of all proposed oxy-fuel carbon capture technologies. Although the theoretical efficiency for the Graz cycle is high, this alone is not what sets it apart from the other designs. Indeed, all of these designs exist only within simulation programs and complex models,

and as such the calculated efficiency numbers will not be accurate when compared to what a plant would produce in the real world. Most of these plants claim efficiencies within 10 percentage points of one another, and as such theoretical efficiency alone would not be a proper metric to determine the most promising cycle design.

The Graz cycle's other advantages lie in its feasibility. The difficulties faced by the Graz cycle in producing a high pressure steam turbine prove easier to solve than the same problems faced by the water cycle. Despite requiring very high pressures, like the water cycle, the input temperature in the Graz cycle, although high, is hundreds of degrees lower than that of the water cycle. With the advent of super-critical rankine cycles that utilize steam turbines operating at higher temperatures and pressures, there is promise that a turbine usable in the Graz cycle may be available faster than a comparable turbine for the water cycle.

The Matiant cycle requires the development of a supercritical CO_2 turbine based on current steam turbine designs. Although this technology may be feasible, it has no other applications to other cycles and therefore carries significant risk for investment. This is especially true if one accepts the arguments of Bolland et al that the cycle is highly sensitive to both parasitic losses and changes in the compressor isentropic efficiency from the assumed value. The E-Matiant cycle suffers from these same vulnerabilities.

The remaining technical challenges, including the development of carbon dioxide based turbines and acidic water in the condenser, are not unique to the Graz cycle, and all the other oxy-fuel cycles require the same technological innovation and investment that would be required for the Graz cycle in these areas. The Graz cycle has the most promise since it offers the highest efficiencies among these cycles. The advantage of focusing on producing the Graz cycle is that should the cycle prove unrealistic in the real world, the technology invested in its development can be used elsewhere in other oxy-fuel designs.

When comparing the Graz cycle to pre- and post-combustion designs, other factors must be considered. If near total CO_2 capture is desired, it is clear that only the

oxy-fuel combustion technologies are viable, since both pre-combustion and post-combustion cycles offer only 90% carbon capture at theoretical efficiencies at or below what is claimed by the oxy-fuel combustion cycles. Post-combustion capture technology also represents a 'band-aid' measure that does not integrate the carbon removal process in the overall cycle. This lack of integration causes inefficiencies and possible points of entropy generation due to this decoupling. As a result, traditional cycles employing post-combustion capture will never be able to approach the efficiency levels of an oxy-fuel or pre-combustion cycle, which make it unattractive as a design for new power generation plants.

Pre-combustion technology offers significant promise in its ability to produce cheap power with carbon capture. With the DOE soon to put out bids on its FutureGen project, a test plant in the Unites States based on this technology is not far off. These cycles have the advantage of using existing technology and layouts, emulating integrated combined cycle (IGCC) plants in many ways. As a result, they are very desirable from a risk standpoint, since there are parallels that can be drawn between the theoretical operation of these plants and the actual operation of IGCC plants worldwide.

Yet the Graz cycle represents a radical idea and a complete rethinking of the power cycle with carbon capture in mind. If computer based models prove to be accurate, the cycle will operate with very high efficiencies with virtually no pollutant release, including carbon dioxide. Investment in the Graz cycle represents a higher risk, since no plants of this type have ever been built and their operation is not well understood. But with significant funding going into the pre-combustion capture sector, it is wise to focus some resources on unconventional designs that, despite the risk, offer the possibility of substantial payoff and reward in the future.

The Graz cycle is analyzed in detail here in an effort to start this process and help ensure that human investment in a world free of carbon dioxide emissions is diversified.

Building a Cycle Model

The analysis of the Graz cycle in this paper is based upon a model developed specifically for the Graz cycle itself. Published documents from the developers of the Graz cycle and other researchers working with the cycle were used to validate this model, which was then used as a basis of further cycle analysis and optimization.

The model was developed using Microsoft Excel 2007 as a graphical frontend. Visual Basic scripts were written to interface with Excel and perform the necessary calculations. The scripts also interfaced with the National Institute of Standards and Technology Standard Reference Database 23: Reference Fluid Thermodynamic and Transport Properties Database Version 7 (NIST REFPROP 7), which provided the thermodynamic data for water, carbon dioxide, oxygen, carbon monoxide, and hydrogen. This database was used to calculate specific state variables, including enthalpy, entropy, pressure, and temperature, of the working fluids in the cycle as a function of any two of the other state variables. The NIST REFPROP 7 database was also used to calculate state variables of mixtures of fluids, most notably the mixture of carbon dioxide and water in the exhaust stream of the Graz cycle burner. The value of an overall specific property for a mixture, such as its specific heat or specific enthalpy, was determined by multiplying the specific property of each individual constituent in the mixture by that constituent's molar fraction, and then adding the results:

$$\psi = \psi_1 \chi_1 + \psi_2 \chi_2 + \cdots$$

where ψ is the specific property of the mixture and ψ_n and χ_n are the specific property and molar fraction of specie n. The database was also used to calculate various transport properties, including specific heat capacity of mixtures and streams.

Turbomachines were modeled in the system using a standard process: the enthalpy change for an isentropic process was found, and this enthalpy change was multiplied by a component efficiency, η:

$$\Delta H = \eta(\Delta H_{isentropic})$$

With this new enthalpy change for the turbomachine, a true output temperature for the working fluid was calculated using its mass flow rate, $\dot{m}$, and its specific heat capacity, c_p:

$$\Delta T = \frac{\Delta H}{(\dot{m}c_p)_{working\ fluid}}$$

Heat exchangers were modeled using the heat exchanger effectiveness, ε, to find the heat load, Q:

$$Q = (\varepsilon)(C_{min})(Thot_{in} - Tcold_{in})$$

where C_{min} is defined as the smaller heat capacity of the hot and cold streams, and $Thot_{in}$ and $Tcold_{in}$ are defined as the inlet temperature for the hot and cold stream, respectively. The model then uses the heat load, the mass flow rates of the hot and cold streams, and the heat capacities of the hot and cold streams to determine the hot and cold stream exit temperatures, $Thot_{out}$ and $Tcold_{out}$:

$$Thot_{out} = Thot_{in} - \frac{Q}{\dot{m}_{hot}c_{p-hot}}$$

$$Tcold_{out} = Tcold_{in} + \frac{Q}{\dot{m}_{cold}c_{p-cold}}$$

In defining the cycle, this model assumed 23 independent variables that fully defined the system. Table 1 enumerates these variables, along with values used for this analysis, derived from a study of the Graz cycle performed by Jericha and Goettlich. [22] All the pressure and temperature values were taken directly from the Jericha paper,

while efficiency, effectiveness, and recycle percentage values were calculated using first order means from the published input and output states. Figure 17 shows the location of these state variables on the Graz cycle flowchart.

Table 1: Independent variables used in model

Variable	Description	Value	Unit
P_{high}	System high pressure in the combustor	40	bar
T_{high}	Output Temperature of the combustor	1312	°C
P_{inject}	Pressure at which water is injected into exhaust	10	bar
$H2O_{in}$	Molar mass flow of water injected into exhaust	0.27	mol/s
P_{mid}	Pressure of the exhaust stream in the boiler	1	bar
P_{low}	Low pressure of the system in the condenser	0.25	bar
T_{boiler}	Water output temperature from the boiler	567.7	°C
$P_{CO2heater}$	Pressure of CO_2 in the feed water heater	2.7	bar
$P_{H2Oheater}$	Pressure of H_2O in the feed water heater	5	bar
P_{H2Omax}	Maximum pressure of H_2O in the boiler	180	bar
$CO2_{recycle}$	Percentage of CO_2 recycled back to burner	78.9	%
C3-entry-T	Temperature of CO_2 at entry to third compressor	25	°C
η_{HTTw}	Efficiency of the injected water turbine	89.8	%
η_{HTT1}	Efficiency of the first stage of the HT turbine	85.5	%
η_{HTT2}	Efficiency of the second stage of the HT turbine	86.16	%
η_{LPT}	Efficiency of the low pressure turbine	75.37	%
η_{HPT}	Efficiency of the high pressure turbine	89.14	%
η_{C1}	Efficiency of the first compressor	90	%
η_{C2}	Efficiency of the second compressor	90	%
η_{C3}	Efficiency of the third compressor	90	%
η_{Pumps}	Efficiency of the water pumps	98.83	%
ε_{boiler}	Effectiveness of the boiler	90	%
ε_{heater}	Effectiveness of the feed-water heater	100	%

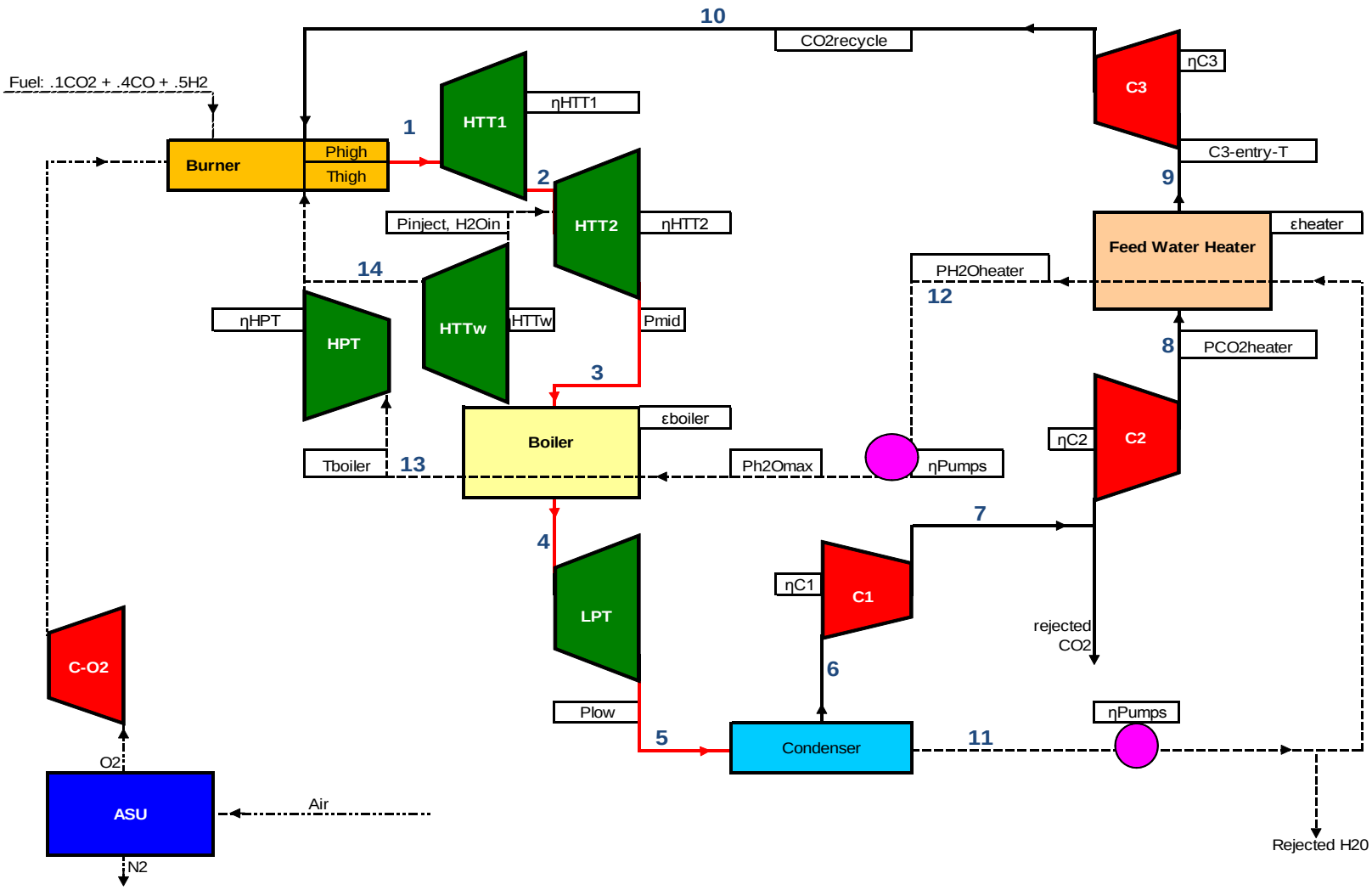

Figure 17: The independent variables on the Graz cycle flowsheet

In addition to these independent variables, the following values, shown in Table 2, are taken in the model as constants:

Table 2: Constant values in the Graz cycle model

Variable	Description	Value	Unit
HHVfuel	The higher heating value of the input syngas	234.409	KJ/mol
Fuel-makeup	The fuel: $0.1CO_2 + 0.4CO + 0.5H_2$	1	mol/s
CO2exitP	The exit pressure of rejected CO_2 before liquefaction (NOTE: constant because a change here results in an offsetting change elsewhere)	1	bar
O2 work	Work done by the oxygen compressor	5880.45	W
ASU work	Work done by the Air Separation Unit	7280.13	W

Another unknown, T_{low}, defined as the temperature at the outlet of the condenser, is a dependant variable that is a function of the pressure in the condenser, P_{low}, and the mass fraction of water in the condenser stream. The temperature here must be low enough to allow water to condense out of the stream, and this temperature is based on the partial pressure of the water at the inlet. This value is calculated by the model according to the following state equation, provided by the NIST REFPROP 7 libraries:

$$T_{low} = -.003{P_{H2O}}^6 + .125{P_{H2O}}^5 - 1.665{P_{H2O}}^4 + 11.17{P_{H2O}}^3 - 40.44{P_{H2O}}^2 + 86P_{H2O} + 40$$

where,

$$P_{H2O} = P_{low}\frac{\dot{m}_{H2O}}{\dot{m}_{H2O}+\dot{m}_{CO2}}$$

In the burner, the HHV of the fuel was used as a heat input, and the combustion products were taken to be at 25°C. The molar flow rate of carbon dioxide into the burner, defined through the independent variables, was used with an estimate of the

input carbon dioxide temperature of 300°C. An input estimate of the incoming water temperature of 300°C fully defined the mixture, and the molar flow rate of water required to reach a burner output temperature defined through the independent variables was calculated. This stream, fully defined in molar fraction, temperature, and pressure, was passed through each component in the Graz cycle in turn via the equations defined above. At the completion of the cycle, new values for the input temperatures for CO_2 and water into the burner were calculated, and the entire Graz cycle was calculated again using these new input parameters. This iteration continued until the H_2O and CO_2 inlet temperatures converged, which occurred to an error of ±0.01°C within five iterations.

Controls were placed on the model to ensure that no water in the exhaust stream condensed before reaching the condenser itself. If water condensed before this point, the efficiency of the plant would falsely increase in this model. This requirement stems from the fact that liquid water within the low pressure turbine would cause damage to the turbine and hinder its operation. Other controls in the model were placed on the boiler and heat exchanger to ensure that no second law violations occurred within the heat exchangers. This means that the hot stream was hotter than the cold stream within the heat exchanger body at all times. A third and final control existed to ensure that the water leaving the boiler unit had been totally converted to high pressure steam.

The result of this calculation for the input parameters given by previous analysis is shown in Figure 18 through Figure 22 below. In all figures, the top value in yellow was calculated using this model, while the bottom value in light blue is the published value from the study performed by Jericha and Göttlich. [22] It should be noted that the efficiency values quoted in this analysis do not include penalties associated with liquefaction of the carbon dioxide product, sequestration of the carbon product, or inefficiencies associated with the gasification of coal.

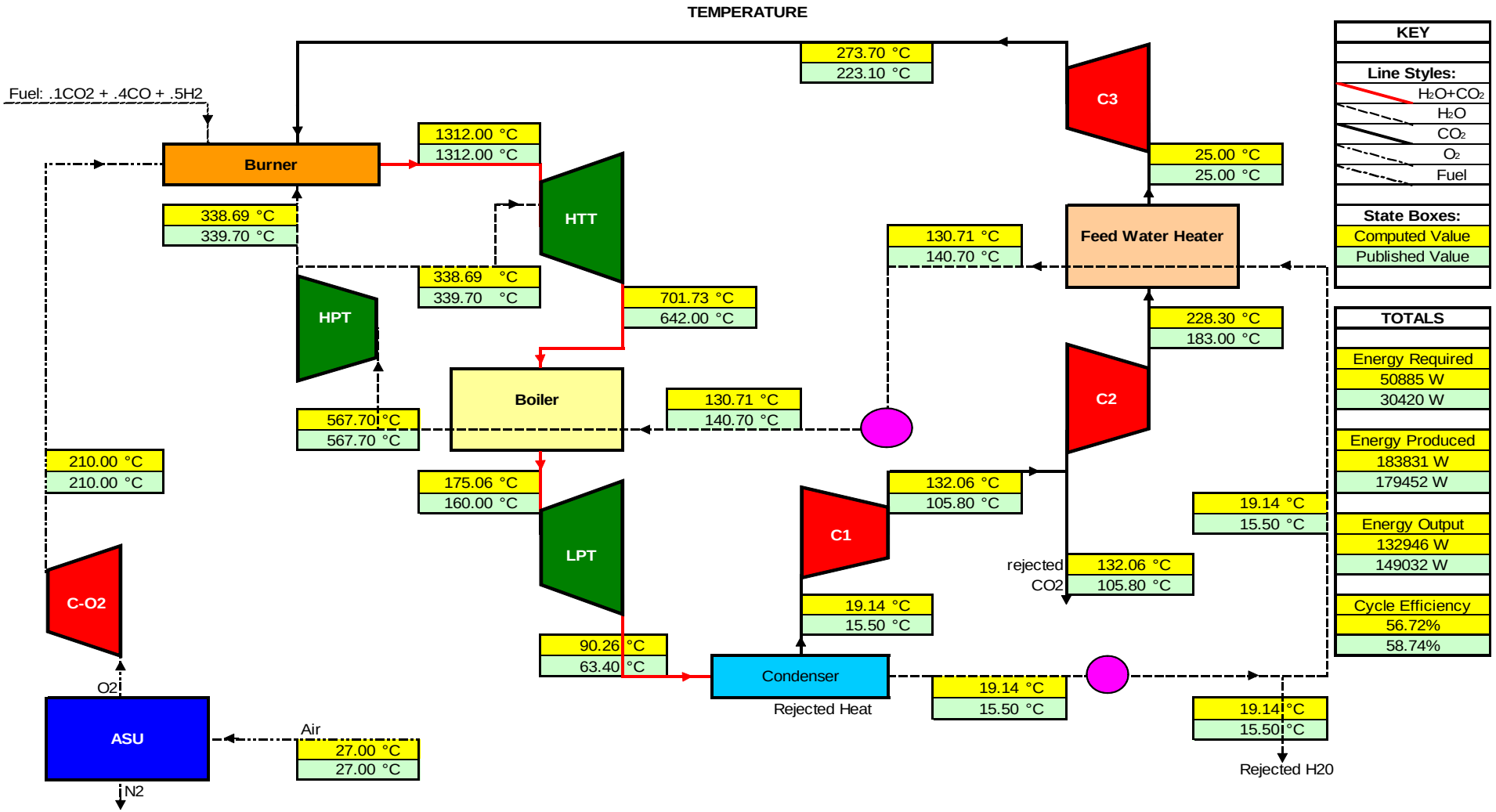

Figure 18: Calculation results: Temperature

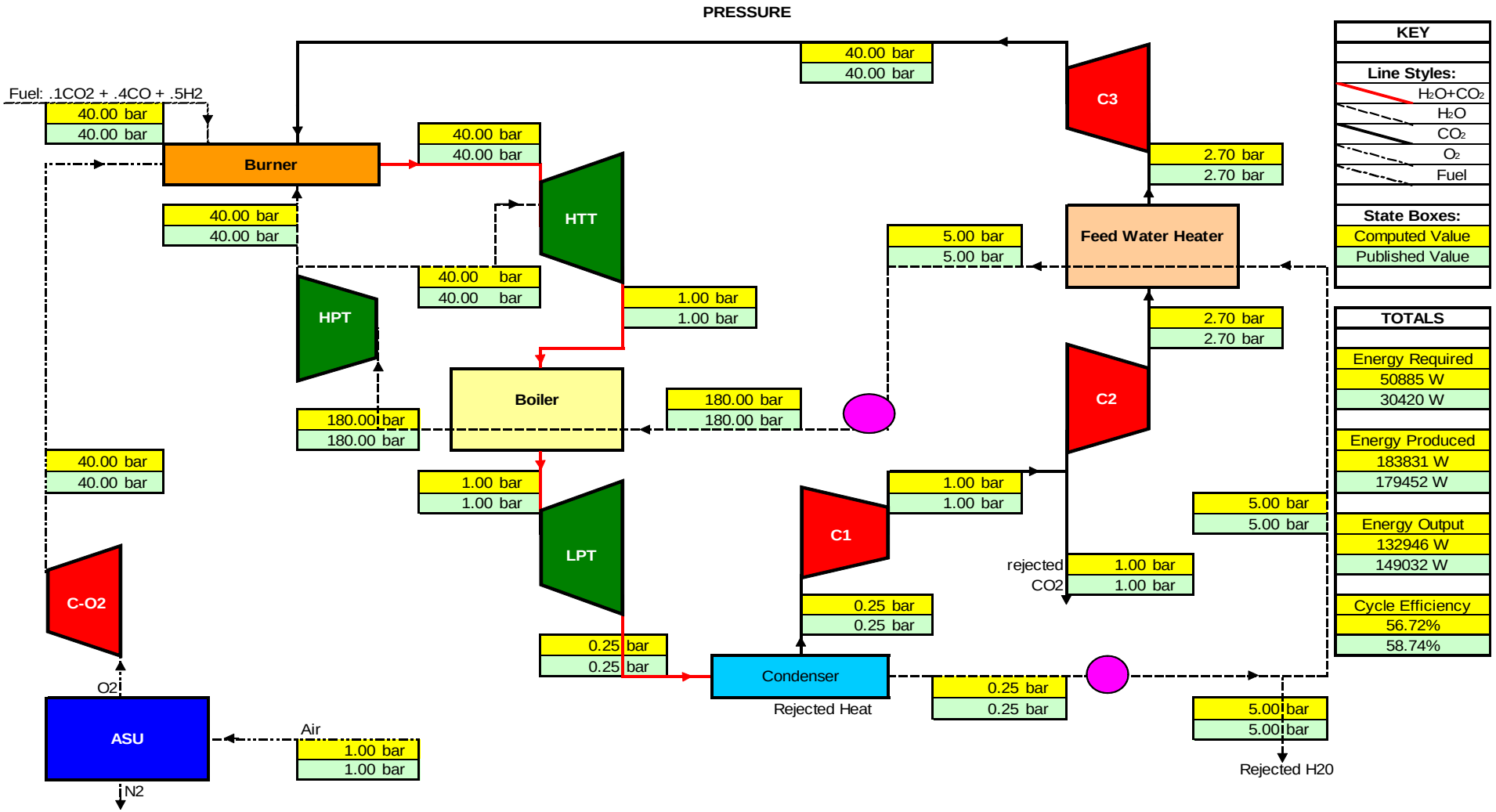

Figure 19: Calculation results: Pressure

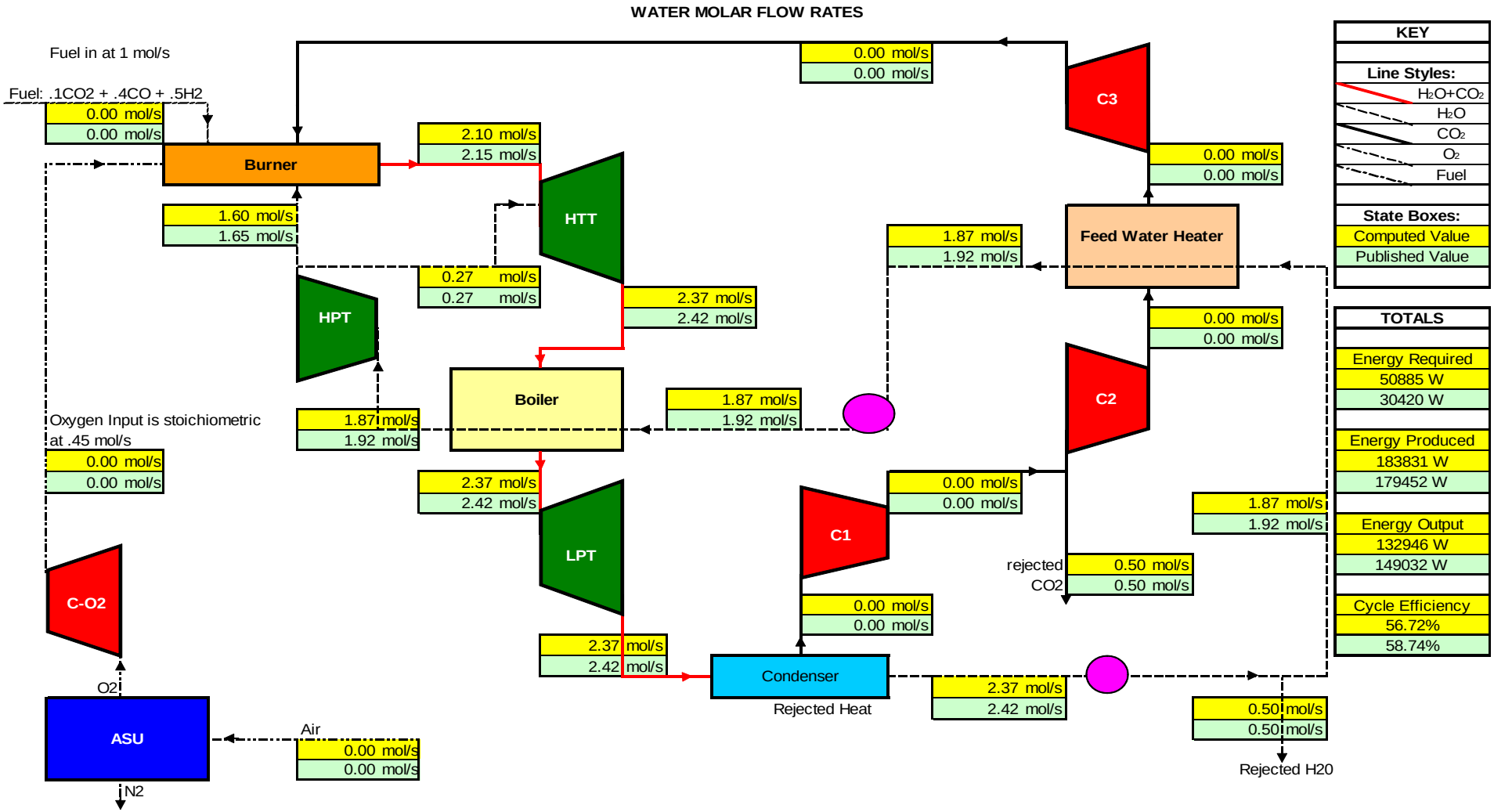

Figure 20: Calculation results: H_2O flow rates

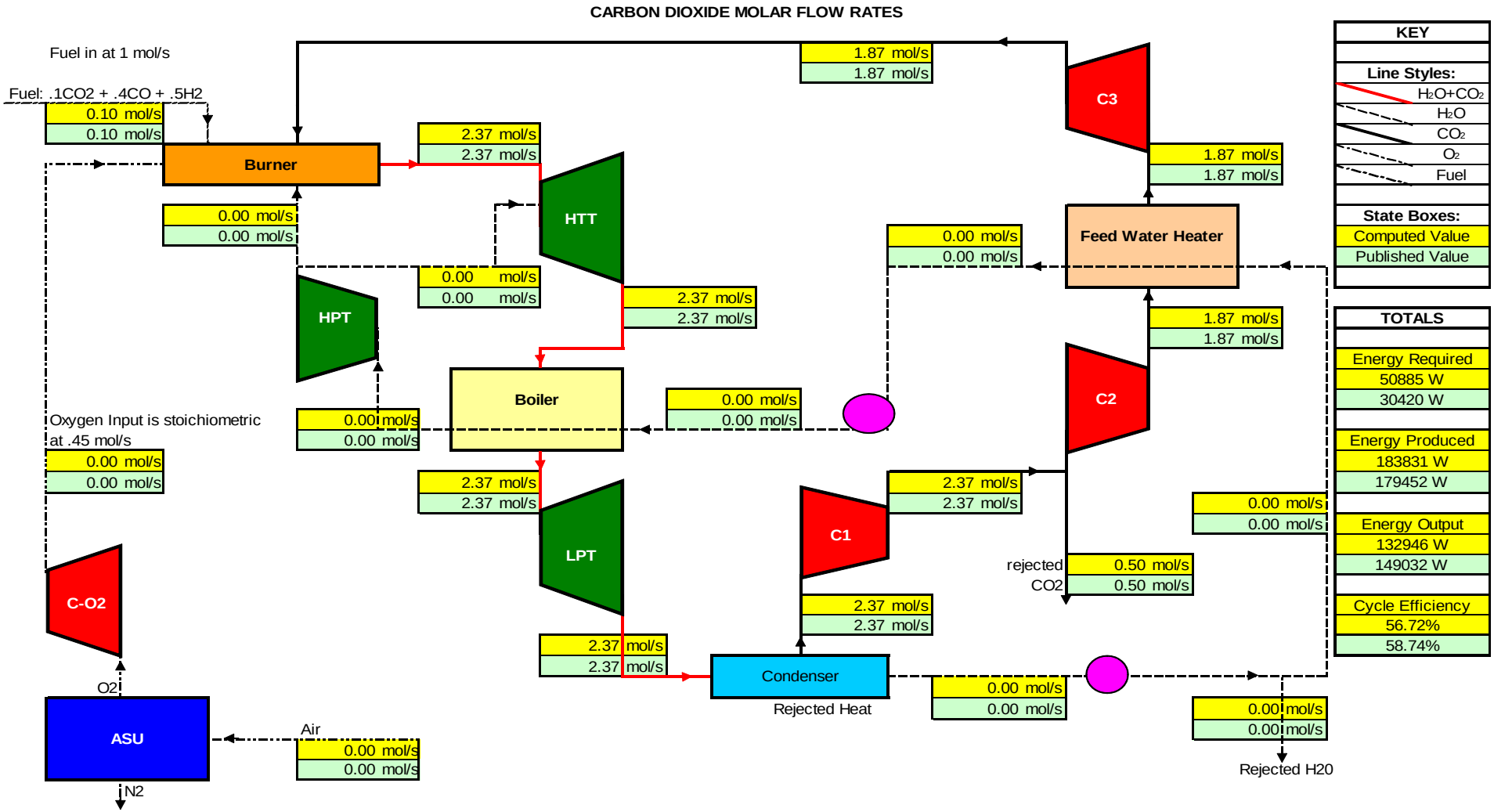

Figure 21: Calculation results: CO_2 flow rates

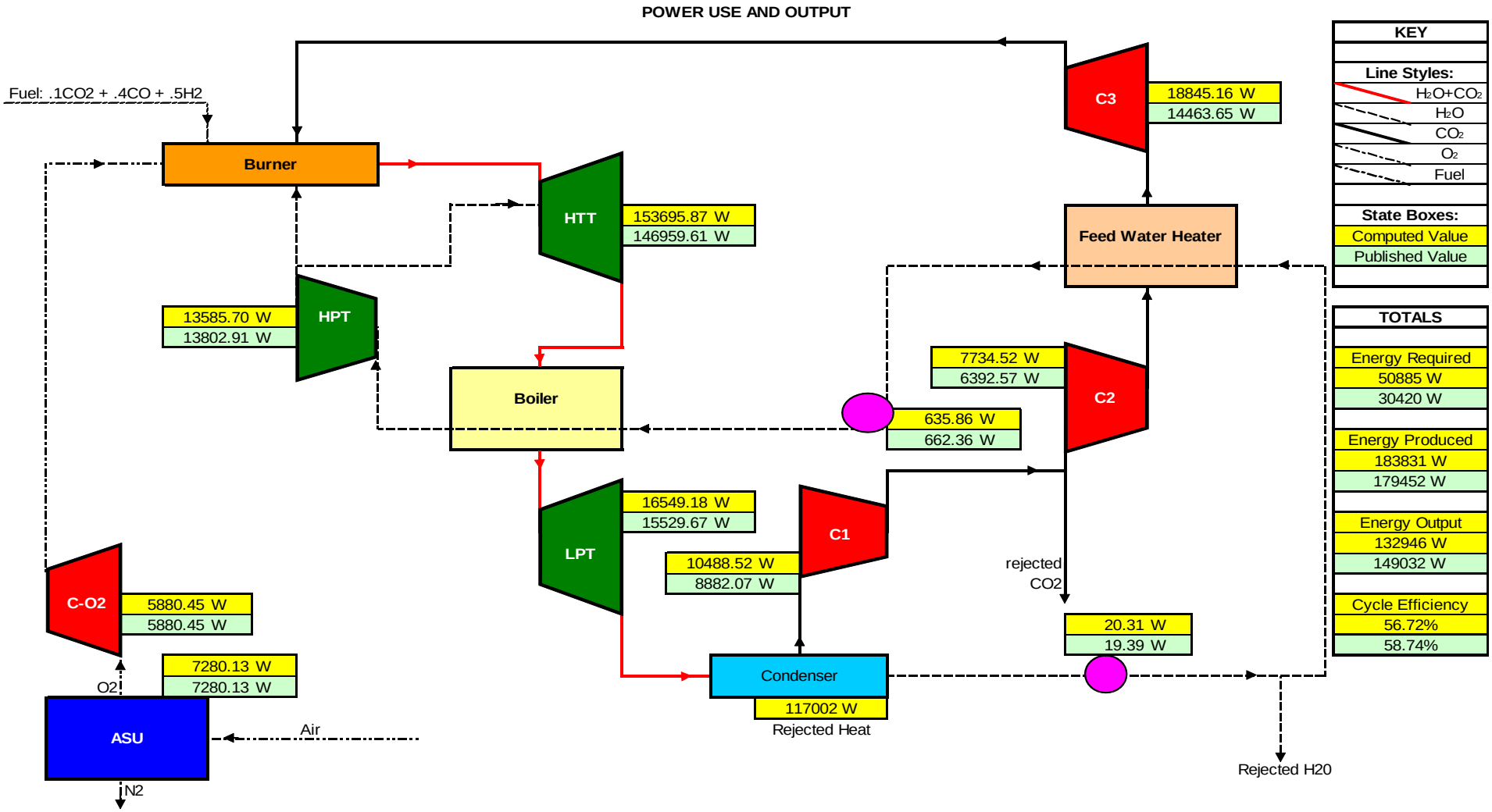

Figure 22: Calculation Results: Power

Figure 23 and Figure 24 show the full T-S diagrams for both the water and carbon dioxide flowing around the full cycle. The numbers at each point in the diagrams correspond to the numbers at different stages of the cycle diagram in Figure 17, and the cycle path is clockwise around the T-S loop:

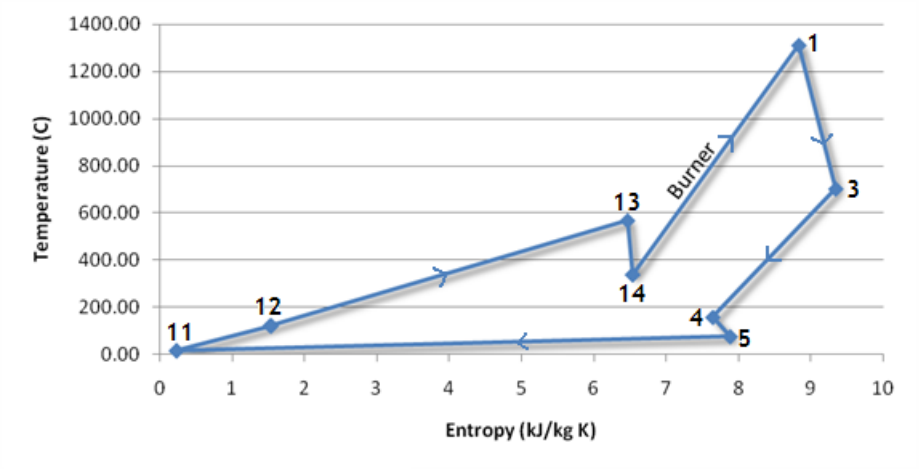

Figure 23: T-S diagram of water in the Graz cycle

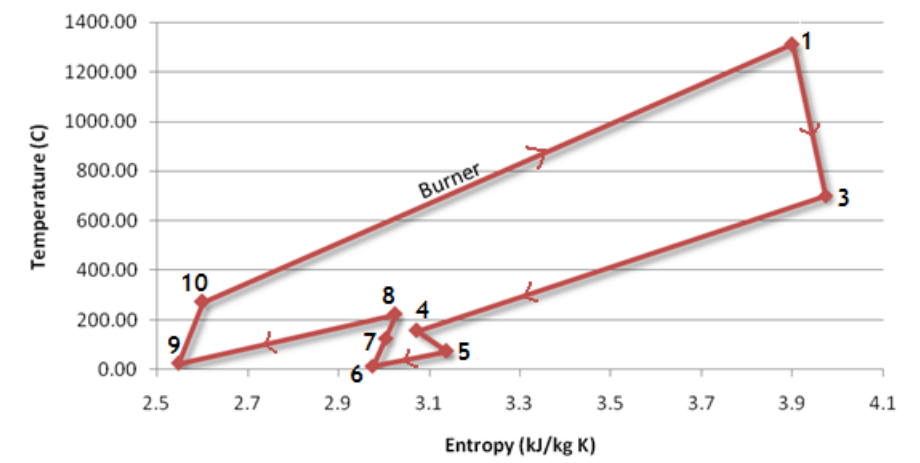

Figure 24: T-S diagram of carbon dioxide in the Graz cycle

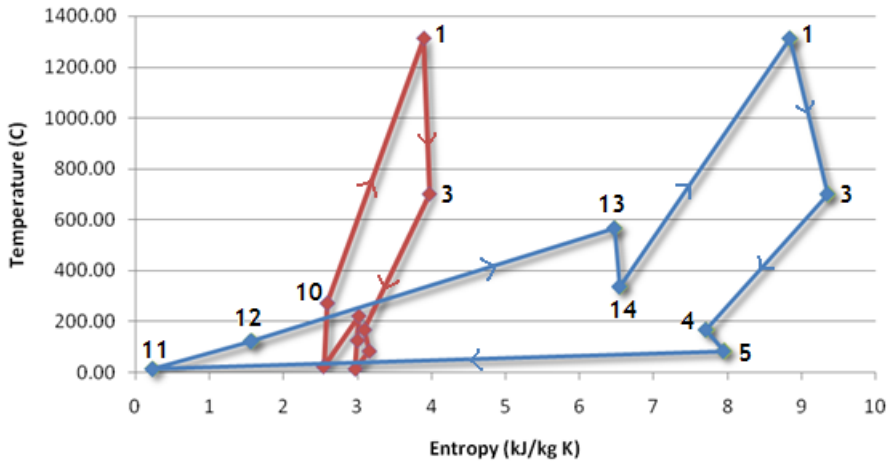

Figure 25: T-S diagram of Carbon Dioxide (red) and water (blue) superimposed on top of each other.

In the water diagram, the water gains entropy and temperature in the burner before losing temperature, but gaining more entropy, in the first expansion. The stream then passes through the boiler where it loses heat and passes entropy to the other stream. After this, another expansion lowers the temperature further and generates more entropy. The condenser acts as a large entropy sink, taking away a large amount of entropy for a small temperature loss. This small temperature loss is a result of the phase change of the water that occurs. The pumping of the water produces no noticeable heat or entropy change on the graph, and the temperature then rises, along with the entropy, in the feed-water heater. After another pumping process that is indistinguishable on the graph due to the low entropy and heat additions, the stream passes through the boiler where it gains significant energy and entropy. The stream then loses heat and gains entropy as it is expanded in the high pressure turbine before passing back into the burner.

In the carbon dioxide stream, significant temperature and entropy increases occur in the burner. Like the water stream, temperature is lost but entropy gained as the first expansion is conducted. With the water stream, the carbon dioxide then loses both heat and entropy in the boiler before losing more heat but gaining entropy in the last expansion. The condenser here represents only a modest decrease in temperature and entropy. The carbon dioxide is then pumped twice before losing heat and entropy

in the feed-water heater. A third compression heats and adds entropy to the stream before it is again injected into the boiler.

Figure 26 shows the entropy generation for each component of the Graz cycle. Note that the burner produces many times more entropy than any other component and is not included on this graph:

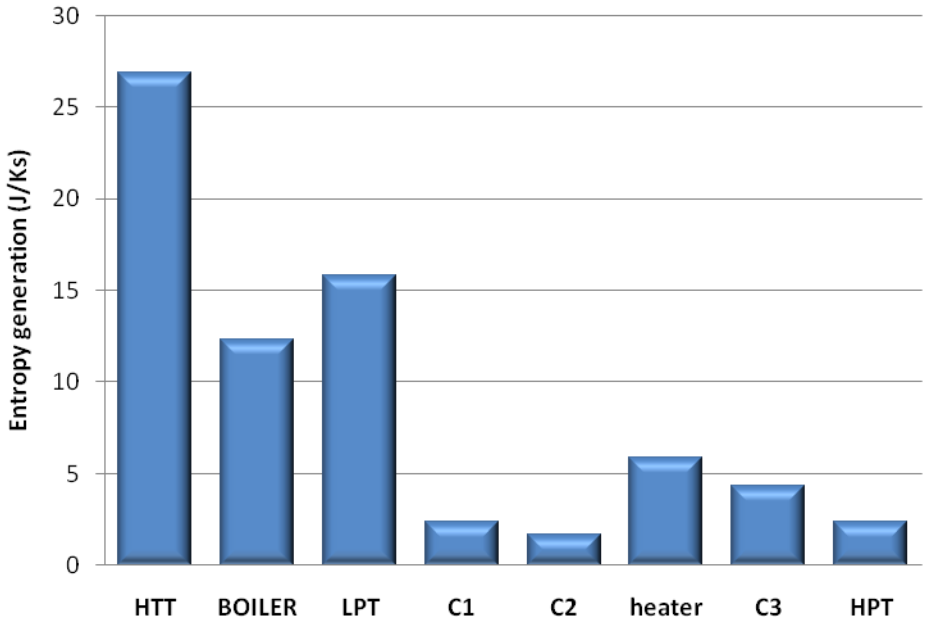

Figure 26: Entropy generation in each unit.

This graph makes it clear that the units with the most irreversibilities are the high temperature turbine (HTT), which includes the HTTw, HTT1, and HTT2, as well as the low pressure turbine (LPT). These losses are due to the efficiency values used during the calculations, and an increase in the efficiencies of any of these units would help decrease the overall entropy generation in that component. This is possible, since the LPT, for example, is assumed to be running at just over 75% efficiency, which is rather low.

Figure 27 shows the change in exergy across the different components in the Graz cycle. The axis has been scaled so that the burner, which has a large positive exergy change (as expected) does not obscure the other components:

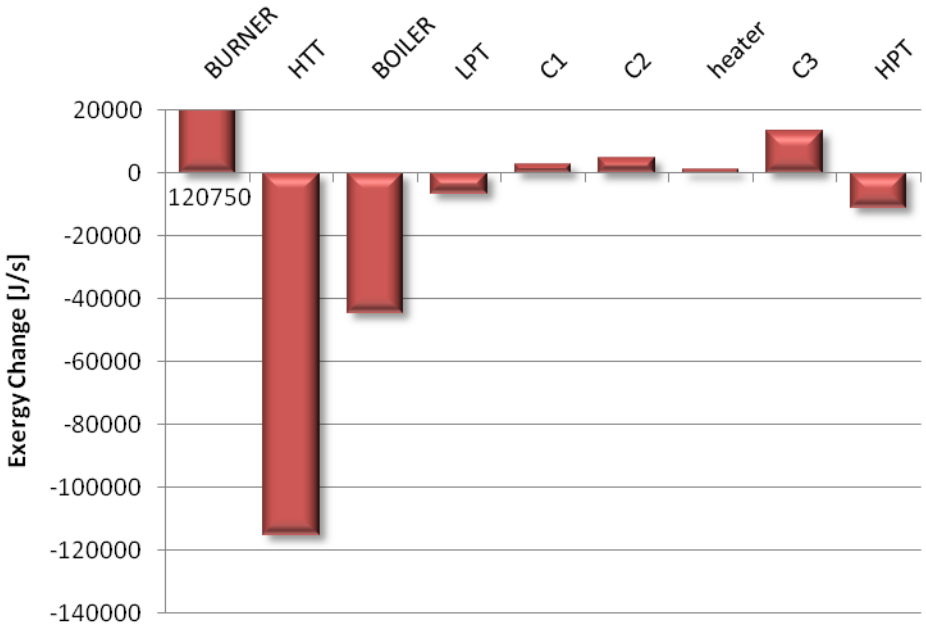

Figure 27: Exergy change over each component. The axis has been scaled.

This figure shows that the largest availability change in this cycle occurs across the HTT. This is expected since the majority of output power in the system is derived in the HTT. The large exergy loss in the boiler represents lost availability, as no usable power is extracted from the boiler unit. This means this availability is totally lost in the boiler as heat to the surroundings, pressure losses, and other parasitic losses. An increase in the effectiveness of this heat exchanger would help reduce this availability loss. The effectiveness used is already high, at 90%, and it is unlikely that much improvement could be made to this unit. Figure 28 shows the temperature profiles of both streams in the boiler, and it can be seen that the pinch point occurs at a temperature difference of roughly 30°C. The area between the two curves represents the availability loss, which is largest as the water completes boiling and the temperature difference is at its largest at 261°C:

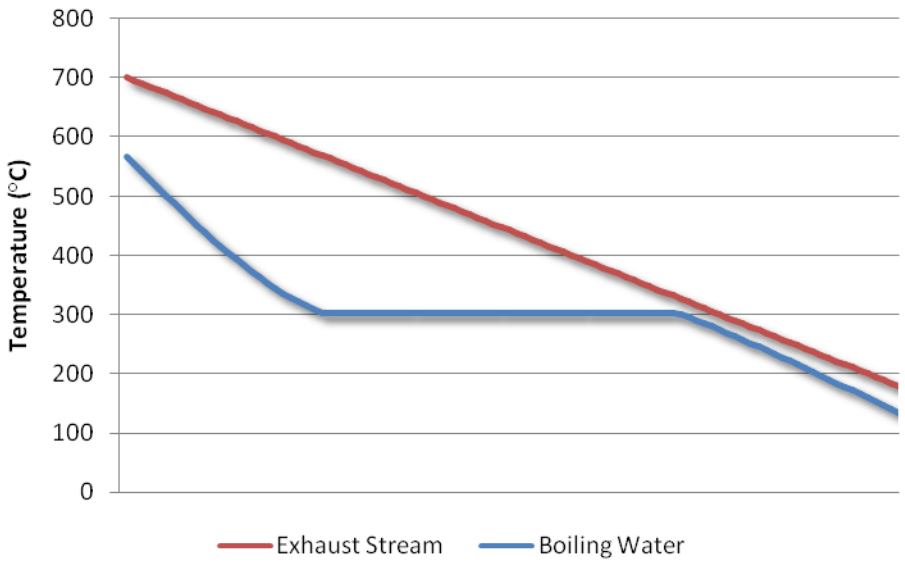

Figure 28: Temperature Profile within Boiler Unit. The x-axis is a linear measure of the change in temperature of the hot stream in the heat exchanger.

A comparison between the results of this analysis and the results of the analysis published by Jericha and Göttlich shows close matching between temperature, pressure, power, and molar flow volumes around the cycle. [22] In nearly all cases, the published values are within 10% of the values predicted by this model, with most values within 2%. These differences can be attributed to the relative complexity of the model used by Jericha and Göttlich. In their paper, the model chosen relies on the program system IPSE developed by SIMTECH Comp. [22] This software takes into account more variables, including the layout and designs of the individual turbines as well as the physical layout of the whole plant, which are neglected within this study. This extra complexity results in slight differences in calculation, which when propagated through the entire cycle lead to the observed errors. The High Temperature Turbine (HTT) is the source of most error due to this simpler model. The forty to one pressure ratio over the turbine represents a large pressure drop, and the model used here results in output temperature and power generation values with errors on the order of 10%. These values are then used as inputs to other components, and as the error propogates through the cycle, it produces states around the cycle different than the states found in the Jericha publication.

Despite this error, the agreement between this model and the published analysis of the cycle is sufficient and serves as a validation of both this cycle model as well as the published model.

Sensitivity Analysis

An important requirement of any power cycle is that the overall cycle efficiency be as constant as possible through a range of different input parameters. The more sensitive the cycle efficiency is to these parameters, the harder it is to build a real plant which can realize and consistently deliver the promised performance. As a result, it is important to know which design parameters in the cycle are dominating and which parameters are less important to the overall efficiency. For these less important parameters, a final design may allow slight changes in their values to achieve lower plant costs or better plant integration.

Sensitivity of System State Parameters

The following figures represent a sensitivity analysis of the Graz cycle plant. Each independent variable that describes a state in the system, such as pressure or temperature, was independently tested, and the overall plant efficiency was determined for a range of these values. These graphs help show the sensitivity of the process to certain parameters and also help point the way to possible optimization. For some of the variables, the model is only valid over a certain range. Beyond this, second law violations or early water condensation occur. For graphs where this happens, a red circle is placed at the end of the graph to signify a bound, at the given conditions, on the variable. When no red circle is drawn, the trend may be continued but was not calculated.

All figures also include a green diamond, which represents the value that was used in the preceding cycle analysis.

Some of the figures depict uneven graphs that signify error. This error is related to the digitization of the model, and the maximum numerical resolution that the computer is capable of calculating with through the model. Although small, these errors

grow and are multiplied as they propagate around the cycle. An orange dashed fit line is included on figures for which the data is particularly erratic.

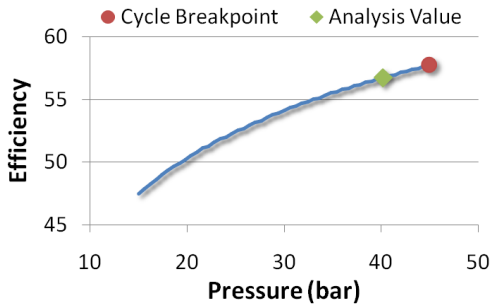

Figure 29: System sensitivity to the boiler pressure (P_{high})

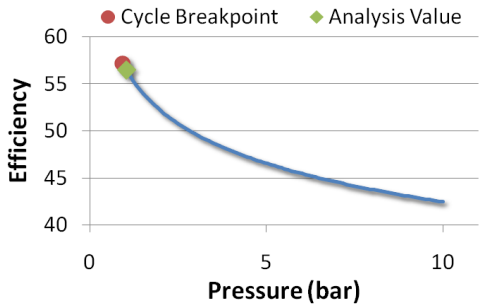

Figure 30: System sensitivity to the exhaust pressure in the boiler unit (P_{mid})

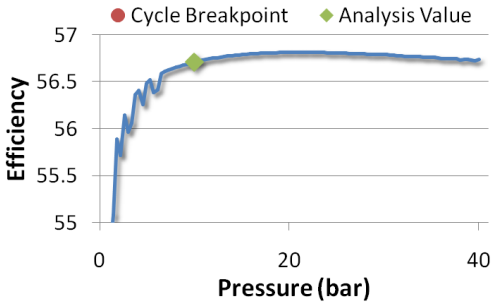

Figure 31: System sensitivity to the water injection pressure (P_{inject})

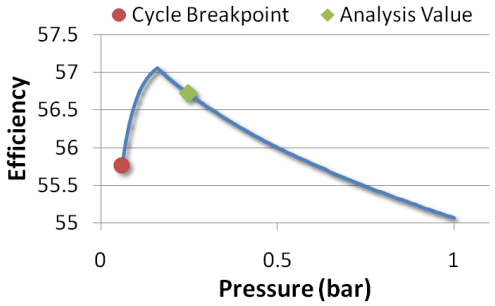

Figure 32: System sensitivity to the condenser pressure (P_{low})

These figures represent the sensitivity of the cycle to changes in the high, medium, and low pressures that the exhaust gases go through on their way to the condenser. The sensitivity of the pressure at which extra water is injected is also shown. As expected, a rise in the high pressure of the system (Figure 29) works to increase overall efficiency. It is this trend that must be reconciled with available equipment, since this high pressure can only be pushed as far as technology allows. Increases in the high pressure must also coincide with increases in the high temperature, otherwise second law violations will occur within the boiler. With the high temperature held constant in this analysis, the second law in the boiler is broken at around 45 bar. Figure 31 shows that the injection pressure for the extra water that is put through the cycle is

largely unimportant above 8 bar, suggesting that this pressure can be picked based on convenience for plant design.

The graph for the middle pressure (Figure 30) is interesting because it shows higher efficiencies at lower pressures. This behavior results from the fact that a rise in this middle pressure produces a rise in the stream temperature as the stream enters the boiler. This higher entry temperature in the boiler results in larger temperature differences over the boiler, and a larger pinch point temperature difference. The larger the temperature differences in a heat exchanger, the more entropy is produced and availability lost. As a result, lower pressures which reduce the pinch point temperature difference within the boiler result in high efficiencies. This can only be pushed so far because at some point the streams will reach the same temperature, and beyond this point the high temperature stream would have to be lower than the temperature of the low temperature stream, which is a second law violation. The diagram shows how the middle pressure reaches a peak at a low pressure and stops when the model determined a second law violation in the boiler.

Figure 32 reveals the sensitivity of the cycle to the low pressure. This figure shows a peak with a decline on both ends. Changing the low pressure value changes the temperature at which the stream enters the condenser. Lower pressures produce a lower condenser entry temperature. This means less heat is thrown away in the condenser and more heat is converted to work in the low pressure turbine. The graph shows an eventual dropoff, however, as the low pressure drops. This occurs because the compressors C1 and C2 must do more work, and as a result the carbon dioxide entry temperature into the feed water heater is higher. This higher temperature results in a release of more energy into the passing water stream and some of the water ends up boiling inside the feed water heater. The consequence of this is a much higher compression work to bring the water to the high pressure of 180 bar since a portion of the water stream is in the vapor phase and it cannot be pumped. As a result, the low pressure must limit itself to pressures above the point at which water boils in the feed water heater. This pressure is easily identifiable in the graph as the peak around 0.2

bar. It is also desirable to have no water condense within the low pressure turbine before it reaches the condenser. As a result, there is another lower bound because the low temperature reached must be above the condensation temperature of water at its partial pressure. This bound is the true lower bound in the graph, represented by the red circle. In all situations, the stricter of these two bounds must be used to bound the low pressure in the system.

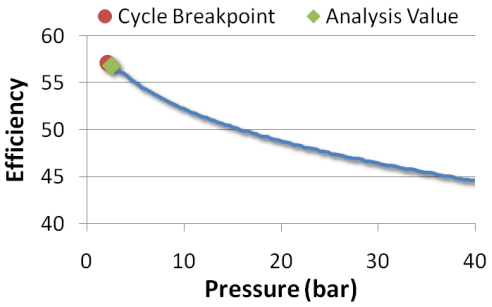

Figure 33: System sensitivity to the carbon dioxide pressure in the feed water heater ($P_{CO2heater}$)

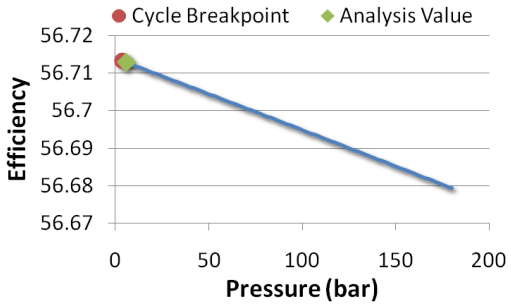

Figure 34: System sensitivity to the water pressure in the feed water heater ($P_{H2Oheater}$)

Figure 33 shows the sensitivity of the overall efficiency to the pressure of the carbon dioxide in the feed water heater. The trend towards higher efficiencies at lower pressure occurs for the same reasons as described above for the middle and low pressure graphs. At lower pressures, the carbon dioxide enters the feed water heater at lower temperatures, and as a result heats the passing water less. This means more energy must be passed from the exhaust stream to the water stream in the boiler to fully heat the water stream. This extra energy loss from the exhaust stream helps to lower the pinch point temperature difference in the boiler, as well as lower the entry temperature into the condenser. The lower bound for the pressure here is determined by the point at which the second law is violated within the boiler.

The dependency of the efficiency on the water pressure in the heater (Figure 34) is nearly completely irrelevant, with only a change of 0.03 percentage points in the overall efficiency for the full range of the possible pressures. As a result, a lower pressure is preferred to simplify piping and construction of the feed water heater.

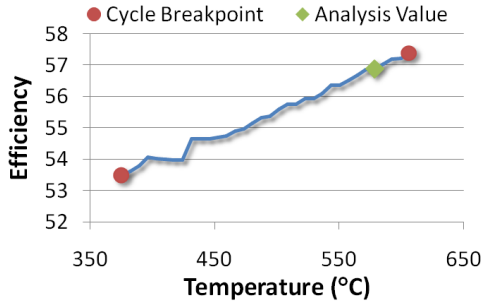

Figure 35: System sensitivity to the water stream output temperature from the boiler (T_{boiler})

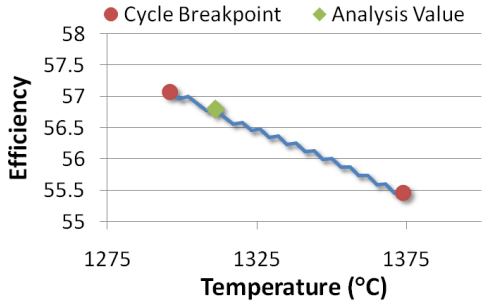

Figure 36: System sensitivity to the burner outlet temperature (T_{high})

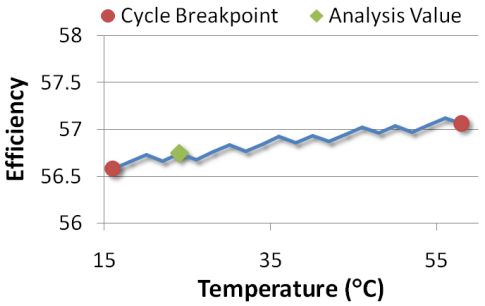

Figure 37: System sensitivity to the carbon dioxide exit temperature from the feed water heater (C3-entry-T)

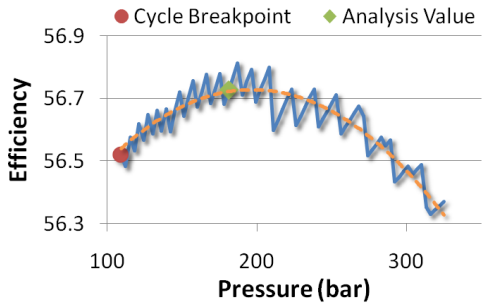

Figure 38: System sensitivity to the water pressure in the boiler (P_{h2Omax})

Figure 35 depicts the sensitivity of the cycle to the boiler outlet temperature. As the temperature rises, more energy is pulled from the exhaust stream flowing through the boiler, which results in a smaller pinch point temperature difference and a lower entry temperature into the condenser. This lower pinch point difference and condenser entry temperature produces a higher efficiency, since less energy is thrown away. The temperature has a maximum which is reached when a second law violation occurs in the boiler itself. Higher values for the boiler outlet temperature will also cause issues with finding machinery to operate in such a demanding environment. As the temperature difference within the boiler decreases, the physical size of the boiler, and therefore its cost, increases. The high pressure turbine is also a technology that does not exist yet, and placing higher demands upon the inlet temperature may delay the availability of a

working turbine. The temperature has a lower bound which is the boiling temperature of water at the high pressure.

The high temperature produces higher efficiencies as the high temperature drops (Figure 36). This is caused by the same reasons discussed for the middle and low pressures before: a lower pinch point temperature difference and a lower condenser entry temperature. Like the boiler outlet temperature, the limit of this occurs when the second law is broken within the boiler unit.

Figure 37 depicts the sensitivity of the C3 compressor entry temperature. Higher C3 entry temperatures produce higher efficiencies because the water exiting the feed water heater is not as hot and more energy must be taken from the exhaust stream in the boiler to heat the water the extra amount. This extra energy loss leads to a lower inlet temperature in the condenser. The C3 entry temperature can only be raised until the second law is broken within the feed water heater unit. The entire cycle is not terribly sensitive to this parameter, which suggests that further efficiency gains would be better found by changing other parameters.

The maximum water pressure (Figure 38), although producing a higher efficiency at a peak around higher pressures, has virtually no effect on the efficiency of the entire system, and as a result it is desirable to lower this pressure as much as possible to alleviate technological hurdles associated with the high pressure turbine. This result occurs because when the pressure is dropped, the temperature of the water entering the burner is higher and therefore more water is needed in the cycle to maintain the maximum temperature. This extra water in the cycle results in extra power produced in the high temperature turbines and the low pressure turbine. This extra power nearly exactly offsets the loss in power in the high pressure turbine that results from the drop in pressure. There is a limit to how low we can push this pressure, however. As the maximum water pressure drops, the low pressure turbine outlet pressure also drops, and eventually drops lower than the condensation temperature for water at its partial pressure in the low pressure turbine. This occurs before the second law is broken within the boiler. Despite this, Figure 38 suggests that many of the technological problems

associated with the high pressure water stream can be mitigated simply by lowering the water high pressure a significant amount without much effect on overall plant efficiency.

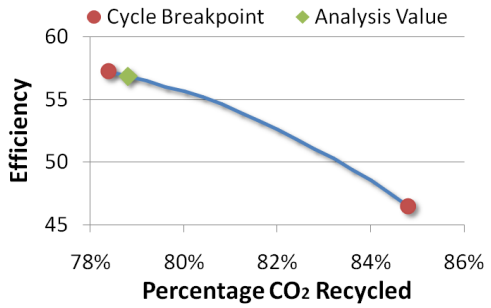

Figure 39: System sensitivity to the carbon dioxide recycle percentage ($CO2_{recycle}$)

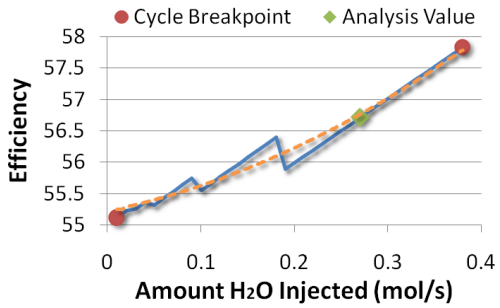

Figure 40: System sensitivity to the water injection rate ($H2O_{in}$)

Figure 39 shows the sensitivity to the carbon dioxide recycle percentage. The final cycle efficiency is very sensitive to this parameter, with only a two percentage point change in the recycle percentage leading to overall efficiency changes of five percentage points or more. This extreme sensitivity makes the carbon dioxide recycle percentage the most important variable in the Graz cycle, and is caused by a number of changes that occur downstream when this value is altered. The amount of water that is needed in the burner unit is directly related to the carbon dioxide recycle percentage. When this percentage changes, the amount of water needed also changes. This produces a shift in the makeup of the exhaust gas, and as a result, it behaves differently than before, registering different temperature drops across turbomachines. The changes also mean less water must be heated in the boiler and feed water heater. As a result, the temperatures around the entire cycle change significantly with only a small change in the recycle percentage, and the new temperatures are not as well matched, leading to cycle irreversibilities. It is important to note is that the change of other system variable could make up for the changes in carbon dioxide recycle percentage, but alone this variable holds importance in maximizing efficiency.

The ideal recirculation percentage is set when the percentage is as low as possible, which minimizes the input temperature into the condenser. The lower bound of the recirculation percentage occurs when the lack of recirculating carbon dioxide

requires more water to flow through the cycle. This extra water takes more energy to boil in the boiler, and a second law violation occurs when the amount of water needed becomes too high. Care must be taken to make sure the exact amount of carbon dioxide desired is recycled in order to avoid incomplete boiling within the boiler or too much carbon dioxide and a decrease in cycle performance.

The amount of water injected into the cycle after the burner is moderately important in the overall efficiency (Figure 40). More water is better, as the extra water in the cycle requires more energy to boil in the boiler, resulting in a lower pinch point temperature and the exhaust stream entering the condenser at a lower temperature. The amount injected must be limited before a second law violation occurs in the boiler.

Sensitivity of Component Efficiencies

The efficiencies of each component can play a large role in the overall efficiency of the plant. When building a plant, it is important to know which components are more important to the overall performance. With this information, extra money and time can be focused on raising the efficiencies of important components instead of other components whose efficiencies do not matter as much to overall system performance.

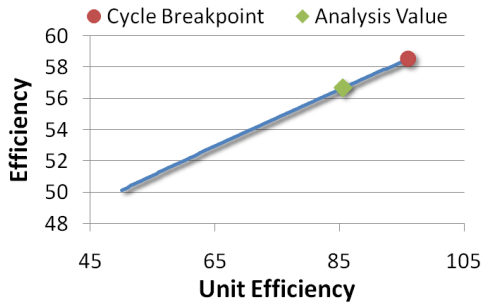

Figure 41: System sensitivity to the first high temperature turbine efficiency (η_{HTT1})

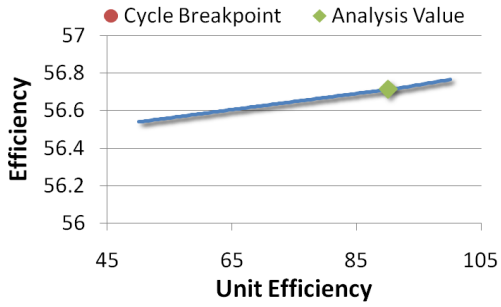

Figure 42: System sensitivity to the water injection high temperature turbine efficiency (η_{HTTw})

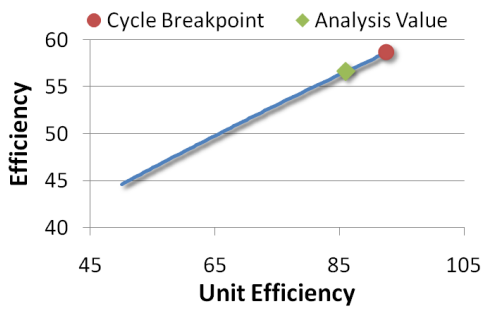

Figure 43: System sensitivity to the second high temperature turbine efficiency (η_{HTT2})

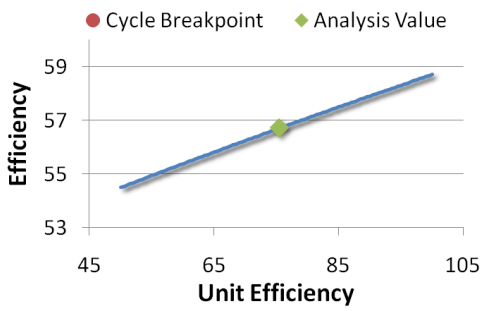

Figure 44: System sensitivity to the low pressure turbine efficiency (η_{LPT})

Figure 41 through Figure 44 show the sensitivity of the overall cycle performance on the efficiencies of the individual turbines in the exhaust flowpath. These turbines represent what would be multi-staged expanders in a real power plant, and the unit efficiency is for the multi-staged turbine unit as a whole.

As expected, a rise in efficiency of any component gives rise to an increase in system efficiency. The turbine which expands the injected water down to the injection pressure (Figure 42) produces very little power, and its efficiency matters very little to the overall plant. The other three turbines in the exhaust flowpath create nearly all of the energy for the plant, and their efficiencies are much more important. For the low pressure turbine (Figure 44), a ten percentage point drop in efficiency represents a one percentage point drop in overall efficiency. The first high temperature turbine (Figure 41) is nearly twice as important to the final efficiency, with a ten point drop in its efficiency contributing a 1.7 point drop in overall efficiency. The most important turbine in the system is the second high temperature turbine (Figure 43). This turbine produces a majority of the power in the cycle and a ten percentage point dip in its efficiency yields a full three percentage point drop in overall efficiency. Both of the high temperature turbines have an upper limit on their efficiency when all other system parameters are held constant. As the turbine efficiencies rise, the outlet temperatures from the turbines decrease. This means that the exhaust stream entrance temperature into the boiler is lower, and at some point a second law violation is reached within the boiler as a result.

The high temperature turbines matter most to the efficiency of the system, and the most time and money should be spent on these two components to ensure that they are as efficient as possible. This also shows that there is relatively little gain in the overall system efficiency from single digit changes in component efficiency. This is good news; if one component falls short of its efficiency design specification by a few percentage points, the overall system will not be adversely affected more than a fraction of a percentage point.

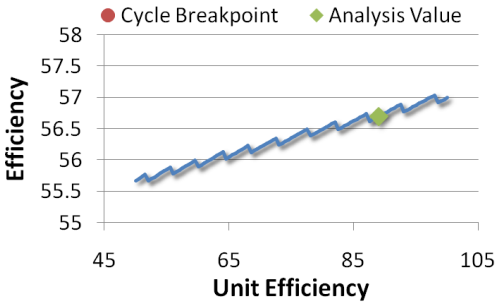

Figure 45: System sensitivity to the high pressure turbine efficiency (η_{HPT})

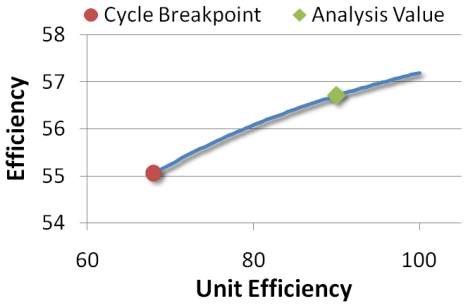

Figure 46: System sensitivity to the first compressor efficiency (η_{C1})

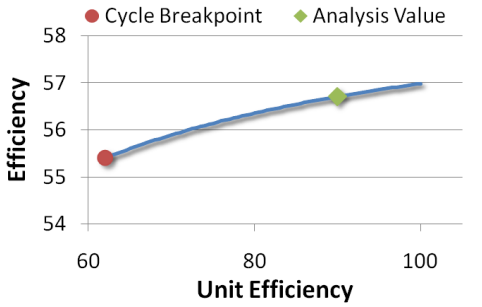

Figure 47: System sensitivity to the second compressor efficiency (η_{C2})

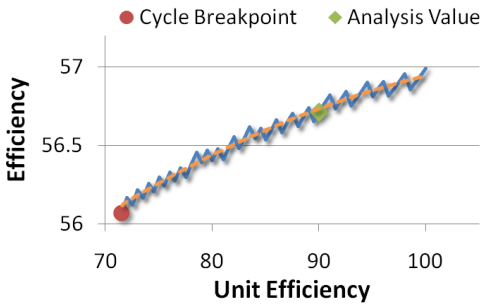

Figure 48: System sensitivity to the third compressor efficiency (η_{C3})

Figure 45 through Figure 48 demonstrate the sensitivity of the high pressure turbine and all three carbon dioxide compressors. It is clear that the high pressure turbine's efficiency (Figure 45) does not play a large role in determining the overall system efficiency. This turbine will represent new technology and having a relaxed requirement for its overall efficiency will go a long way towards helping the technology develop faster towards a usable state.

The overall performance is not very sensitive to the efficiency of each carbon dioxide compressor. Despite this, the first two compressors, C1 (Figure 46) and C2 (Figure 47), have bounds on their lower efficiency. Should the efficiency of either of these units fall below a threshold value, the carbon dioxide entering the feed water heater will be of an elevated temperature. Extra energy will pass into the water and at the threshold value, the water in the feed water heater will begin to turn to steam. This steam will have a large impact on overall system performance, as the requirements to compress the water to its high pressure value are drastically increased when the water is in the vapor phase. It is vitally important to ensure that the compressors have high enough efficiencies to ensure no water boils within the feed water heater unit.

The third compressor's efficiency (Figure 48) is also relatively unimportant. Like C1 and C2, C3 has a lower limit on its efficiency when all other parameters are held constant. When the efficiency for C3 is too low, the temperature of the carbon dioxide exiting the compressor is very high. More water is required in the burner to cool the combustion, and this extra water in the streams leads to a second law violation within the boiler.

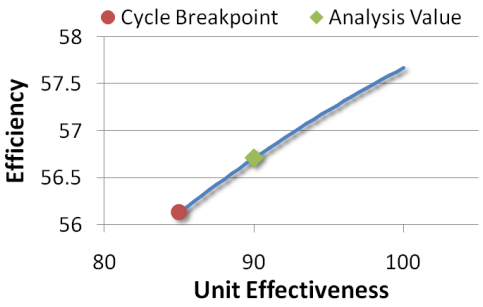

Figure 49: System sensitivity to the boiler effectiveness (ε_{boiler})

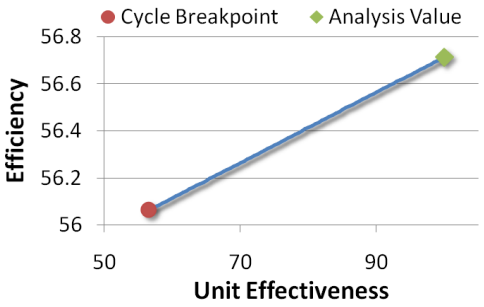

Figure 50: System sensitivity to the feed water heater effectiveness (ε_{heater})

Figure 49 and Figure 50 represent the sensitivity of the effectiveness of the boiler and feed water heater, respectively. For both, it is clear that as effectiveness increases, cycle efficiency does as well. Although the overall performance is not terribly sensitive to either effectiveness, the lower bound of the boiler occurs when the water in the boiler does not completely turn to steam and superheat. The design of the system must ensure that this lower bound is not reached. The feed water heater's lower

effectiveness bound is hit when the exhaust stream entering the condenser is below the condensation temperature for water at its partial pressure. This occurs because the water entering the boiler is at a lower temperature for lower feed water heater effectiveness values, which results in more energy being taken from the exhaust stream and a lower exhaust outlet temperature.

The sensitivity of the water pumps is not displayed here. This is due to the fact that these pumps require minimal power to operate and their efficiencies have insignificant effects on the cycle efficiency.

Optimizing the Graz Cycle

Difficulties of Optimization

The sensitivity analysis gives insight into possible ways that the Graz cycle can be optimized to maximize its efficiency. A higher maximum pressure clearly elevates the theoretical efficiency, but at what cost to the feasibility of the plant? The sensitivity analysis can also be misleading. The burner outlet temperature sensitivity graph shows that the plant efficiency grows as the temperature drops towards its lower bound. To conclude, however, that this means a lower burner outlet temperature is the key to maximizing plant efficiency is incorrect. The figure is really saying that plant efficiency is maximized when the temperature at the condenser inlet is as low as permitted without water condensing before the unit or a second law violation occurring in the boiler. The burner outlet temperature graph produces the highest efficiency when the temperature is closest to the point that minimizes the temperature entering the condenser without violating the second law in the boiler. Similarly, the middle and low pressure sensitivities, as well as nearly all the other sensitivity graphs, show maximums approaching limits that minimize the condenser entry temperature.

The question then becomes, with what combination of changing parameters is the condenser entry temperature minimized to produce a maximum cycle efficiency? The answer to this question is not trivial, and its answer cannot be known by simply studying the above sensitivity graphs.

If the efficiencies of each component are ignored (since it is obvious that higher efficiency components produce a higher efficiency plant. No matter the values of the other parameters, simply raising the component efficiencies will always raise the cycle efficiency), there are still twelve system parameters that define the cycle, and the effect one has on the overall cycle efficiency is coupled to the values of all the other parameters. A rise in the burner outlet temperature alone, for example, will only serve to lower the cycle efficiency. A rise in the temperature coupled with changes in other variables, however, may raise the total overall cycle efficiency above 56.72% value computed in the analysis above. Conversely, the change may also end up lowering the overall efficiency. Due to this coupling of the system parameters, it becomes very hard to analytically optimize the system. With so many variables, it would take an enormous amount of computing time to calculate every single combination of parameter values to determine the best solution. In order to solve this problem and effectively optimize the cycle, a technique must be used that does not rely on an analytical solution or equation to solve, and can find a maximum without searching the entirety of the parameter space.

The Modified Simulated Annealing Algorithm

A modified version of the simulated annealing algorithm can be used to find a near-best solution. This algorithm was originally inspired by the annealing of crystals in metallurgy. It is well known that the speed at which a material cools directly relates to the order of its molecules when solidified. Materials that are cooled very quickly do not have time to form crystals and its molecules end up jumbled and disorganized, like in glass. When a material is cooled slowly, however, its molecules have time to arrange themselves into ordered sets and crystals form.

When the material is cooled slowly, the extra heat lingering around the material allows the molecules in the material to 'unstick' themselves from a position of lower energy and temporarily exist in a higher energy stage. As the molecule of higher energy moves around, it has the ability to find stable conditions of still lower energy than the energy level it was originally at. In this way, the extra heat allows the molecule to move

from a local energy minimum to a global energy minimum by passing through higher energy states.

The algorithm works by analogy to this natural process. A cost function is derived for the problem that needs to be solved, and during each iteration, a random 'neighbor' to the current state is calculated. If the neighbor is of a lower cost, the neighbor state is taken as the new state. If the neighbor cost is higher, its state is taken with a probability *p*, which is an exponential function of a global parameter *T* as well as the difference in cost between the two states. Over the course of the algorithm *T* is decreased, and with it *p*. Near the beginning of the calculation the state fluctuates wildly from high cost to low cost situations and back. As the calculation continues and *T* is decreased, the state is allowed to move to higher cost situations less and less, and eventually allows virtually no moves to higher cost states. This allowance for moves to higher cost at the beginning of the algorithm allows the calculation to seek out the global minimum without becoming stuck in local minima.

In order to make use of this algorithm, a cost function must be defined for the problem as well as a way to calculate 'neighbor' states. The probability *p* of taking a higher cost neighbor state must also be defined. This is easier stated than done, for the definition of *p* and choice of the neighbor function have a large impact on the success and computation time of the algorithm. The annealing schedule is particularly important: if the computation decreases *T* too fast, the global minimum will not be found. If *T* is decreased too slowly, the algorithm will converge to the true solution, but at a significantly slower pace than is necessary. A poor choice of the neighbor function will also impact the speed at which the algorithm converges. As a result, finding the best definition for the algorithm parameters is a trial and error process that can be regarded as more of an art than a science.

For the Graz cycle optimization, the cost function *C* can be defined as:

$$C = -\eta_{cycle}$$

where η_{cycle} is the overall cycle efficiency of the Graz cycle and is between zero and one. This cost function means that minimizing the cost of a state will maximize its efficiency.

The probability parameter *p* at iteration step *n* is defined as:

$$p(n) = e^{\frac{C(n)-C(n-1)}{T(n)}}$$

where *C*(*n*) is defined as the cost of the state used in iteration step *n*, and where *T*(*n*) is defined as:

$$T(n) = 5 - \frac{1}{6}\text{floor}\left(\frac{n}{36}\right)$$

where the 'floor(x)' function rounds any fraction *x* down to the nearest integer less than the fraction value [floor(2.3)=2 and floor(1.99999)=1]. With these definitions, the calculation will run for 1080 iterations until *T*(*n*) becomes zero.

To determine a state, the algorithm will vary the twelve system state parameters, with a neighbor state calculated using the definitions put forth in Table 3. The initial state is defined as the state put forth in the Jericho paper and analyzed above.

Table 3: Independent variables used in algorithm and their neighbor definition. 'Random' is defined as a function which produces a random (equal distribution) number between -1 and 1.

Variable	Neighbor Calculation	Limits	Initial Value	Units
P_{high}	$P_{high}(n) = P_{high}(n\text{-}1)$ + Random	30-50	40	bar
T_{high}	$T_{high}(n) = T_{high}(n\text{-}1)$ + 10*Random	1000-1370	1312	°C
P_{inject}	$P_{inject}(n) = P_{inject}(n\text{-}1)$ + Random	P_{mid} - P_{high}	10	bar
$H2O_{in}$	$H2O_{in}(n) = H2O_{in}(n\text{-}1)$ + Random/10	0-1	0.27	mol/s
P_{mid}	$P_{mid}(n) = P_{mid}(n\text{-}1)$ + Random	0.25-10	1	bar
P_{low}	$P_{low}(n) = P_{low}(n\text{-}1)$ + Random/4	0.01- P_{mid}	0.25	bar
T_{boiler}	$T_{boiler}(n) = T_{boiler}(n\text{-}1)$ + 10*Random	400-800	567.7	°C
$P_{CO2heater}$	$P_{CO2heater}(n) = P_{CO2heater}(n\text{-}1)$ + Random	1- P_{high}	2.7	bar
$P_{H2Oheater}$	$P_{H2Oheater}(n) = P_{H2Oheater}(n\text{-}1)$ + Random	P_{low} - P_{H2Omax}	5	bar

P_{H2Omax}	P_{H2Omax} (n) = P_{H2Omax} (n-1) + 5*Random	80-200	180	bar
$CO2_{recycle}$	$CO2_{recycle}$ (n) = $CO2_{recycle}$ (n-1) + Random/10	70-85	78.9	%
C3-entry-T	P_{H2Omax} (n) = P_{H2Omax} (n-1) + 10*Random	0-150	25	°C

During each iteration a new neighbor is found and its values are plugged into the Graz model to determine its efficiency. This efficiency is used to calculate the neighbor cost. If the model determines that the neighbor values do not fall within the set of working solutions (for example, the second law is violated or water condenses in the low pressure turbine), the cost is set to 1 and the neighbor is automatically discarded, meaning the probability parameter *p* is not used to determine if the neighbor should be taken. In this way, the algorithm avoids picking states as solutions which violate physical laws. This process confines the parameter space to the real solution space. Figure 51 shows pseudo-code for the modified simulated annealing algorithm:

```
State=Set Initial Condition                 Set the initial state of the system
Beststate=State                             Set the best state found so far
For n=1:1081                                Repeat until n=1080, starting with n=1
   Newstate=Neighbor(State)                 Create a new neighbor from the current state
   If Cost(Newstate) < Cost(State)          Test to see if the neighbor state is cheaper
      State=Newstate                           If it is, we will make the neighbor the state
   Else                                     Otherwise
      If Rand < p(n)                           Test to see if random number is less than p
         If Cost(Newstate) < 1                    If so, Test to see if neighbor is valid solution
            State=Newstate                           If so, take the neighbor as new state
         End
      End
   End
   If Cost(State) < Cost(Beststate)         Test to see if current state is better than best state
      Beststate=State                          If so, take current state as the best state found
   End
End                                         Return to the 'For' line and repeat with n=n+1
Display Beststate                           Display the best found solution
```

Figure 51: Pseudo-code for the modified simulated annealing algorithm

Optimization Results

The optimization of the Graz cycle using the modified simulated annealing algorithm resulted in a design that yields an overall efficiency of 60.11%. This efficiency is directly comparable to the efficiency of 56.72% found in the original analysis in this paper and does not include penalties associated with the liquefaction of the carbon dioxide product, carbon dioxide sequestration, or inefficiencies associated with coal gasification. It is encouraging to note that had the sensitivity analysis alone been used to optimize this system, the highest efficiency attainable by altering only one of the original variables while holding the others constant was a high value of 57.84%. This value was found when the amount of water injected in the system was raised to 0.38 mol/s.

The efficiencies of the states used in the optimization are shown as an iteration series in Figure 52:

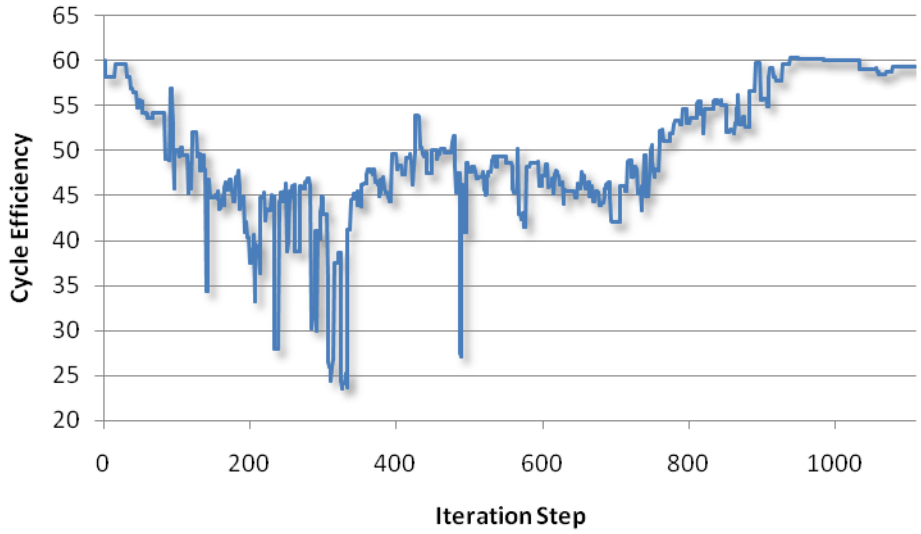

Figure 52: Efficiency of Found States at every iteration

The figure shows how during the first iterations, the high probability of taking a state with a higher cost (and therefore a lower efficiency) results in a wildly fluctuating set of used states that has a decreasing nature. As the probability of accepting states of lower efficiency decreases at high iterations, the fluctuations become small and increases in the state efficiencies are preferred. Towards the end of the optimization, with the

probability of accepting a state of lower efficiency at near zero, the optimization shows a distinctly positive trend as it approaches its eventual maximum value. The shape of this graph suggests that the optimization had to pass through a series of states of higher cost, and therefore lower efficiency, to find the overall state of lowest cost and highest efficiency.

Figure 53 through Figure 57 show the results of the optimization compared against the results of the previous analysis, which was used as a base case. The algorithm did not significantly change many of the variables, with P_{high}, T_{high}, P_{H2Omax}, T_{boiler}, P_{low}, and $P_{H2Oheater}$ only varying a few percentage points. The optimization seems to have worked by adjusting the carbon dioxide recycle rate, and altering necessary parameters, such as the C3 entry temperature, to ensure no second law violations occurred around the cycle. The higher CO_2 flow rate in the cycle resulted in a higher production of power from the high and low temperature turbines and a lower water flow rate through the cycle resulted in less heat rejection in the condenser:

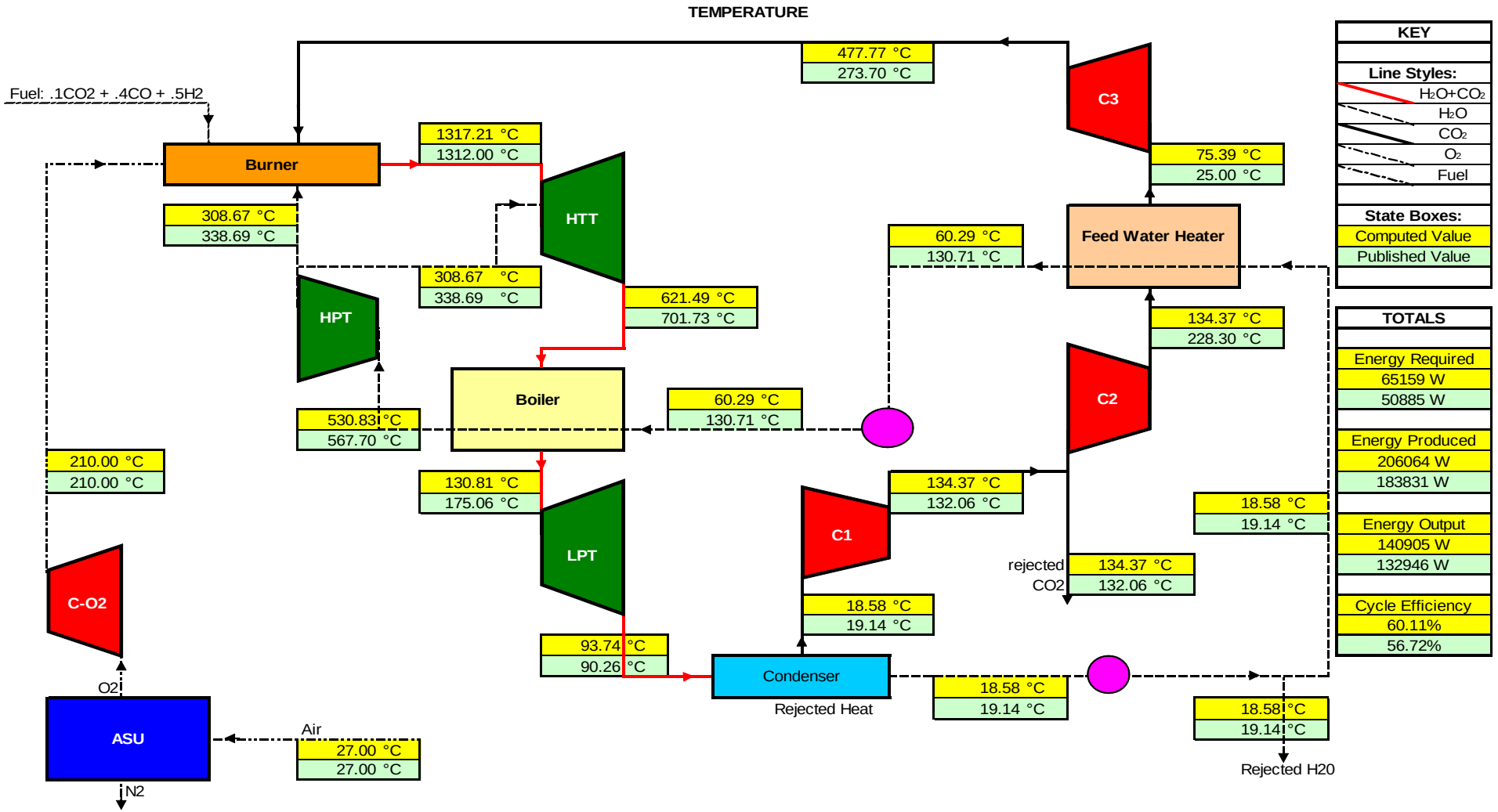

Figure 53: Results of Optimization: Temperature

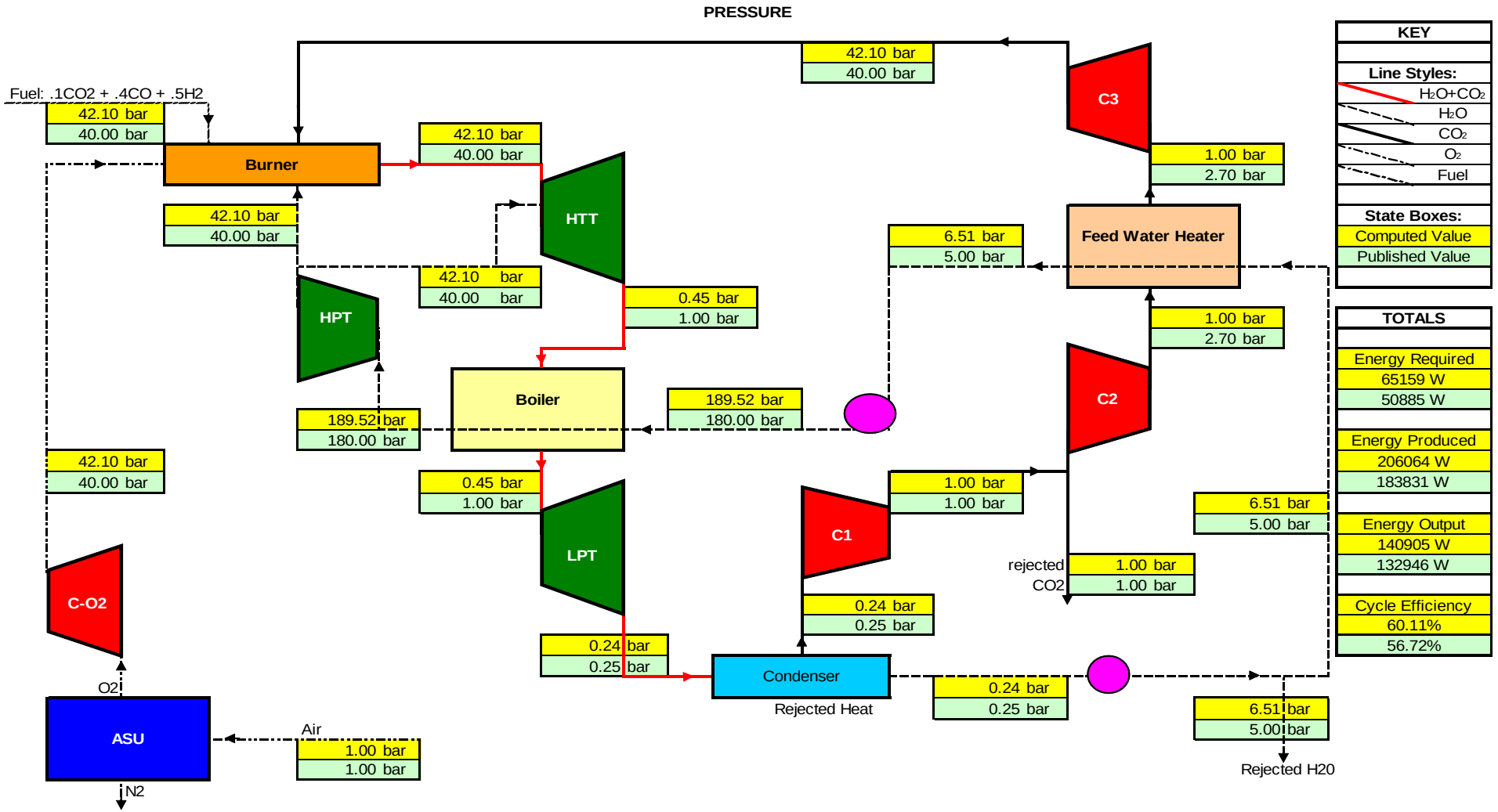

Figure 54: Results of Optimization: Pressure

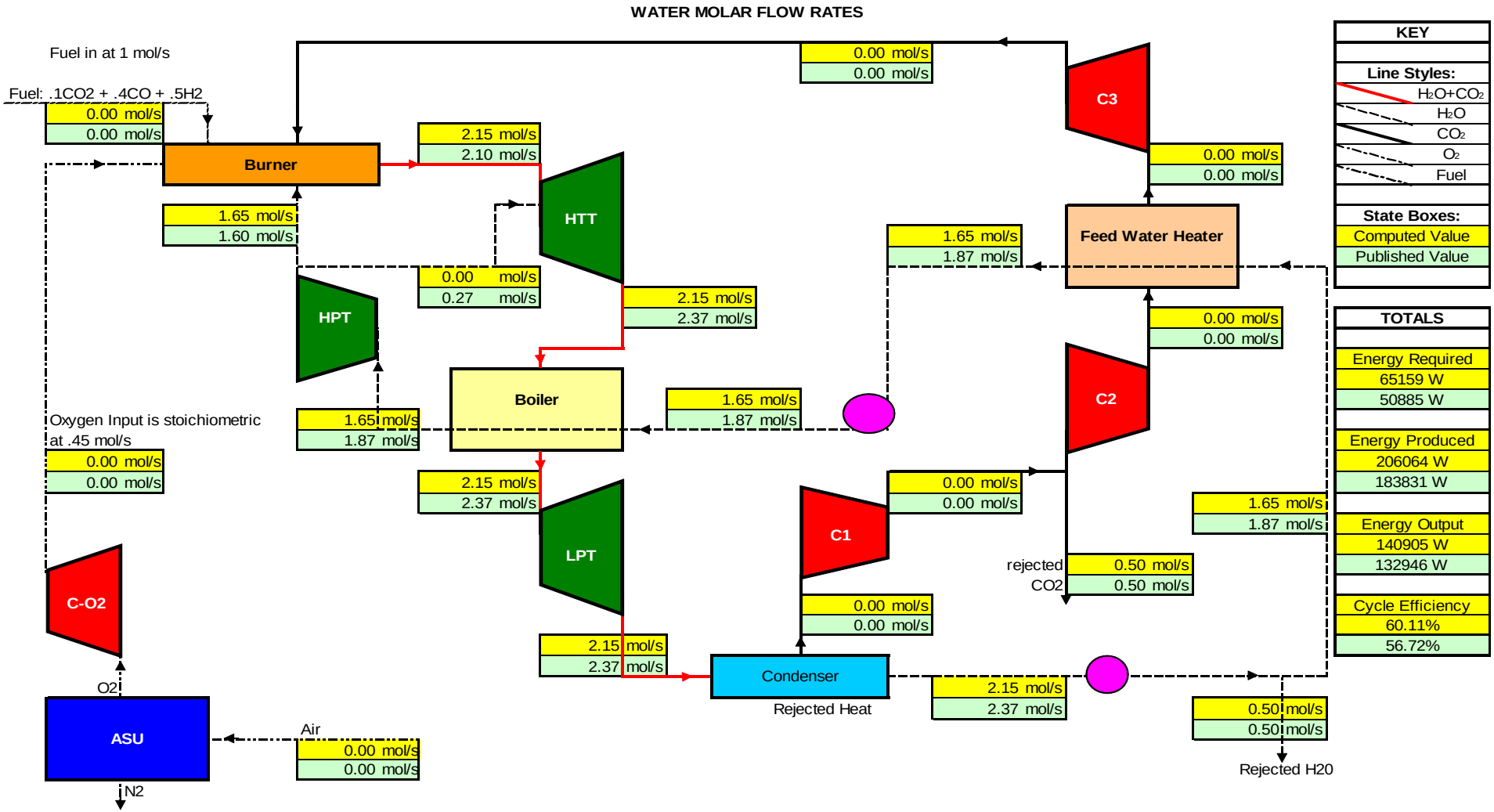

Figure 55: Results of Optimization: Water Molar Flow Rates

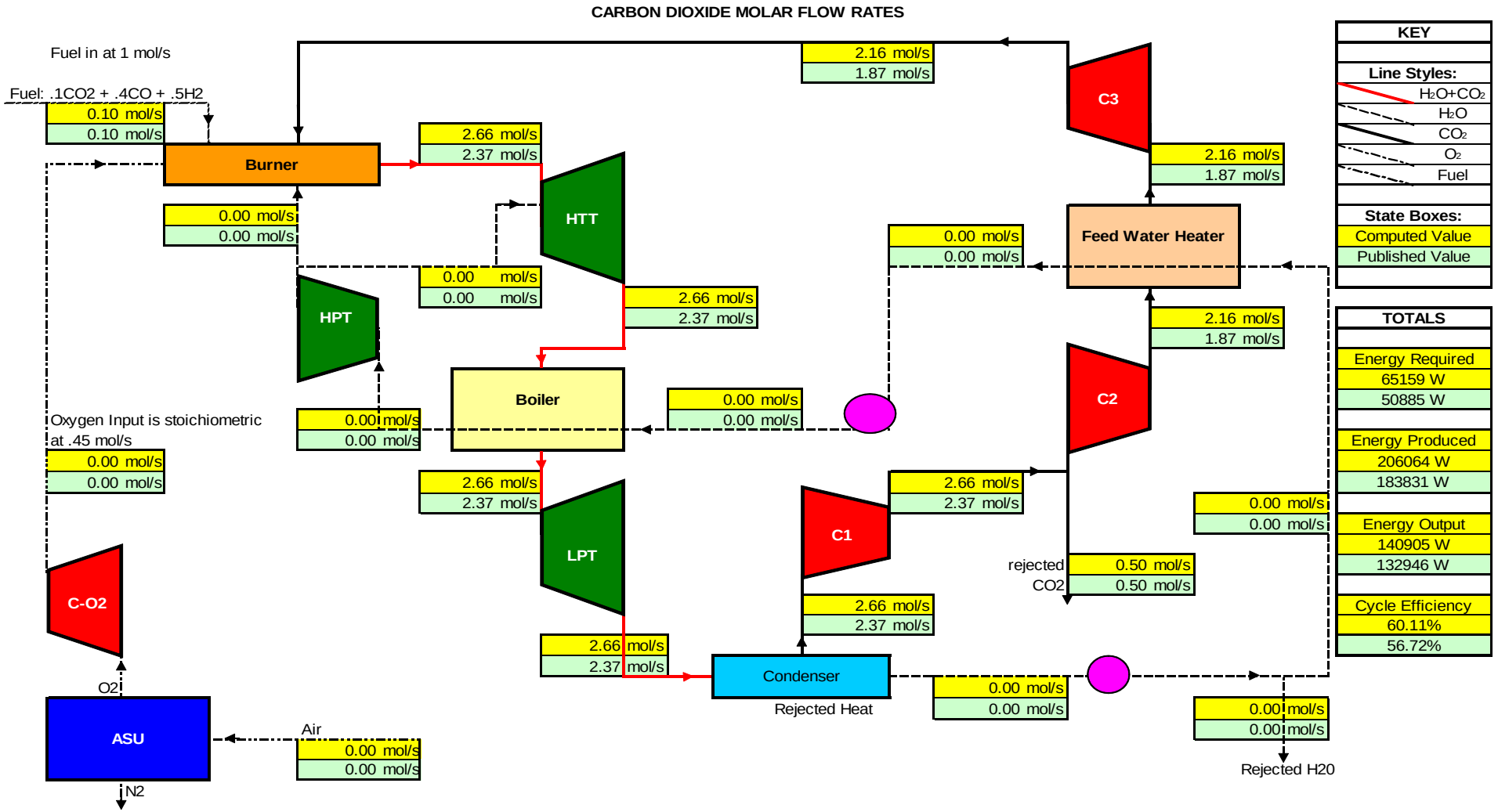

Figure 56: Results of Optimization: Carbon Dioxide Molar Flow Rates

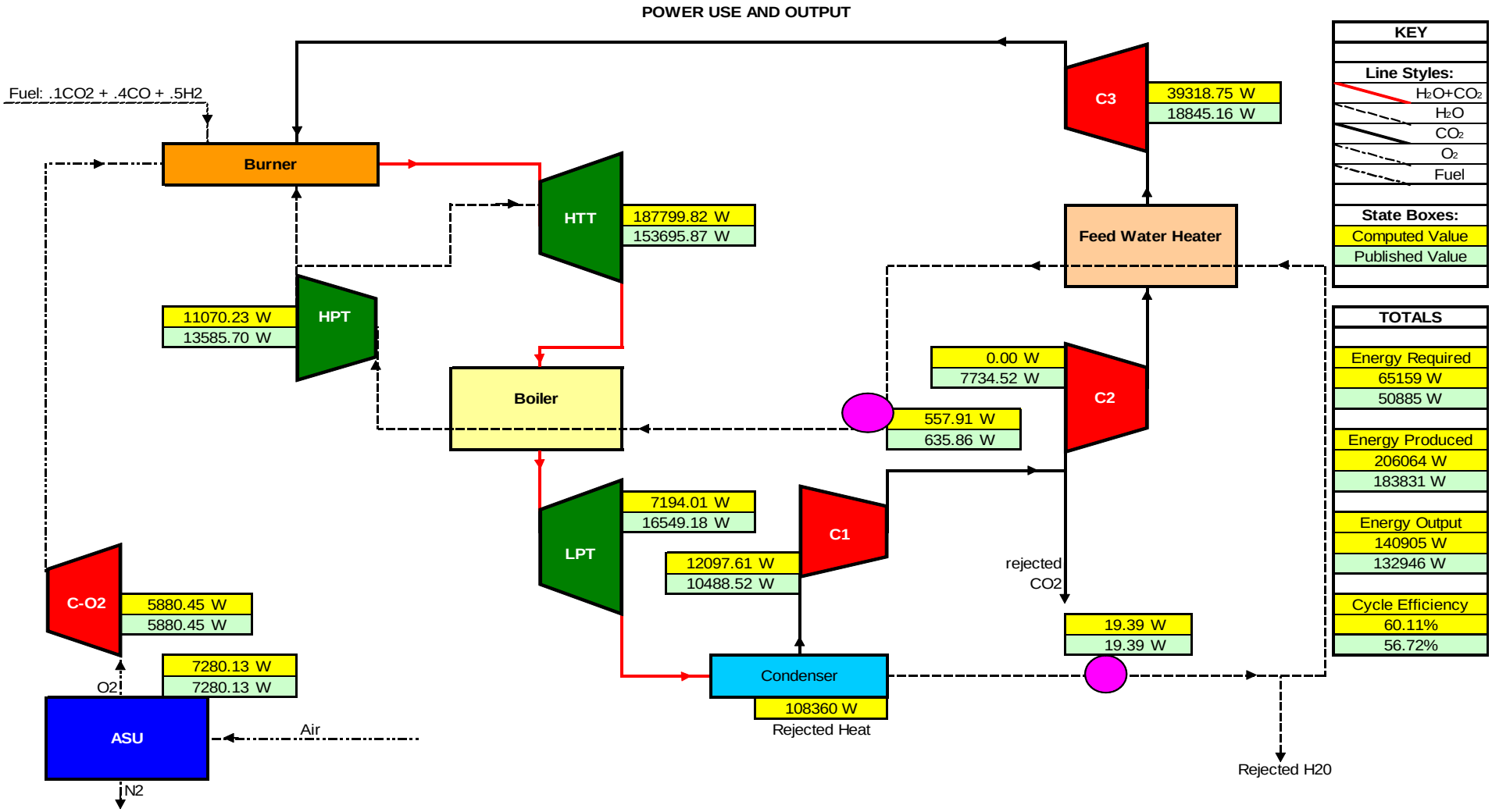

Figure 57: Results of Optimization: Power Output

After analyzing the optimization result, it is clear the optimization found its largest gains by altering the amount of water and carbon dioxide flowing through the cycle. The system both raised the carbon dioxide in the system and lowered the water content, and the energy rejected through the condenser dropped, resulting in the increase in efficiency. What seems odd is that the temperature into the condenser is higher now than in the previous case. The lower amount of rejected heat makes sense, due to the lower amount of water in the stream, but it seems that simply lowering this temperature could improve upon this optimization further to reduce the heat rejected in the condenser even more. A look inside the boiler shows that the optimization has decreased the entropy generation in the boiler as much as possible and produced a pinch point of only 9°C. This lowering of the pinch point, however, is a double edged sword; lower pinch point values also lead to very large heat exchange and boiler equipment that may prove impractical. Figure 58 shows the temperature profiles in the boiler:

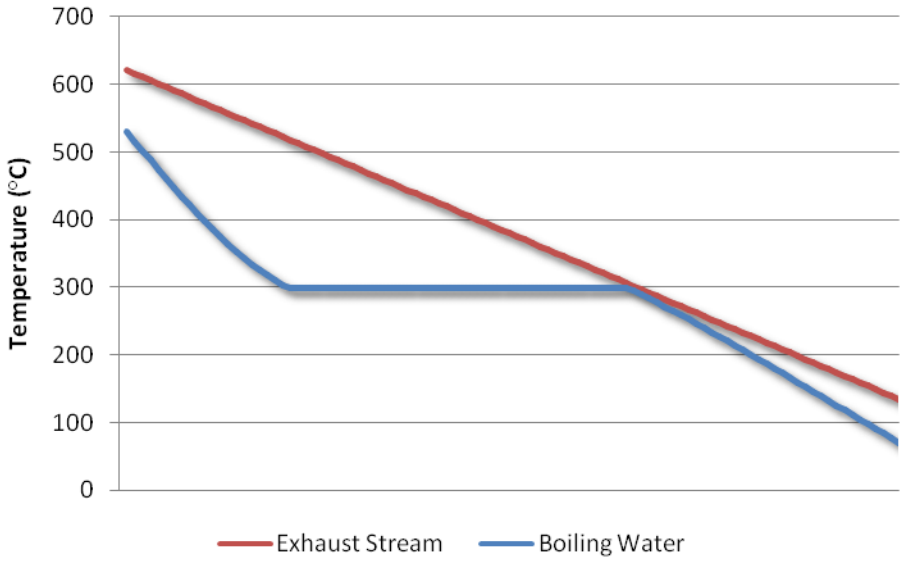

Figure 58: Temperature Profile within Boiler Unit. The x-axis is a linear measure of the change in temperature of the hot stream in the heat exchanger

The algorithm has done a good job of minimizing the pinch point within the boiler, and as can be seen in Figure 59, resulted in a reduction in entropy generation within the boiler unit itself, resulting in the higher cycle efficiency obtained. There was more

entropy generation within the high temperature turbine due to a new pressure ratio closer to 80 to 1. This rise in entropy generation in the HTT is more than offset by drops in entropy generation in the low pressure turbine (LPT) and compressors:

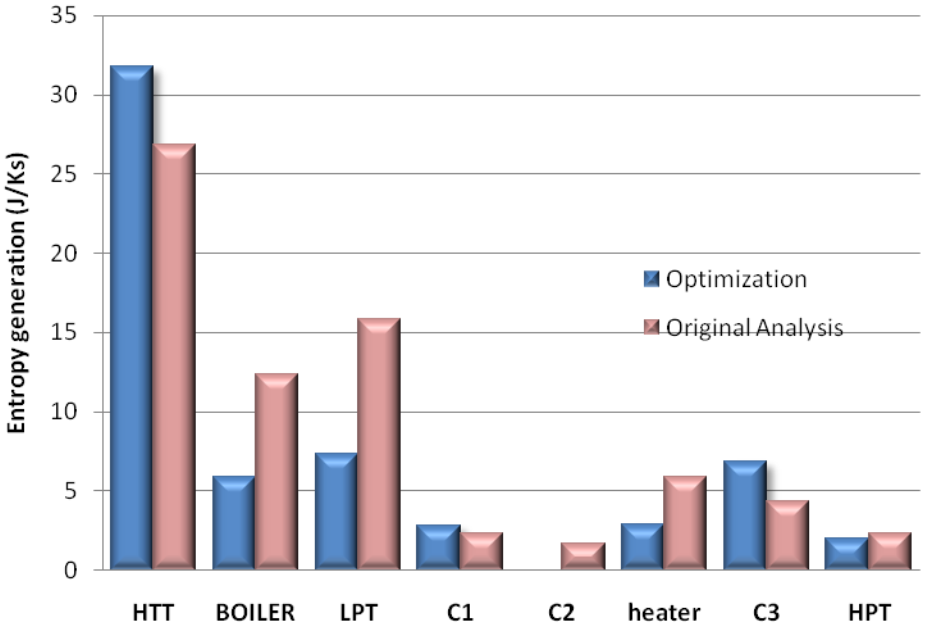

Figure 59: Entropy Generation per Unit for the Optimization and the Original Cycle

Figure 60 and Figure 61 show the changes in the T-S diagrams for both carbon dioxide and water as they flow around the cycle. The T-S diagram from the original analysis is shown as a dashed grey line in both figures. The numbers in the figures refer to the numbers from the cycle diagram in Figure 17. It is clear that the water cycle was fairly well optimized already, but the carbon dioxide cycle was improved:

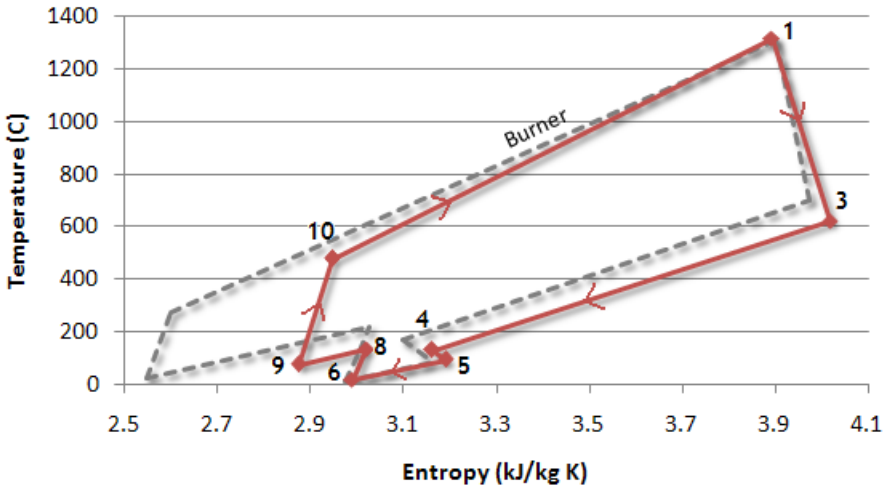

Figure 60: CO_2 T-S diagram

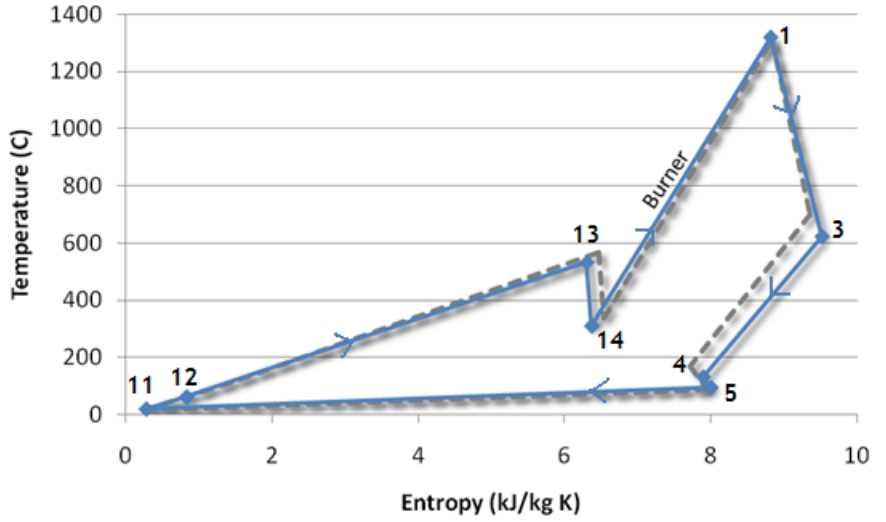

Figure 61: H_2O T-S diagram

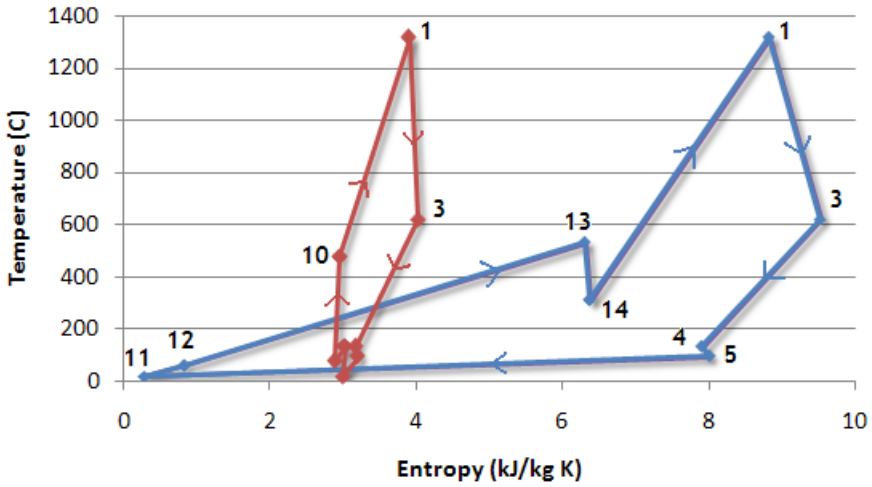

Figure 62: T-S diagram showing carbon dioxide (red) and water (blue) superimposed on the same coordinate system

Another interesting result of this optimization is that the scheme reduced the water injection rate to zero moles per second and effectively removed the second compressor from the cycle by setting the pressure ratio across the unit equal to one. In addition to providing a cycle with higher efficiency, there is now also a simpler cycle which results in less plumbing. The cycle no longer needs a high temperature water turbine (HTTw) and the first two high temperature turbines, HTT1 and HTT2, can effectively be combined into a single unit without the need to inject water between them. It also means that the second compressor can be completely removed, saving the need for a separate compressor unit before the feedwater heater and allowing the compression that took place in the second unit to be integrated into the third compressor. Figure 63 shows the original Graz cycle layout, while the modified layout of this optimized plant is presented in Figure 64:

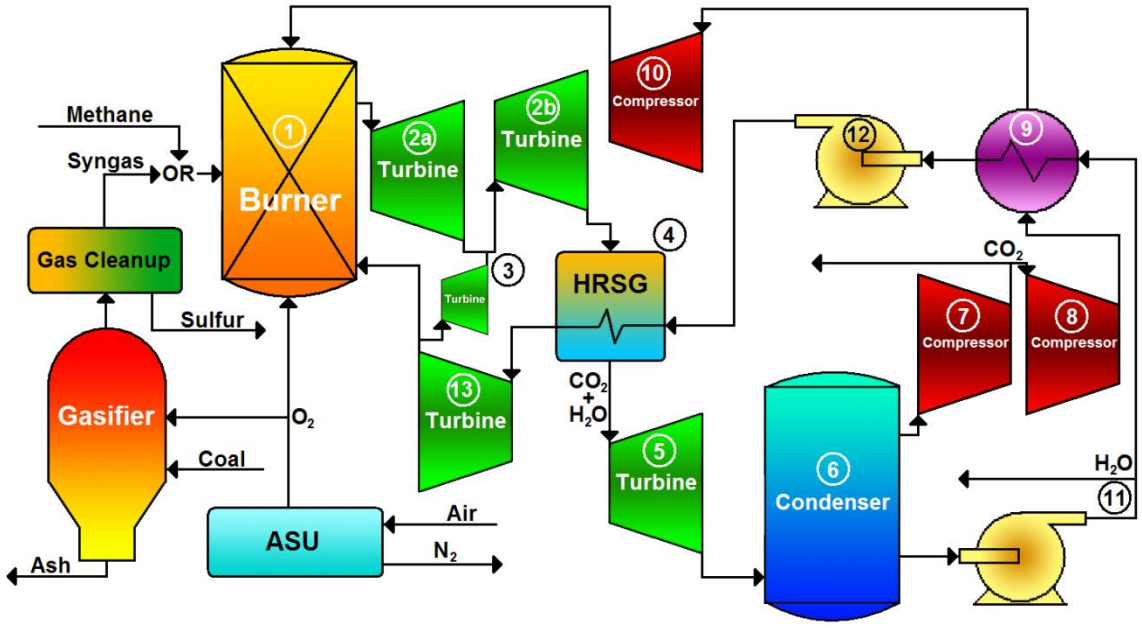

Figure 63: Original Graz cycle layout

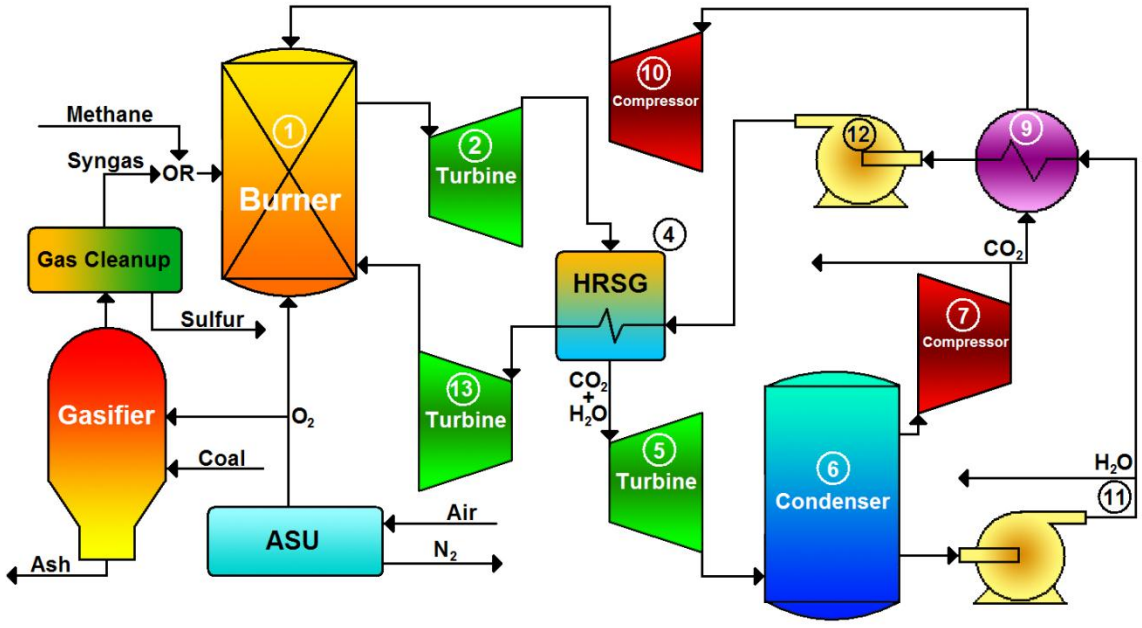

Figure 64: Layout of the optimized Graz cycle. The 2a and 2b turbine set has been replaced with a single unit, while the water injection turbine has been removed. In addition, the compressor at step 8 has also been removed.

An Alternative Cost Function

The simulated annealing algorithm has extra power in optimizing this cycle because the cost function used in the optimization can be defined specifically for

optimizing different cycle parameters at once. In general, the cost function can be defined as:

$$C = \sum \omega_i \zeta_i$$

where ζ_i is a non-dimensionalized parameter of interest and ω_i is its assigned weight.

The optimization performed above was aimed at maximizing the efficiency of the cycle, but in real applications it may be ideal to accept a lower plant efficiency if it means the capital costs of the plant would decrease. The optimization above, for example, found a high water pressure of 189 bar, which is high enough to present technological challenges for plumbing and the high pressure steam turbine.

To combat these high pressures and temperatures in the cycle, an alternative cost function can be defined that weighs the importance of lowering the high pressure and temperature along with the importance of maximizing plant efficiency. In practice, the cost function used for this would be based on capital costs of different components, as well as projected energy and fuel costs over the lifetime of the plant. Such analysis of economic forces is outside the scope of this analysis, but a sample cost function that could be used to perform this type of analysis is presented:

$$C = \frac{P_{high}}{1\text{bar}} + \frac{P_{H2Omax}}{1\text{bar}} + \frac{T_{boiler}}{100°\text{C}} + \frac{T_{high}}{100°\text{C}} - 100\,\eta_{cycle}$$

This function will be higher for high values of the maximum pressures and temperatures in the cycle, but is offset by being lowered by an increase in efficiency. In this way, the desire to minimize the cost function accounts for both rises in the high pressures and temperatures as well as rises in the efficiency of the plant. The weights of each term in this cost function are estimates and the analysis performed using this cost function is provided as a demonstration of the possible uses of the algorithm for optimizing a cycle.

The same optimization that was performed in the previous section was performed again using this modified cost function. The iteration history of the algorithm is show in Figure 65:

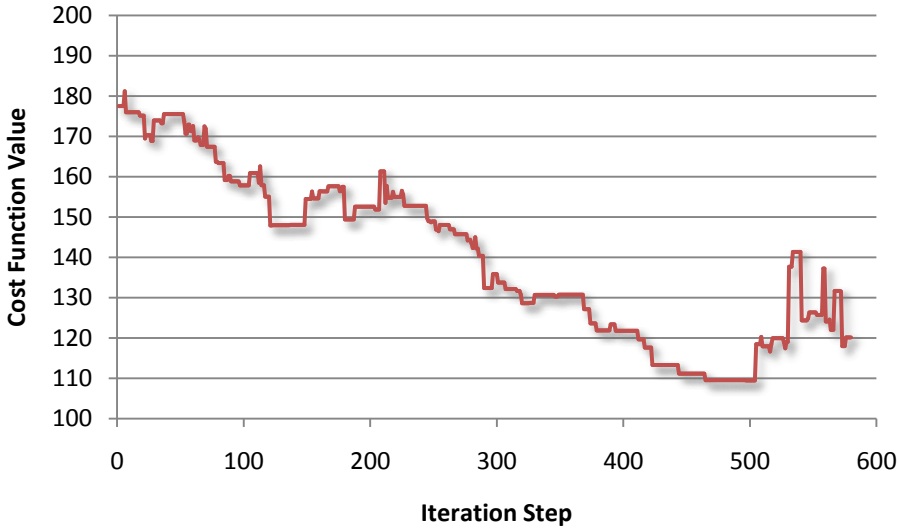

Figure 65: Cost of states at each iteration step

The iteration history of this optimization shows a steady decline over the life of the algorithm, and does not exhibit the same wild variation that was evident in the iteration history of the previous analysis (Figure 52). This suggests that for the cost function used, the initial state of the system was not on or near a minimum. This means that the randomly found neighbors had a high probability of being of lower cost, resulting in the steady decrease in the cost function value. As the cost function approached the optimized minimum, the probability of finding a state of still lower cost decreased, and at the end of the algorithm more fluctuation is seen as the algorithm attempted to jump around different states.

The end result of this algorithm was a modest increase in plant efficiency, to 58.76%, with a large decrease in the maximum water pressure, to 110 bar, and a small decrease in the maximum water temperature, to 532°C. The burner outlet temperature and pressure did not change a substantial amount. This result is not surprising, as Figure 38 in the sensitivity analysis, which plotted the sensitivity of the cycle efficiency against the maximum water pressure, demonstrated that the maximum water pressure

could be lowered to near 110 bar with only fractions of a percentage drop in overall efficiency. The algorithm did more than the sensitivity analysis could have allowed us to do, by heavily adjusting the water and carbon dioxide flow rates in the cycle. As in the previous analysis, the optimization resulted in a higher carbon dioxide flow rate throughout the cycle and a lower water flow rate. This helped contribute to extra power output from the turbine stages and less heat rejection in the condenser unit, which provided the modest two percentage point gain in system efficiency. Figure 66 through Figure 70 show the results of this optimization run compared against the base case analysis:

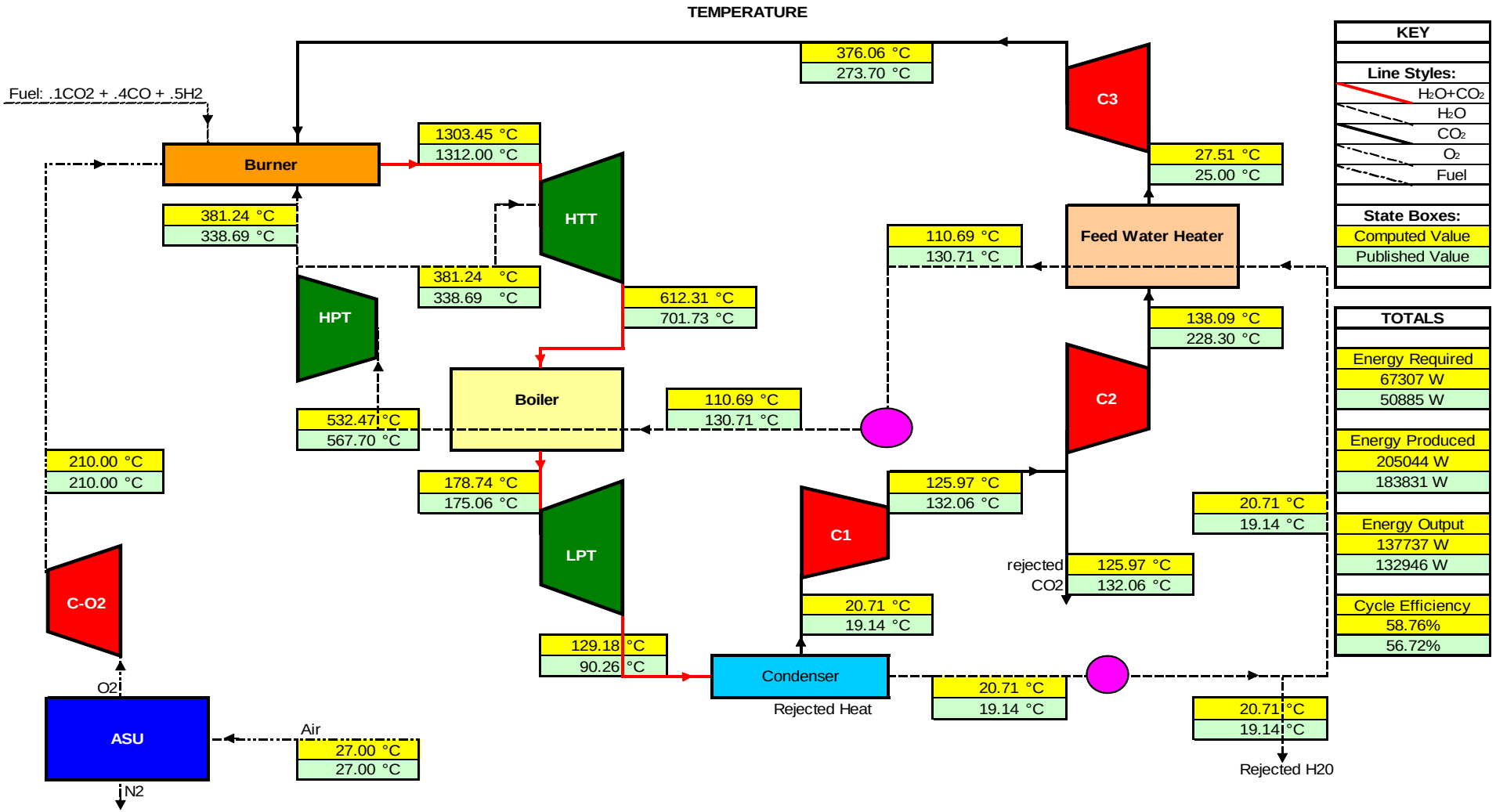

Figure 66: Results of Optimization: Temperature

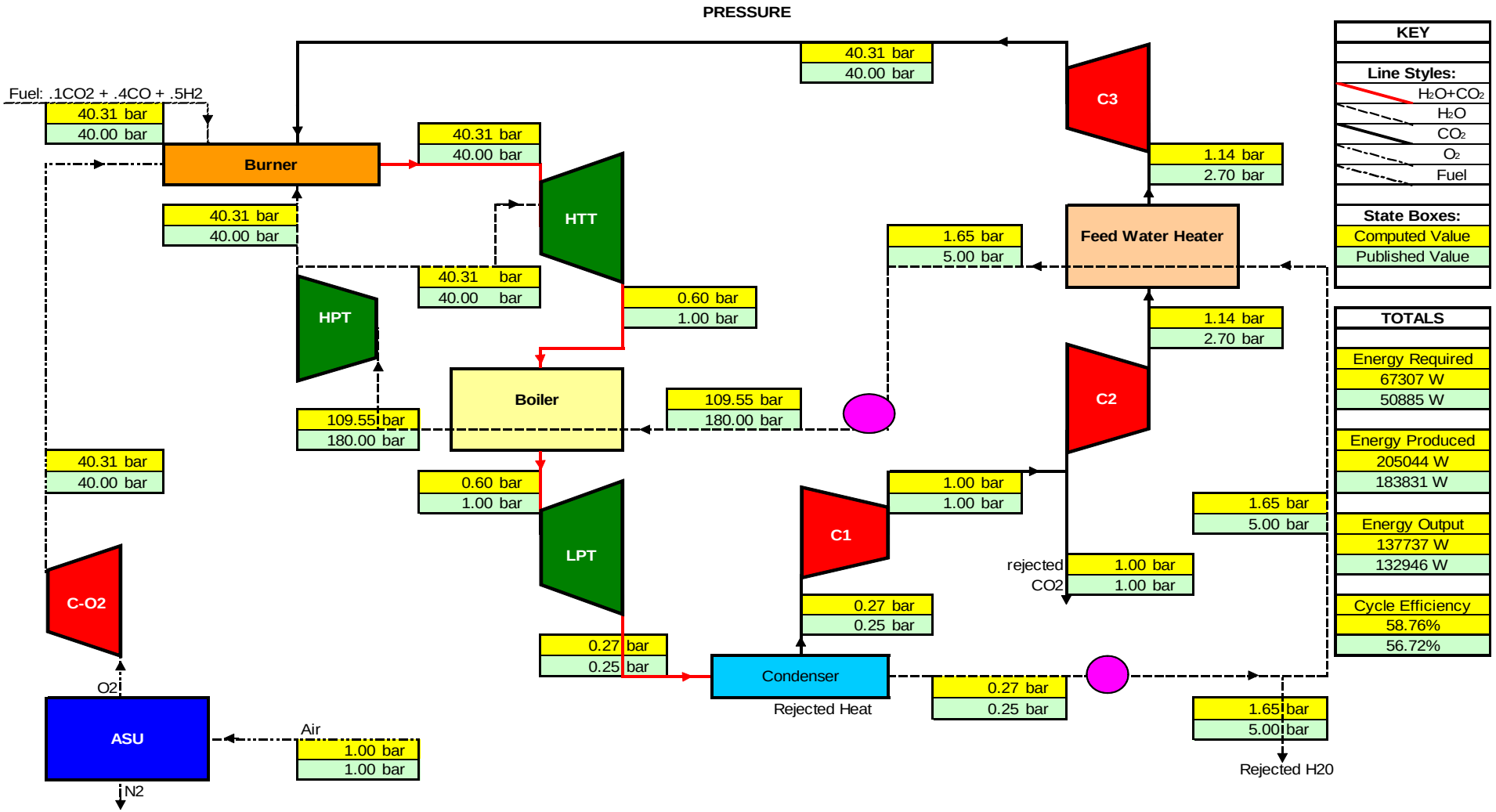

Figure 67: Results of Optimization: Pressure

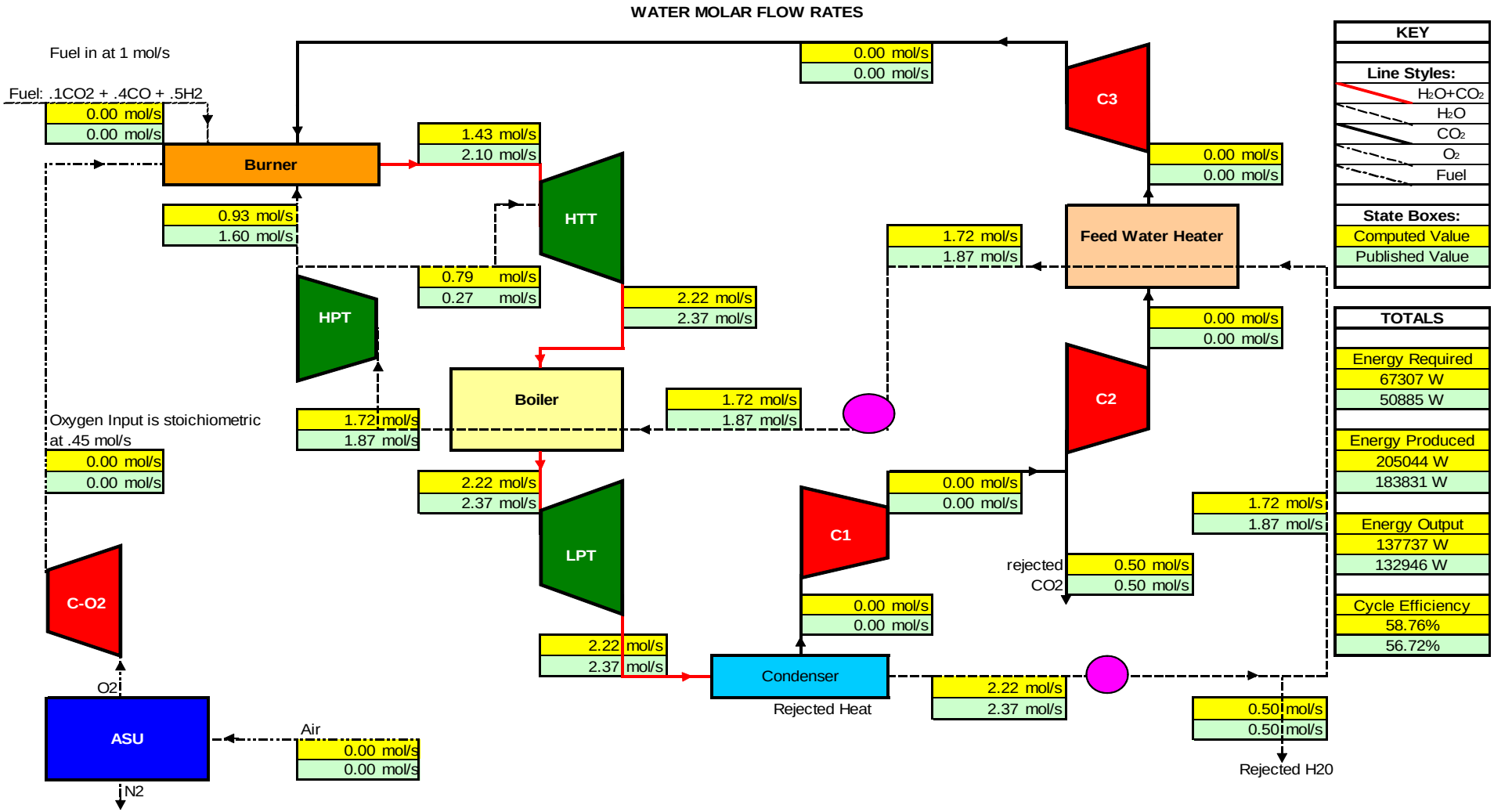

Figure 68: Results of Optimization: Water Flow Rates

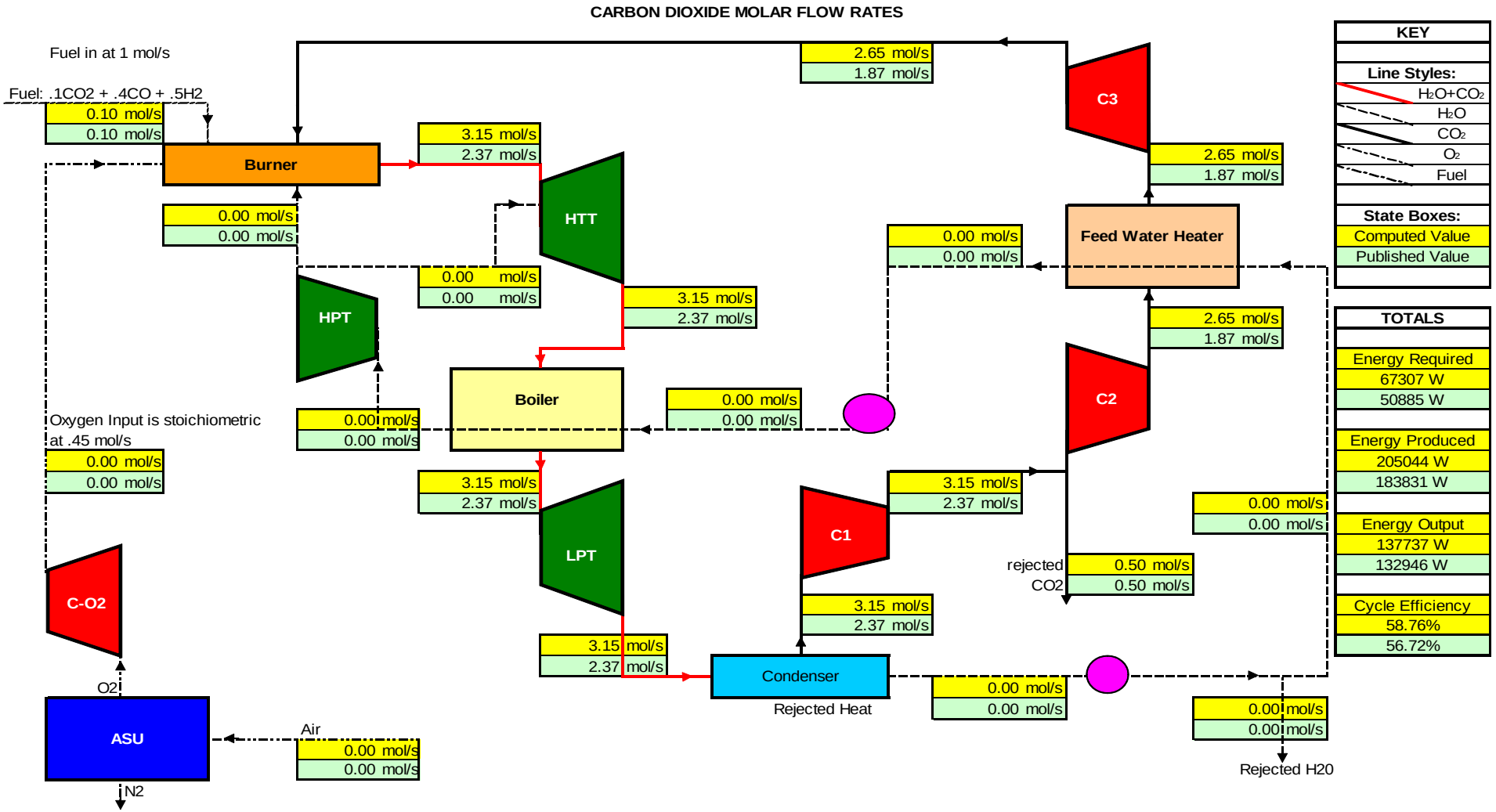

Figure 69: Results of Optimization: Carbon Dioxide Flow Rates

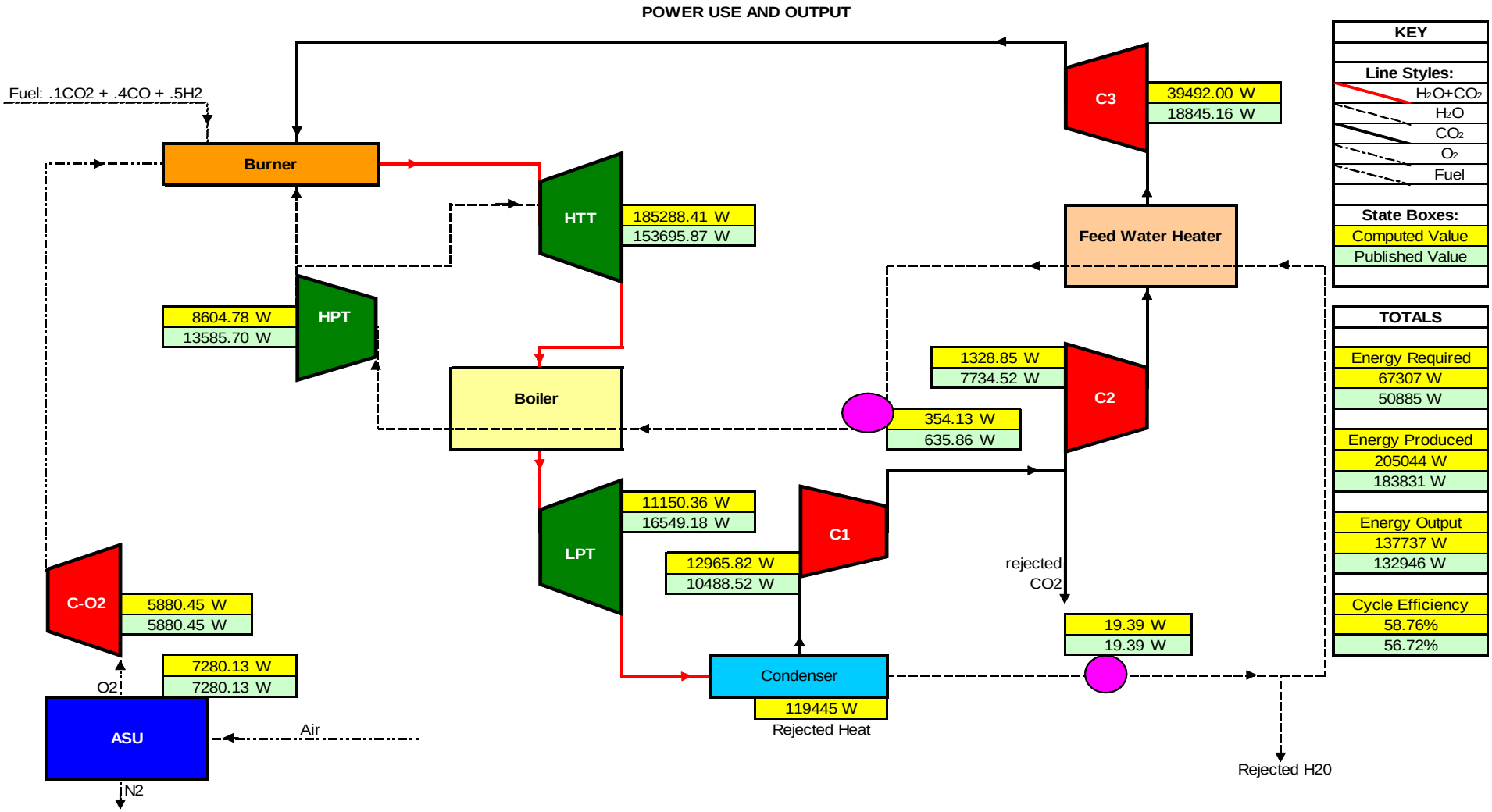

Figure 70: Results of Optimization: Power Output

Future Work

The analysis and optimization performed in this paper are based on a first law model of the Graz cycle. The model provides a good estimate for overall plant design and function, however more sophisticated models of the cycle which employ more realistic turbomachine models should be employed in a similar analysis and optimization to ensure valid results.

The Graz cycle must also be analyzed from other viewpoints. One important analysis that needs to be performed is an economic study for the lifetime of a typical plant. Capital costs, fuel costs, and expected energy prices must be weighed to determine the overall economic feasibility of a Graz cycle plant. Similarly, an analysis must be done to determine the possible costs associated with developing the technology necessary to build a Graz cycle type power plant. Although these costs can be spread across multiple plants, they present a significant barrier to the adoption of this cycle and must be carefully tabulated in order to understand funding levels required to develop this technology.

This analysis also fails to include the gasification step or the liquefaction and sequestration steps. Including the liquefaction and sequestration work as well as the cold gas conversion efficiency of the gasifier unit will no doubt lower the overall efficiency of a Graz plant by tens of percentage points. The magnitude of this efficiency drop is critical to understanding the long-term vitality of a Graz cycle plant, and a close study of these effects should be conducted. In addition, a strong effort should be made to incorporate the gasification and liquefaction steps in the overall Graz cycle layout. Such integration of cycle components allows for better heat recovery within the cycle and generally higher plant efficiencies. Only by integrating the entire plant into one design can the Graz cycle expect to become a viable alternative to other clean coal technology.

The Graz cycle represents a promising solution to the current global warming predicament. High efficiencies coupled with near-zero carbon emissions and a cheap,

abundant fuel warrant further investigation into the feasibility of the Graz cycle solution.

Bibliography

1. **Martin M Halman, Meyer Steinberg.** *Greenhouse Gas Carbon Dioxide Mitigation: Science and Technology.* New York : Lewis Publishers, 1999.

2. Monthly Mean Atmospheric Carbon Dioxide at Mauna Loa Observatory, Hawaii. *NOAA ESRL Global Monitoring Division.* [Online] 11 5, 2006. http://www.cmdl.noaa.gov/ccgg/trends/co2_data_mlo.php.

3. Annual Energy Outlook with Projections to 2030. *Energy Information Administration (EIA).* [Online] 2 2007. http://www.eia.doe.gov/oiaf/aeo/index.html.

4. **Hendriks, Chris.** *Carbon Dioxide Removal from Coal-Fired Power Plants.* Utrecht, The Netherlands : Kluwer Academy Publishers, 1994.

5. Monthly Energy Review. *Energy Information Administration (EIA).* [Online] 4 27, 2007. http://www.eia.doe.gov/emeu/mer/overview.html.

6. US Natural Gas Prices. *Energy Information Administration (EIA).* [Online] 5 6, 2007. http://tonto.eia.doe.gov/dnav/ng/ng_pri_sum_dcu_nus_a.htm.

7. World Crude Oil Prices. *Energy Information Administration (EIA).* [Online] 5 6, 2007. http://tonto.eia.doe.gov/dnav/pet/pet_pri_wco_k_w.htm.

8. Annual Energy Review. *Energy Information Administration (EIA).* [Online] 7 27, 2006. http://www.eia.doe.gov/emeu/aer/coal.html.

9. Coal Gasification and Related Technologies. *Idaho National Laboratory (INL).* [Online] 6 20, 2006. http://www.inl.gov/scienceandtechnology/alternativefuels/coalgasification.shtml.

10. **Goettlicher, Gerold.** *The Energetics of Carbon Dioxide Capture in Power Plants.* s.l. : US Department of Energy, Office of Fossil Energy, National Energy Technology Laboratory, 2004.

11. *Performance modelling of a carbon dioxide removal system.* **Umberto Desideri, Alberto Paolucci.** 1899, Perugia, Italy : Energy Conversion & Management, 1999, Vol. 40, p. 1915.

12. **Undrum, Olav Bolland and Henriette.** *REMOVAL OF CO2 FROM NATURAL GAS FIRED COMBINED CYCLE PLANTS.* s.l. : Norwegian University of Science and Technology, Statoil R&D Centre.

13. *Future Directions of Membrane Gas Separation Technology.* **Baker, Richard W.** 6, s.l. : American Chemical Society, 2002, Vol. 41, p. 1393.

14. DOE's FutureGen Initiative. *DOE - Fossil Energy.* [Online] 3 7, 2007. http://www.fossil.energy.gov/programs/powersystems/futuregen/.

15. *COMPARISON OF TWO CO2 REMOVAL OPTIONS IN COMBINED CYCLE POWER PLANTS.* **MATHIEU, OLAV BOLLAND and PHILIPPE.** 16 18, Great Britain : Energy Convers. Mgmt, 1998, Vol. 39, pp. 1653-1663.

16. *BENCHMARKING OF GAS-TURBINE CYCLES WITH CO2 CAPTURE.* **Hanne M. Kvamsdal, Ola Maurstad, Kristin Jordal, and Olav Bolland.** Trondheim, Norway : SINTEF Energy Research.

17. **Olav Bolland, Hanne M. Kvamsdal, John C. Boden.** *A THERMODYNAMIC COMPARISON OF THE OXY-FUEL POWER CYCLES WATER-CYCLE, GRAZ-CYCLE AND MATIANT-CYCLE.* s.l. : CO2 Capture Project (CCP).

18. *TECHNO-ECONOMIC COMPARISON OF DIFFERENT OPTIONS OF VERY LOW CO2 EMISSION TECHNOLOGIES.* **S. HOUYOU, Ph. MATHIEU, R. NIHART.** Liège, Belgium : University of Liège, Dept. of Power Generation, Institute of Mechanical Engineering.

19. *Conceptual Design and Cooling Blade Development of 1700°C Class High-Temperature Gas Turbine.* **Ito, Shoko.** Yokohama, Japan : ASME, 2005, Vol. 127, p. 358.

20. *HIGHLY EFFICIENT ZERO EMISSION CO2-BASED POWER PLANT.* **MATHIEU, E. IANTOVSKI and Ph.** Great Britain : Energy Convers. Mgmt, 1997, Vol. 38 Suppl, pp. S141-S146.

21. *The Graz Cycle – a Zero Emission Power Plant of Highest Efficiency.* **Franz Heitmeir, Wolfgang Sanz, Emil Göttlich, Herbert Jericha.** Dresden : XXXV Kraftwerkstechnisches Kolloquium, 2003.

22. *CONCEPTUAL DESIGN FOR AN INDUSTRIAL PROTOTYPE GRAZ CYCLE POWER.* **H. Jericha, E. Göttlich.** Amsterdam, The Netherlands : ASME TURBO EXPO 2002, 2002.

23. *An advanced oxy-fuel power cycle with high efficiency.* **C Gou1, R Cai, and H Hong.** Part A: J. Power and Energy, s.l. : Proc. IMechE, 2006, Vol. 220.

24. *DESIGN OPTIMISATION OF THE GRAZ CYCLE PROTOTYPE PLANT.* **H. Jericha, E. Göttlich, W. Sanz, F. Heitmeir.** Atlanta, GA : Proceedings of ASME Turbo Expo, 2003.

25. **Scott Klara, Erik Shuster.** *Tracking Coal Fired Power Plants.* s.l. : NETL, 2007.

26. International Energy Outlook 2005. *Energy Information Administration (EIA).* [Online] 11 5, 2006. http://www.eia.doe.gov/oiaf/ieo/highlights.html.